



ALEXANDRIA UNIVERSITY  
FACULTY OF ENGINEERING

# **RANDOM ACCESS PROTOCOLS FOR FUTURE OPTICAL CDMA NETWORKS**

A Thesis Submitted to the Electrical Engineering Department  
in Partial Fulfillment of the Requirements for the Degree of

**Master of Science**

in

**Electrical Engineering**

By

**Ziad Ahmed Rashad El-Sahn**

*B.Sc. in Electrical Engineering (Communications & Electronics), June 2002*

Supervisors

**Prof. Dr. El-Sayed A. El-Badawy      Prof. Dr. Hossam M. H. Shalaby**

*Electrical Engineering Department, Faculty of Engineering, Alexandria University*

Registered: September 2002

Submitted: April 2005

بِسْمِ اللَّهِ الرَّحْمَنِ الرَّحِيمِ

ذَلِكَ فَضْلُ اللَّهِ يُؤْتِيهِ مَن يَشَاءُ ۗ وَاللَّهُ ذُو الْفَضْلِ الْعَظِيمِ

٤

وَقُلْ رَبِّ زِدْنِي عِلْمًا

١١٤

# EVALUATION COMMITTEE

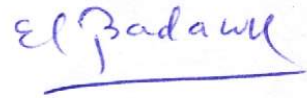
We certify that we have read this thesis and that, in our opinion, it is fully adequate in scope and quality as a dissertation for the degree of Master of Science in Electrical Engineering.

## Evaluation Committee

*Signature*

- **Prof. Dr. El-Sayed A. El-Badawy**

Department of Electrical Engineering,  
Alexandria University, Alexandria, Egypt.  
Higher Institute of Engineering, Thebes Academy, Cairo, Egypt.



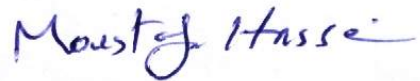
- **Prof. Dr. Hossam M. H. Shalaby**

Department of Electrical Engineering, Faculty of Engineering,  
Alexandria University, Alexandria, Egypt.



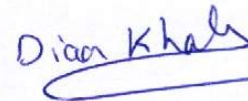
- **Prof. Dr. Moustafa Hussein Aly**

Department of Electronics and Communication Engineering,  
Arab Academy for Science & Technology, Alexandria, Egypt.



- **Prof. Dr. Diaan Abdel Meguid M. Khalil**

Department of Electronics and Communication Engineering,  
Faculty of Engineering, Ein-Shams University, Cairo, Egypt.



For the faculty council

**Prof. Dr. Ossama Rashed**

Vice Dean for graduate and research  
Faculty of Engineering, Alexandria University.  
Alexandria 21544, Egypt.



# SUPERVISORS

## **Prof. Dr. El-Sayed A. El-Badawy**

Dean, Higher Institute of Engineering, Thebes Academy, Cairo 11434, Egypt.

Professor Emeritus, Department of Electrical Engineering,

Faculty of Engineering, Alexandria University,

Alexandria 21544, Egypt.

Email: [sbadawy@ieee.org](mailto:sbadawy@ieee.org)

## **Prof. Dr. Hossam M. H. Shalaby**

Professor, Department of Electrical Engineering,

Faculty of Engineering, Alexandria University,

Alexandria 21544, Egypt.

Email: [shalaby@ieee.org](mailto:shalaby@ieee.org)

# VITAE

## Personal Information

- Date of Birth: 22<sup>nd</sup> November, 1979.
- Place of Birth: Alexandria, Egypt.

## Education

1984 – 1997 **College Saint-Marc** Alexandria, Egypt

- Alliance Française 1996.
- Diplôme de Langue Française 1997 signé par L'Ambassadeur de France.

1998 – 2002 **Faculty of Engineering** Alexandria University

- B.Sc. in Electrical Engineering (Communications and Electronics), June 2002.
- Overall Grade: Excellent with Degree of Honour.
- Overall Rank: 3<sup>rd</sup> over a class of 300 students.
- Graduation Project: Multimedia Mobile Communications.

## Professional and Work Experience

1999 Training **Arabia Computer Systems** Alexandria, Egypt

2000 Training **Federal Arab Maritime Company** Alexandria, Egypt

2001 Training **Schlumberger - Wireline** Shukeir, Egypt

2002 – Present **Faculty of Engineering, Alexandria University**  
Teaching Assistant (Full Time), Department of Electrical Engineering, Communications and Electronics Section.

## ACKNOWLEDGEMENTS

نحمد الله عز وجل أن هدانا لهذا وما كنا لنهتدي لولا أن هدانا الله

First, I would like to express my heartfelt gratitude to my supervisors Prof. Dr. El-Sayed A. El-Badawy, and Prof. Dr. Hossam M. H. Shalaby, for their academic advice, constant encouragement, guidance, and support during my graduate school years. I am really grateful to them for contributing many suggestions and improvements.

My appreciation also goes to my colleagues at the Department of Electrical Engineering (Alexandria University) for the friendly academic atmosphere, and their encouragement. In addition, I would like to express my thanks to Eng. Yousef Abdel Malek for his help and useful discussions; I really feel so proud working hand in hand with him all throughout the research program.

I am extremely grateful to my parents who have sacrificed themselves to give me the best education. From my early childhood, they raised me to love learning, and supported me to develop my interest in science and engineering. Their unreserved love and support for these many years is what makes this M.Sc. degree possible. I would also like to thank them for their continuous support, for their patience, encouragement and extra care.

**Thank you all.**

## PUBLICATIONS AND AWARDS

- [1] Z. A. El-Sahn, Y. M. Abdel-Malek, H. M. H. Shalaby, and El-S. A. El-Badawy, "Performance limitations in the  $R^3T$  optical random access CDMA protocol," *Submitted for possible publication to OSA J. Optical Networking*, March 2005.

**This paper won the 1<sup>st</sup> position in paper evaluation and 3<sup>rd</sup> position after presentation, *IEEE Egyptian Student Branch Contest 2004, AAST, Cairo, Egypt, January 2005.***

- [2] Z. A. El-Sahn, Y. M. Abdel-Malek, H. M. H. Shalaby, and El-S. A. El-Badawy, "The  $R^3T$  optical random access CDMA protocol with queuing subsystem," *Submitted for possible publication to the IEEE/OSA J. Lightwave Technol., also a summary submitted to the 31<sup>st</sup> European Conference on Optical Communication, (ECOC 2005), Glasgow, Scotland, 25-29 September 2005.*

- [3] Z. A. El-Sahn, Y. M. Abdel-Malek, H. M. H. Shalaby, and El-S. A. El-Badawy, "Proposed optical random access CDMA protocol with stop & wait ARQ," *Submitted for possible publication to OSA J. Optical Networking, also a summary submitted to the 31<sup>st</sup> European Conference on Optical Communication, (ECOC 2005), Glasgow, Scotland, 25-29 September 2005.*

**This paper was presented in part at the *Fifth Workshop on Advanced Photonics, The National Institute of Laser Sciences, Cairo University, Egypt, May 2005.***

- [4] Z. A. El-Sahn, Y. M. Abdel-Malek, H. M. H. Shalaby, and El-S. A. El-Badawy, "Optical random access CDMA protocol with stop & wait ARQ and a queuing subsystem," *Submitted for possible publication to OSA Optics Letters.*

# **ABSTRACT**



# ABSTRACT

In this thesis we present an overview on optical code division multiple access (CDMA) communication systems. Both physical and optical link layers are studied. Focus is oriented towards random access protocols and media access control (MAC) protocols for future optical CDMA networks.

One of the main objectives of this research is to study the performance of the optical CDMA round robin receiver/transmitter ( $R^3T$ ) protocol in noisy environments and dispersive channels. We proved by numerical analysis that the effect of thermal noise dominates the performance only for low population networks, whereas the effect of multiple access interference (MAI) becomes dominant for larger networks. We found out that there are optimum values for the operating wavelength and the average peak laser power of the transmitter to compensate for this degradation.

Then, we suggest a queuing model to the  $R^3T$  protocol in order to enhance its performance. A detailed state diagram is outlined and a mathematical model based on the equilibrium point analysis (EPA) technique is presented. Our results reveal that significant improvement in terms of the steady state system throughput and the protocol efficiency can be achieved by only adding a single buffer to the system which does not add considerably to the network complexity. The modified protocol significantly outperforms the  $R^3T$  protocol for larger population networks and at higher traffic loads. Furthermore, the modified  $R^3T$  protocol exhibits an acceptable timeout probability under different network parameters.

Finally, we propose an optical random access CDMA protocol based on stop & wait automatic repeat request (ARQ). A mathematical description of this protocol is outlined using a detailed state diagram. Several performance measures are considered; namely, the steady state system throughput, the blocking probability, the average packet delay, and the protocol efficiency. We proved by numerical analysis that the proposed protocol is less complex and significantly outperforms the  $R^3T$  protocol (which is based on a go-back  $n$  technique) at higher population networks. Our results also show that the performance of the proposed protocol with correlation receivers is nearly close to that of the  $R^3T$  protocol with chip-level receivers, which significantly reduces the overall system cost.

# TABLE OF CONTENTS

<b>TABLE OF CONTENTS</b>	<b>viii</b>
<b>LIST OF FIGURES</b>	<b>xii</b>
<b>LIST OF TABLES</b>	<b>xv</b>
<b>LIST OF SYMBOLS</b>	<b>xvi</b>
<b>ACRONYMS</b>	<b>xix</b>
<b><u>CHAPTER 1: INTRODUCTION AND THESIS SURVEYS</u></b>	<b>1</b>
1.1 Introduction	1
1.2 Contributions of the Thesis	2
1.3 Organization of the Thesis	3
<b><u>CHAPTER 2: RESEARCH AND DEVELOPMENT IN OPTICAL CDMA COMMUNICATION SYSTEMS</u></b>	<b>5</b>
2.1 Introduction	5
2.2 Basic Optical CDMA Communication Systems	5
2.2.1 System Architecture	5
2.2.2 Optical Orthogonal Codes (OOCs)	6
2.3 Optical CDMA Encoding - Decoding Techniques	7
2.3.1 Time Domain Encoding Using Optical Delay Line Loops	7
2.3.2 Spectral Intensity Encoding CDMA Systems	8
2.3.3 Optical Fast Frequency Hop CDMA (FFH-CDMA)	10
2.3.4 Important Design Issues in Optical CDMA	11
2.4 Various Optical CDMA Receivers	11
2.4.1 Correlation Receivers	12
2.4.1.1 Passive Correlation Receivers	12
2.4.1.2 Active Correlation Receivers	13
2.4.1.3 Correlation Receivers with Optical Hard-Limiters	13
2.4.2 Chip-Level Receivers	15
2.4.2.1 High-Speed Chip-Level Receivers	15
2.4.2.2 All Optical Chip-Level Receivers	16
2.4.3 Comparison of Various Optical CDMA Receivers	17

2.5 Performance of Optical CDMA Receivers	18
2.5.1 Correlation Receivers without Hard-Limiter	19
2.5.2 Chip-Level Receivers	20
2.5.3 Simulation Results	21
2.5.4 Conclusions	24
<b><u>CHAPTER 3: OPTICAL CDMA RANDOM ACCESS PROTOCOLS</u></b>	<b>25</b>
<b>FOR FUTURE LOCAL AREA NETWORKS</b>	
3.1 Introduction	25
3.2 Background and Basic Information	25
3.2.1 Traditional Random Access Protocols	26
3.2.1.1 Pure ALOHA	26
3.2.1.2 Slotted ALOHA	27
3.2.1.3 CSMA and CSMA/CD	28
3.2.2 The Need for MAC Protocols for Optical Networks	28
3.3 Optical CDMA Protocols with and without Pretransmission Coordination	29
3.3.1 System Architecture	29
3.3.2 Optical CDMA Protocols' Description	30
3.3.2.1 First Protocol: Pro 1	30
3.3.2.2 Second Protocol: Pro 2	30
3.3.2.3 Variation of Pro 2	30
3.3.3 Optical CDMA Protocols' Performance	31
3.3.3.1 The Effect of MAI	31
3.3.3.2 Performance Metrics	32
3.3.4 Results and Conclusions	32
3.4 Round Robin Receiver/Transmitter ( $R^3T$ ) Protocol	34
3.4.1 Network and System Design	35
3.4.1.1 Physical Layer Implementation	35
3.4.1.2 Optical Link Layer	35
3.4.2 Mathematical Model and Theoretical Analysis	35
3.4.2.1 State Diagram and Protocol Description	36
3.4.2.2 Performance Evaluation	38
3.4.3 Simulation Results	40
3.4.4 Summary and Conclusions	43

<b><u>CHAPTER 4: IMPAIRMENTS IN THE <math>R^3T</math> OPTICAL RANDOM</u></b>	<b>44</b>
<b>ACCESS CDMA PROTOCOL</b>	
4.1 Introduction	44
4.2 Impairments in Fiber Optic Communication Systems	44
4.2.1 Receiver Noise	44
4.2.1.1 Shot Noise	45
4.2.1.2 Thermal Noise	45
4.2.2 Light Dispersion in Fibers	45
4.2.2.1 Modal Dispersion	46
4.2.2.2 Chromatic Dispersion	46
4.3 Performance of the $R^3T$ Protocol in a Noisy Environment	47
4.3.1 System Architecture and Hardware Implementation	48
4.3.2 Effect of Thermal Noise	48
4.3.2.1 Mathematical Analysis	48
4.3.2.2 Numerical Results	51
4.3.3 Effect of Light Dispersion	55
4.3.3.1 Mathematical Analysis	56
4.3.3.2 Numerical Results	57
4.4 Conclusions	59
<b><u>CHAPTER 5: THE <math>R^3T</math> OPTICAL RANDOM ACCESS CDMA</u></b>	<b>60</b>
<b>PROTOCOL WITH QUEUING SUBSYSTEM</b>	
5.1 Scope and Motivation	60
5.2 System Architecture	60
5.2.1 Optical CDMA Network	60
5.2.2 Optical CDMA Protocol	61
5.3 Mathematical Model	62
5.4 Theoretical Analysis	68
5.4.1 State Diagram Analysis	68
5.4.1.1. Transmission Mode	68
5.4.1.2. Reception Mode	70
5.4.1.3. Acknowledgement Mode	71
5.4.1.4. Requesting Mode	71
5.4.2 Performance Measures	73

5.4.2.1 Steady State Throughput	73
5.4.2.2 Protocol Efficiency	74
5.4.2.3 Timeout Probability	74
5.5 Simulation Results	75
5.6 Conclusions	80
<b><u>CHAPTER 6: PROPOSED OPTICAL RANDOM ACCESS CDMA</u></b>	<b>81</b>
<b>PROTOCOL WITH STOP &amp; WAIT ARQ</b>	
6.1 Introduction	81
6.2 System and Hardware Architecture	82
6.3 Mathematical Model	83
6.3.1 Protocol Assumptions	83
6.3.2 State Diagram Description	84
6.4 Performance Analysis	86
6.4.1 State Diagram	86
6.4.1.1 Transmission Mode	87
6.4.1.2 Reception Mode	87
6.4.1.3 Acknowledgement Mode	88
6.4.1.4 Requesting Mode	88
6.4.2 Performance Metrics	88
6.4.2.1 Steady State System Throughput	88
6.4.2.2 Blocking Probability	89
6.4.2.3 Protocol Efficiency and Average Delay	89
6.5 Numerical Results	90
6.6 Conclusions	95
<b><u>CHAPTER 7: CONCLUSIONS AND FUTURE WORK</u></b>	<b>97</b>
7.1 Conclusions	97
7.2 Future Research Avenues	98
<b>REFERENCES</b>	<b>100</b>

# LIST OF FIGURES

Fig. 2.1	Optical CDMA network configuration.	6
Fig. 2.2	Time domain optical CDMA encoding of high peak intensity ultra-short pulses using delay line loops: (a) Encoder, (b) Decoder.	8
Fig. 2.3	Spectral intensity encoded optical CDMA system: (a) Encoder, (b) Decoder.	9
Fig. 2.4	Optical FFH-CDMA system: (a) Encoder, (b) Decoder.	10
Fig. 2.5	Passive correlator structure.	12
Fig. 2.6	Active correlator structure.	13
Fig. 2.7	Optical hard-limiters' characteristics: (a) An ideal optical hard-limiter, (b) A practical optical hard-limiter.	14
Fig. 2.8	(a) Optical correlation receiver with hard-limiter, (b) Optical correlation receiver with double hard-limiters.	15
Fig. 2.9	(a) High-speed chip-level receiver, (b) All optical chip-level receiver.	16
Fig. 2.10	Bit error probabilities for OOK-CDMA receivers, under a Poisson shot-noise-limited assumption, versus average photons/bit.	18
Fig. 2.11	Packet success probability versus number of active users for different packet sizes.	22
Fig. 2.12	Packet success probability versus number of active users and code length for correlation receivers.	23
Fig. 2.13	Packet success probability versus number of active users and code length for chip-level receivers.	23
Fig. 3.1	Normalized throughput versus offered traffic for ALOHA systems.	27
Fig. 3.2	Optical CDMA network architecture.	29
Fig. 3.3	Throughput versus average activity for different protocols.	33
Fig. 3.4	Throughput and delay versus average activity for different protocols.	33
Fig. 3.5	Complete state diagram of the $R^3T$ optical CDMA protocol.	36
Fig. 3.6	Throughput and blocking probability versus average activity for different number of users.	40

Fig. 3.7	Throughput and blocking probability versus number of users for different propagation delays.	41
Fig. 3.8	Throughput and delay versus timeout duration for different activities.	42
Fig. 4.1	Typical dispersion versus wavelength curves.	47
Fig. 4.2	Bit error probabilities for OOK-CDMA chip-level receivers versus the decision threshold.	50
Fig. 4.3	Packet success probability and decision threshold versus the average peak laser power and the receiver noise temperature for different number of active users.	52
Fig. 4.4	Throughput versus average peak laser power for different propagation delays.	53
Fig. 4.5	Packet delay versus throughput for different propagation delays.	54
Fig. 4.6	Protocol efficiency versus blocking probability for different number of users.	55
Fig. 4.7	Throughput versus message length for different interstation distances and wavelengths.	57
Fig. 4.8	Throughput versus user bit rate for different interstation distances.	58
Fig. 5.1	An optical CDMA network in a star configuration.	61
Fig. 5.2	Complete state diagram of the $R^3T$ optical CDMA protocol with a single buffer in the queue.	63
Fig. 5.3	Detailed state diagram of the requesting mode.	64
Fig. 5.4	Detailed state diagram of the acknowledgement mode.	65
Fig. 5.5	Detailed state diagram of the reception mode.	66
Fig. 5.6	Detailed state diagram of the transmission mode.	67
Fig. 5.7	(a) State $r_n$ , (b) State $T_{X_{t+i}}$ , (c) State $W_{X_i}$ .	67
Fig. 5.8	Throughput versus number of users for different propagation delays.	76
Fig. 5.9	Available packets and throughput versus average activity.	76
Fig. 5.10	Protocol efficiency versus message length for different number of users.	77
Fig. 5.11	Timeout probability versus average activity and timeout duration.	78
Fig. 5.12	Timeout probability versus number of users.	79

Fig. 6.1	Optical CDMA network topology.	82
Fig. 6.2	State diagram of the proposed optical CDMA protocol with stop & wait ARQ.	85
Fig. 6.3	Transmission states, $T_{xi}$ and reception states, $R_{xi}$ .	86
Fig. 6.4	Throughput versus number of users for different receivers.	91
Fig. 6.5	Blocking probability versus user activity for different interstation distances.	92
Fig. 6.6	Throughput and delay versus activity for different number of users and different interstation distances.	93
Fig. 6.7	Throughput versus number of users for different interstation distances.	94
Fig. 6.8	Efficiency versus message length for different number of users.	94
Fig. 6.9	Throughput versus number of users and average peak laser power per chip.	95



# LIST OF TABLES

Table 2.1	Comparison of various optical CDMA receiver structures.	17
Table 2.2	Examples of optimal $(L,3,1,1)$ optical orthogonal codes.	22
Table 3.1	Notations and description for states in the $R^3T$ protocol state diagram.	37
Table 4.1	Typical values of simulation parameters.	52
Table 4.2	Light source and optical fiber specifications.	57
Table 6.1	Parameters used for numerical calculations.	90

# LIST OF SYMBOLS

$A$	Average user activity
$a$	Acknowledgement states
$C$	Number of pulses with $Y_i \geq \theta$
$ C $	Maximum achievable number of codes
$c$	Speed of light in free space
$D$	Average packet delay
$d$	Average delay spent in the backlog mode
$D_{chrom}$	Chromatic dispersion parameter
$e$	Retransmission states
$F$	APD excess noise factor
$G$	Offered traffic
$G_{APD}$	Average APD gain
$I_d$	APD dark current
$K$	Number of bits in a packet
$\bar{k}$	Interference vector
$K_B$	Boltzmann's constant
$k_{eff}$	APD effective ionization ratio
$L$	Code length
$\ell$	Message length in packets
$m$	Initial state
$m_{b_j}$	Conditional mean of the decision variable $Y_j$
$N$	Number of users
$n$	number of backlogged users
$n_1$	Core refractive index
$NA$	Numerical aperture
$P_{av}$	Received average peak laser power
$P_B$	Blocking probability

$P_{bc}$	Conditional bit correct probability
$P_{bt}$	Blocklogged probability
$P_{in}$	Input power
$P_{out}$	Output power
$P_S$	Packet success probability
$P_{th}$	Thinking probability
$P_{to}$	Timeout probability
$p_1$	Probability of 1 chip interference
$p_w$	Probability of w chip interference
$Q$	Photon count within a chip interval
$Q(x)$	Normalized Gaussian tail probability
$Q_d$	Photon count due to dark current within a chip interval
$q$	Requesting states
$q_e$	Magnitude of the electron charge
$R_{APD}$	APD responsivity at unity gain
$R_b$	User bit rate
$R_L$	Load resistor
$R_{xx}$	Auto-correlation function
$R_{xy}$	Crosscorrelation function
$r$	Transmission states
$r'$	Number of active users
$S_o$	Zero dispersion slope
$s$	Reception states
$T$	Bit duration
$t$	Two-way propagation time
$T_c$	Chip duration
$T^o$	Receiver noise temperature
$T_s$	Slot duration
$u$	Constant output of an optical hard-limiter

$v$	Speed of light inside a fiber
$v'$	Threshold level of an optical hard-limiter
$W^e$	Waiting after retransmission states
$W^q$	Waiting after request states
$W^r$	Waiting after transmission states
$W^s$	Waiting after reception states
$w$	Code weight
$Y_i$	Photon count within weighted chip $i$
$Z$	Total number of received pulses
$z$	Interstation distance
$\beta$	Steady state system throughput
$\gamma$	Probability to receive an acknowledgement
$\Delta t_{chrom}$	Pulse spreading due to chromatic dispersion
$\Delta t_{modal}$	Pulse spreading due to modal dispersion
$\Delta\lambda$	Spectral line width of a light source
$\eta$	Protocol efficiency
$\theta$	Decision threshold
$\lambda$	Wavelength
$\lambda_a$	Auto-correlation constraint
$\lambda_c$	Cross-correlation constraint
$\lambda_o$	Zero dispersion wavelength
$\pi_n$	Stationary probabilities
$\sigma$	Probability to find a connection request
$\sigma_{b_j}^2$	Conditional variance of the decision variable $Y_j$
$\sigma_n^2$	Variance of thermal noise within a chip interval
$\tau$	Timeout duration

# ACRONYMS

APD	Avalanche Photodiode
ARQ	Automatic Repeat Request
BER	Bit Error Rate
CDMA	Code Division Multiple Access
CLSP	Channel Load Sensing Protocols
CRC	Cyclic Redundancy Check
CSMA	Carrier-Sense Multiple-Access
CSMA/CD	CSMA with Collision Detection
DC	Direct Current
EPA	Equilibrium Point Analysis
FBGs	Fiber Bragg Gratings
FFH-CDMA	Fast Frequency Hop CDMA
FTTB	Fiber To The Building
FTTC	Fiber To The Curb
FTTCab	Fiber To The Cabinet
FTTH	Fiber To The Home
IEEE	Institute of Electrical and Electronics Engineering
IM-DD	Intensity Modulation and Direct Detection
ISI	Intersymbol Interference
LAN	Local Area Network
LED	Light Emitting Diode
MAC	Media Access Control
MAI	Multiple Access Interference
OOCs	Optical Orthogonal Codes
OOK	On Off Keying
OSI	Open Systems Interconnection
PAC	Packet Avoidance Collision
PPM	Pulse Position Modulation
QOS	Quality Of Service
$R^3T$	Round Robin Receiver/Transmitter

SNR	Signal to Noise Ratio
WDMA	Wavelength Division Multiple Access

# CHAPTER 1

## INTRODUCTION AND THESIS SURVEYS

### Outline:

- **Introduction**
- **Contributions of the Thesis**
- **Organization of the Thesis**

# CHAPTER 1

## INTRODUCTION AND THESIS SURVEYS

### **1.1 Introduction**

While applications drive the development for faster and more efficient network technology, on the other hand network technology opens up the opportunity for the development of new applications. Applications that were not feasible or even imaginable a few years ago are now widely used. The most current example is the development of multimedia applications for the World Wide Web. Web browsers permit us to receive not only text-based information, but also audio and video from a wide variety of sources such as research institutions, governments, businesses, and individuals. These new applications are pushing the limits on current networks, since they require a great amount of bandwidth and have specific quality of service (QOS) requirements. The increasing demand makes imperative the use of some new technology that is not only capable of meeting today's demands but is also flexible to accommodate tomorrow's growth.

Fiber based optical communication networks offer an efficient way to meet these requirements [1]-[8]. Therefore, optical transmission has taken over in the backbone networks during the last decade and is continuously being deployed closer to the edge of the networks. In the access network, there is an increased interest in fiber to the home (FTTH), fiber to the building (FTTB), fiber to the curb (FTTC), and fiber to the cabinet (FTTCab) technologies. For access networks and local area networks (LANs), low cost is a very important factor and thus systems with low complexity must be proposed.

Spread spectrum signaling has been recently proposed to achieve multi-user capability in fiber-optic code division multiple access (CDMA) networks [9]-[11]. The main advantage of using CDMA in an optical network is that it allows a flexible multiple access method for asynchronous traffic with a graceful degradation at high interference. Furthermore, variable requirements on bit error rates (BER) can be satisfied by suitable choices of codes. An additional advantage is that some processing



can be moved into the optical domain, which is important since certain operations can be implemented with very low complexity using optical components. Because there are no standards or commercial implementations available for optical CDMA networks, the question of the best implementation method is still open. Furthermore, it is not clear whether CDMA is a suitable solution for optical networks. According to studies by Stok and Sargent, CDMA can offer a higher capacity than wavelength division multiple access (WDMA) for local area networks if noise is neglected [2]. Furthermore, CDMA can be efficiently used in conjunction with WDMA on multimedia communication networks where multiple services with different traffic requirements are to be integrated. However, when shot noise and thermal noise are taken into consideration, CDMA is much more sensitive to the signal to noise ratio than WDMA [3]. Therefore, it is not clear that the comparison will hold when also other noise types are taken into account.

One of the motivating factors for the work in this thesis was the small amount of research concerning the network or link layer of optical CDMA communication systems [4]-[8]. In this thesis focus will be mainly on protocols and solutions for LANs, but many of the principles can also be used for access networks.

## **1.2 Contributions of the Thesis**

As current network technologies evolve to an all optical largely passive infrastructure, design and implementation problems take on new significance and raise a number of challenging issues that require novel solutions. In [7], Shalaby has proposed an optical random access CDMA protocol called *round robin receiver/transmitter ( $R^3T$ )* protocol. This protocol is based on a go back- $n$  automatic repeat request (ARQ) and is suitable for only low population networks. In his analysis, Shalaby assumed that each node is equipped with a single buffer to store only a single message (the message that is being served); thus any arrival to a nonempty buffer was discarded. This of course gives rise to a blocking probability which was not studied and thus limits the system throughput. Also focus was oriented towards only multiple access interference (MAI), the effect of receiver's noise and other impairments were neglected.

This thesis makes the following contributions, focusing on the design and analysis of

MAC and link layer protocols for optical CDMA networks. The main contributions of the thesis work can be summarized as follows:

- 1- Studying the impact of the receiver's thermal noise on the performance of the  $R^3T$  protocol. Also the effect of light dispersion on limiting the user bit rate is considered. Chip-level receivers are considered in the analysis because of their high ability to overcome the effect of MAI.
- 2- Introducing a queuing subsystem to the  $R^3T$  protocol, namely increasing the number of available buffers. The steady state system throughput, the protocol efficiency, and the timeout probability are derived, simulated and compared with the previous results in [7]. Our results show that significant improvement in the performance of the  $R^3T$  protocol can be achieved by only adding a single buffer to the system.
- 3- Developing a new optical random access CDMA protocol based on a stop & wait ARQ. The performance of this protocol is evaluated in terms of the system throughput, the blocking probability, the protocol efficiency, and the average packet delay. Our results reveal that the proposed protocol outperforms the  $R^3T$  protocol in large population networks.

### **1.3 Organization of the Thesis**

Following the introduction in Chapter 1; which summarizes the motivation, objectives, and achievements in this research, Chapter 2 presents an overview of the physical layer of optical CDMA communication systems. Different CDMA encoding techniques and receiver structures are outlined. In Chapter 3, we give a quick review for the different MAC protocols that were proposed in literature. The link layer of an optical direct-detection CDMA packet network is then considered. Finally, we present a mathematical analysis for several proposed random access protocols in [6] and [7]. Chapter 4 is concerned with the major sources of limitations in optical CDMA systems. Both receiver noise and light dispersion in fibers are studied. Also the performance of the  $R^3T$  protocol in noisy environments and dispersive channels is investigated. The performance of the  $R^3T$  protocol with a queuing subsystem is discussed in Chapter 5. A mathematical model based on the equilibrium point analysis (EPA) is presented. In addition, the steady state system throughput, the protocol

efficiency, and the timeout probability are derived and evaluated under several network parameters and compared with the results in [7]. In Chapter 6, we propose a new optical random access CDMA protocol which is based on a stop & wait ARQ in order to reduce the complexity of the previously proposed protocols. The performance of this protocol is evaluated for different receiver structures and under different network parameters. Furthermore, the effect of the receiver thermal noise is analyzed. Finally, Chapter 7 presents the conclusions of this thesis and suggests directions for a further research in this area.

## **CHAPTER 2**

# **RESEARCH AND DEVELOPMENT IN OPTICAL CDMA COMMUNICATION SYSTEMS**

### **Outline:**

- **Introduction**
- **Basic Optical CDMA Communication Systems**
- **Optical CDMA Encoding - Decoding Techniques**
- **Various Optical CDMA Receivers**
- **Performance of Optical CDMA Receivers**

# CHAPTER 2

## RESEARCH AND DEVELOPMENT IN OPTICAL CDMA COMMUNICATION SYSTEMS

### **2.1 Introduction**

Over the last one to two decades, there has been a lot of interest and research in optical CDMA systems. More than 250 papers have been written in this area since 1985 [12]. A vast number of different schemes using time domain or frequency domain encoding approaches have been proposed [13]-[17]. Coherent and non-coherent manipulations of optical signals have been used in different proposals and various codes have been devised for optical CDMA systems. In this chapter, we try to give a general review of the previous work done in this field.

Also we consider different receiver structures proposed for fiber-optic CDMA systems [18], [19] and discuss their major strengths and drawbacks. The receiver structures introduced and studied here are those structures with minimum electronic processing. The main electronic functions used in these structures are integration and comparison with a threshold value. These are the simplest electronic functions that can be implemented with relatively high speeds. Other receiver structures can be introduced which massively benefit from electronic signal processing. Such receivers can employ for example pattern recognition or multi-user detection techniques to improve the performance of the systems. However, the intensive electronic processing required is not desirable for high-speed optical CDMA signal processing due to its complexity.

### **2.2 Basic Optical CDMA Communication Systems**

#### **2.2.1 System Architecture**

A typical fiber-optic CDMA communication system is best represented by an information data source followed by a laser when the information is in electrical

signal form, and an optical encoder that maps each bit of the output information into a very high rate optical sequence, which is then coupled into the single-mode fiber channel. At the receiver end, the optical pulse sequence would be compared to a stored replica of itself (correlation process) and to a threshold level at the comparator for the data recovery. In fiber-optic CDMA there are  $N$  such transmitter and receiver pairs (users). Figure 2.1 shows one such network in a star configuration. The set of the different fiber-optic CDMA pulse sequences essentially becomes a set of address codes or signature sequences for the network. One of the primary goals of optical CDMA is to extract data with the desired optical pulse sequence in the presence of all other users' optical pulse sequences.

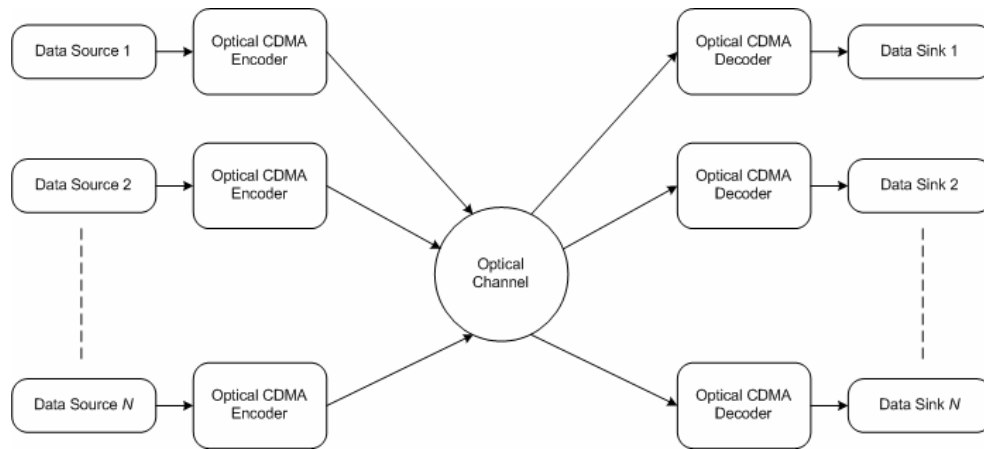


Fig. 2.1. Optical CDMA network configuration.

### **2.2.2 Optical Orthogonal Codes (OOCs)**

Central to any successful code division multiple-access scheme, whether electrical or optical, is the choice of the high rate sequences; namely, the signature sequences, on which the information data bits of different users is mapped. In CDMA, many asynchronous users occupy the same channel simultaneously. A desired user's receiver must be able to extract its signature sequence in the presence of other user's signature sequences. Therefore, a set of signature sequences that are distinguishable from time shifted versions of themselves and for which any two such signature sequences are easily distinguishable from each other is needed. The design of sequences with these properties for communication systems, such as spread-spectrum CDMA, ranging systems, radar systems, etc., has been a topic of interest to many

communications scientists and mathematicians in the last two decades [20]. These traditional codes cannot be used in optical CDMA systems. A new family of unipolar codes named Optical Orthogonal Codes (OOCs) has been proposed for optical CDMA systems by J. A. Salehi [9].

An optical orthogonal code is a family of (0,1) sequences with good auto- and cross-correlation properties, i.e., the autocorrelation of each sequence exhibits the 'thumbtack' shape and the cross-correlation between any two sequences remains low throughout. A family of OCC's is denoted by  $\phi(L, w, \lambda_a, \lambda_c)$  where  $L$  is the code length,  $w$  is the code weight,  $\lambda_a$  and  $\lambda_c$  are the auto-correlation and cross-correlation constraints, respectively. Thus, for any two sequences  $x, y \in \phi(L, w, \lambda_a, \lambda_c)$  we have:

- The auto-correlation function

$$R_{xx} = \sum_{n=0}^{L-1} x_n \cdot x_{n+l} \begin{cases} = w & \text{if } l = 0 \\ \leq \lambda_a & \text{if } l \neq 0 \end{cases} \quad (2.1)$$

- The cross-correlation function

$$R_{xy} = \sum_{n=0}^{L-1} x_n \cdot y_n \leq \lambda_c \quad (2.2)$$

For any OOC family, the number of codes cannot exceed a certain value (which is called the cardinality  $|C|$ ) depending on the code length, code weight and the maximum auto- and cross-correlation values. Traditionally,

$$\lambda_a = \lambda_c = 1 \quad \Rightarrow \quad |C| = \left\lfloor \frac{L-1}{w(w-1)} \right\rfloor, \quad (2.3)$$

where  $\lfloor x \rfloor$  denotes the largest integer not greater than  $x$ . This constraint on the code correlations guarantees minimal interference between the users at the expense of limiting the maximum number of codewords (subscribers). To increase the possible number of subscribers, we can relax a bit the constraint on the code correlations.

## **2.3 Optical CDMA Encoding - Decoding Techniques**

### **2.3.1 Time Domain Encoding Using Optical Delay Line Loops**

The first optical CDMA proposals were found in Hui [13] and in Prucnal [14], and [15]. It was intended as a multiple access protocol in a local area network (LAN).

Intensity modulation and direct detection (IM-DD) has been established as the most suitable signal modulation and detection scheme in optical communication systems. In order to preserve the simplicity of IM-DD, optical CDMA systems are designed very differently from their radio versions. In direct detection optical CDMA system, a spreading code or a signature sequence is used to spread the data signal. Each user in the system has its own sequence, and all signature sequences should be orthogonal.

The earliest optical CDMA proposals made use of optical delay line networks (Fig. 2.2) to encode a high-peak ultra-fast optical pulse into  $w$  low intensity pulses placed at the mark positions of the user's signature code. A similar delay line decoder network is used at the receiver to reconstruct the high-peak narrow pulse using conjugate delay lines. The decoding operation is an intensity correlation process.

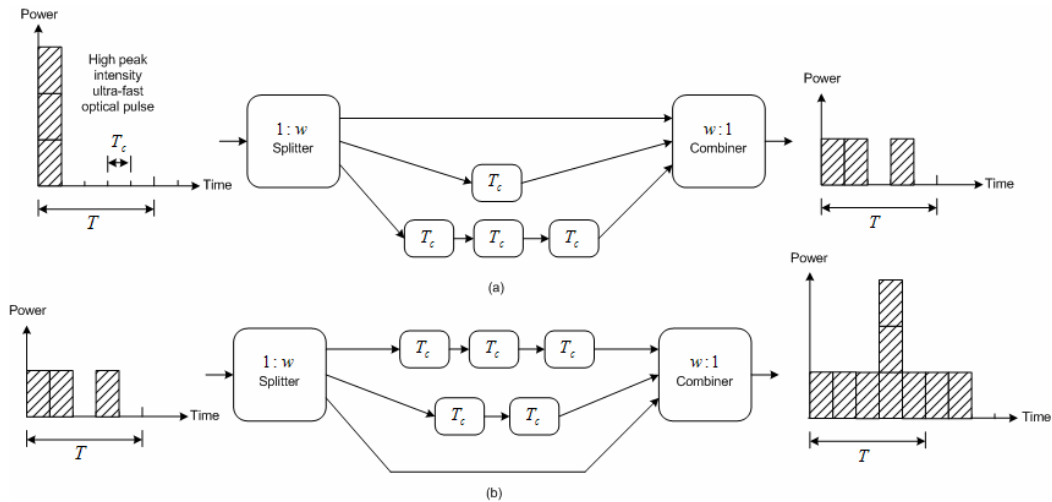


Fig. 2.2. Time domain optical CDMA encoding of high peak intensity ultra-short pulses using delay line loops: (a) Encoder, (b) Decoder.

Because of the effect of multiple access interference (MAI), the bit error rate (BER) is usually quite high and the number of allowable active users is very limited, [9]-[11], and [21]. The delay line encoder and decoder used are also very energy inefficient because of the splitting process. It is known that a splitting loss of  $10\log w$  dB is incurred when  $w$  branches are combined.

### 2.3.2 Spectral Intensity Encoding CDMA Systems

Zacarrin and Kavehrad first described this approach [16]. It is similar to the



coherent phase encoded system in the sense that the frequency components from a broadband optical source are resolved first. Each code channel then uses a spectral amplitude encoder to selectively block or transmit certain frequency components (as shown in Fig. 2.3).

A balanced receiver with two photodetectors is used as a part of the receiver. The receiver filters the incoming signal with the same spectral amplitude filter (called the direct filter) used at the transmitter as well as its complementary filter. The outputs from the filters are detected by the two photodetectors connected in a balanced fashion. For an unmatched transmitter, half of the transmitted spectral components will match the direct filter and the other half will match the complementary filter. Since the output of the balanced receiver represents the difference between the two photodetector outputs, unmatched channels will be cancelled, while the matched channel is demodulated. Since there is a subtraction between the two photodetectors, it is possible to design codes so that full orthogonality can be achieved with the non-coherent spectral intensity encoding approach. In principle, orthogonality eliminates the crosstalk from other users.

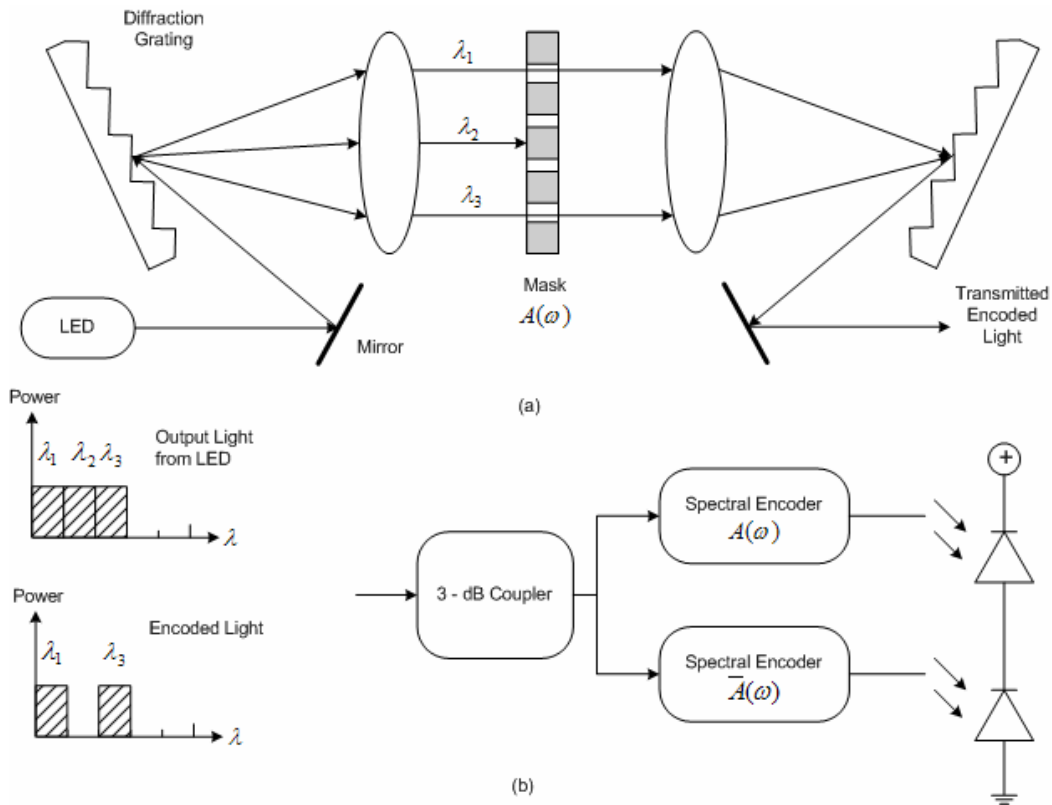


Fig. 2.3. Spectral intensity encoded optical CDMA system: (a) Encoder, (b) Decoder.

Bipolar signaling can also be obtained by sending complementary spectrally encoded signals [22]. There is a 3-dB power advantage for bipolar signaled systems. However, the performance of this type of systems is spoiled by the intensity fluctuations arising from the beating between optical waves at the same wavelength, but coming from different users, which we call speckle noise.

### 2.3.3 Optical Fast Frequency Hop CDMA (FFH-CDMA)

In frequency hop systems, the input signal is encoded in both time and frequency domains. This goal can be achieved using a series of Fiber Bragg Gratings (FBGs) arranged according to the signature code (hop pattern). The spacing between any two FBGs is adjusted such that the two way propagation time is equivalent to one chip duration. Figure 2.4 illustrates the operation of the basic FFH-CDMA system. The tuning of each FBG at the transmitter will determine the code used. At the receiver, this order is reversed to achieve the decoding function, i.e., matched filtering. The FFH-CDMA requires two dimensional codes that represent the hopping sequence between wavelengths in successive time chips, [23] and [24].

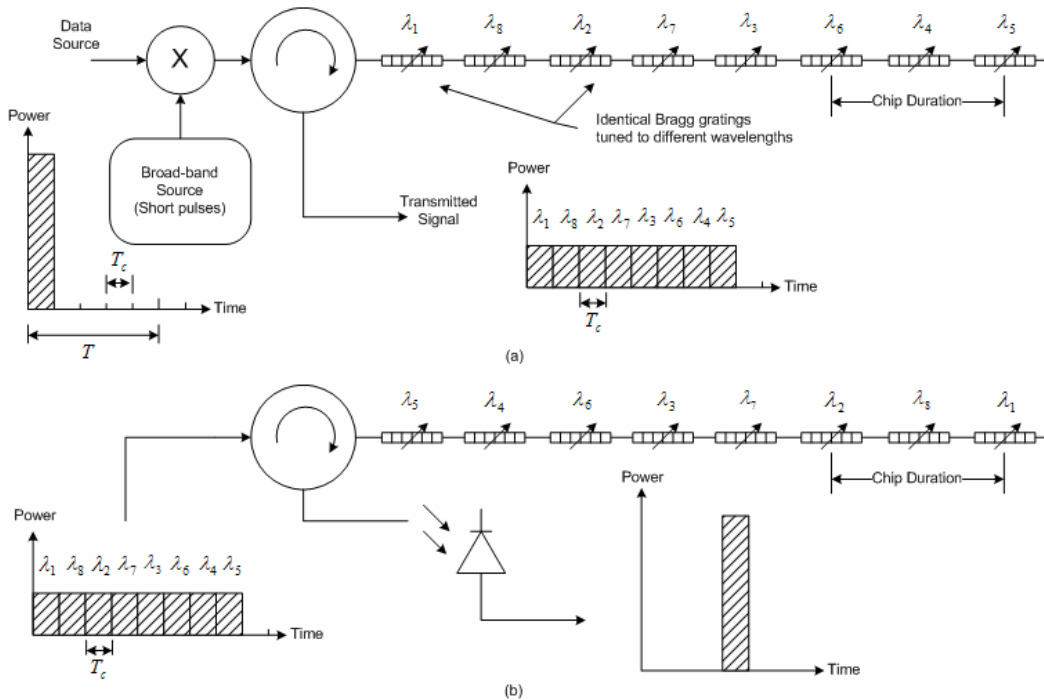


Fig. 2.4. Optical FFH-CDMA system: (a) Encoder, (b) Decoder.

### **2.3.4 Important Design Issues in Optical CDMA**

As pointed out before, in order to achieve efficient spectral usage and to obtain the good performance that the telecommunications community is striving for, it is important to have systems with full orthogonality so that co-channel crosstalk can be minimized. To achieve full orthogonality, while preserving the simplicity of intensity detection, is not straightforward. This forms the main challenge in this research. All optical CDMA networks are generally broadcast and select systems. In a broadcast and select network, the receiver receives the signals from all the transmitters. Ideally, all the unmatched channel signals are cancelled due to orthogonal encoding. Nevertheless, a receiver detects the optical energy from the unmatched transmitters. In spite of signal orthogonality, shot noise does not subtract but is always additive, and is increasing with the total detected signal intensity. Therefore, detecting the signals from all users gives rise to cumulative shot noise, which amounts to cross-talk and interference. Other important issues in the design of optical CDMA systems are the thermal noise and light dispersion in fibers, which will be studied in Chapter 4. Our first contribution in this dissertation is to take the effect of the thermal noise and light dispersion on an optical random access CDMA protocol for LANs.

### **2.4 Various Optical CDMA Receivers**

In this section, we will consider different receiver structures proposed for fiber-optic CDMA and discuss their major strengths and drawbacks. The receiver structures introduced and studied here are those structures with minimum electronic processing. The main electronic functions used in these structures are integration and comparison against a threshold value. These are the simplest electronic functions that can be implemented with relatively high speeds. Other receiver structures can be introduced which massively benefit from electronic signal processing. Such receivers can employ for example pattern recognition or multi-user detection techniques to improve performance of the systems. However, the intensive electronic processing required is not desirable for high-speed optical CDMA signal processing due to its complexity.

### 2.4.1 Correlation Receivers

The optical CDMA correlation receiver was first introduced by Salehi [10]. Simply, this receiver acts as an optical matched filter that collects the spreaded optical power from mark positions and compares it to a certain threshold.

#### 2.4.1.1 Passive Correlation Receivers

In this receiver, the received signal will be compared against the transmitter signature sequence, Fig. 2.5. The whole receiver performs as a matched filter to the input signal. Incoming signal will be divided into  $w$  equal parts each undergoing a time delay complement to one of the delay elements of the CDMA encoder, to form a filter inversely matched to the transmitted signature sequence. The output of these delay lines will be combined and after photodetection and integration, the output voltage will be sampled at the end of each bit interval. If the transmitted bit is '1', an optical pulse will appear at the sampling chip-time with a power that is  $w$  times the power of each incoming chip pulse.

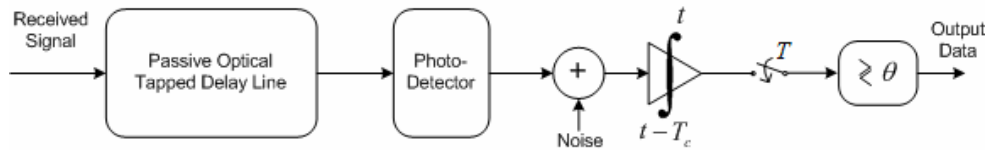


Fig. 2.5. Passive correlator structure.

The major strength of this design is its passive optical correlator. However, this receiver needs a very high-speed electronic circuitry which should operate at a chip-rate speed and thus limits this structure, and other similar structures using passive correlator, only to relatively low-speed applications. Another drawback of this system is the strong power loss in optical splitters. The original pulse will split to  $w$  parts at the encoder and then each pulse will be divided to  $N$  parts at the star coupler and again to  $w$  parts at the optical decoder. Therefore, the energy of the original transmitter encoded laser pulse, will be divided to  $N.w^2$  and forms the energy of each chip pulse at the receiver.

Hence, the transmitter should produce strong enough pulses so that the decision variable has enough energy for reliable decision. The sampled value, which

is the output voltage of an integrator, will be compared against a threshold level  $\theta$  and an estimation of the transmitted bit will be given.

#### 2.4.1.2 Active Correlation Receivers

This receiver performs the same operation as the passive correlation receiver, but an active multiplier that can be implemented for example using an acousto-optic modulator will perform code multiplication, Fig. 2.6. Therefore, the integration time after the photodetector should be extended to  $T$  (bit duration) seconds and this receiver has a lower speed electronic design comparing with passive correlation receiver, but it uses a more complicated optical technology. Although longer integration times makes the electronic circuits more feasible, it increases the contribution of collected noise in decision variable.

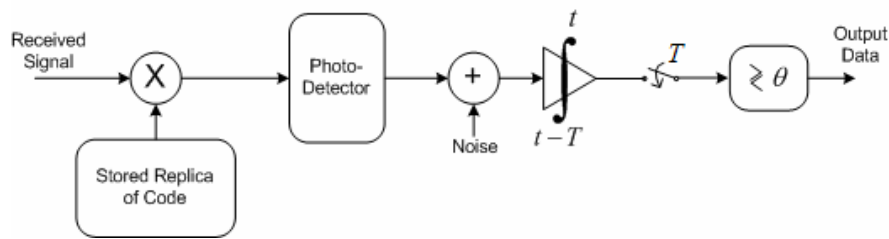


Fig. 2.6. Active correlator structure.

Using an active multiplier, only pulses at mark positions will enter the receiver and therefore the integration should be performed over the entire bit duration. Therefore, this receiver needs electronic circuitry in bit-rate speed, not chip-rate speed, which is more feasible than electronic circuit in passive correlation structure. This structure is also more efficient regarding required power and does not split the received power as in passive correlator. However, the receiver needs an optical multiplier which itself has speed limitations and is a costly device.

#### 2.4.1.3 Correlation Receivers with Optical Hard-Limiters

This structure removes many interference patterns using an optical hard-limiter placed before the correlation receiver [11]. The characteristics of an optical hard-limiter are represented in Fig. 2.7, where we have plotted the relation between output power and input power  $P_{out}$  and  $P_{in}$ , respectively.

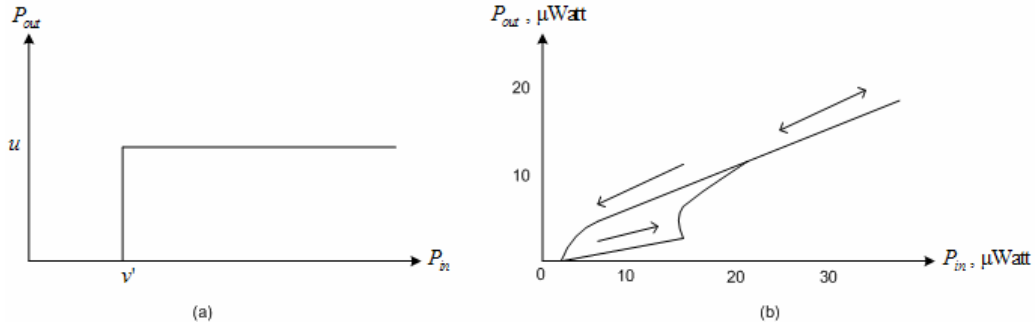


Fig 2.7. Optical hard-limiters' characteristics: (a) An ideal optical hard-limiter, (b) A practical optical hard-limiter.

The transfer function of an ideal optical hard-limiter can be written as [18]:

$$g(x) = \begin{cases} u & \text{if } x \geq v' \\ 0 & \text{otherwise} \end{cases}, \quad (2.4)$$

where  $x$  denotes the input power,  $g(x)$  is the output power,  $v'$  is the threshold level of the optical hard-limiter and  $u$  is a constant. The function of an optical hard-limiter at the input of the correlator is to limit the energy of input pulses to the equivalent of one pulse. Therefore, if a transmitted bit is '0' and there are several interfering pulses at a specified mark position, the optical hard-limiter, limits the incoming optical energy to the energy of just one pulse. Therefore, the number of input pulses to the correlator is limited to one pulse at each chip time position, thus considerably reduces the possibility of detecting '1' when '0' has been transmitted. For example, if  $w = 4$  and a transmitted bit is '0', assuming that the number of received pulses at four positions are (3, 2, 0, 0). A correlation receiver adds these numbers, compares the result with the code weight, and erroneously decides that data bit '1' is transmitted. However, a hard-limiter converts the interference pattern to (1, 1, 0, 0) allowing the correlator a sufficient margin to make a correct decision about the transmitted bit.

To enhance the performance of the correlation receiver with single hard-limiter, Ohtsuki [25] proposed an optical CDMA correlation receiver with double optical hard-limiters. Double optical hard-limiter structure removes many interference patterns, which will pass through a simple optical hard-limiter. The first hard limiter clips the energy of incoming pulses, but the second hard-limiter removes the stray pulses produced by passive optical correlator (delay lines) not contributing to the decision criteria.

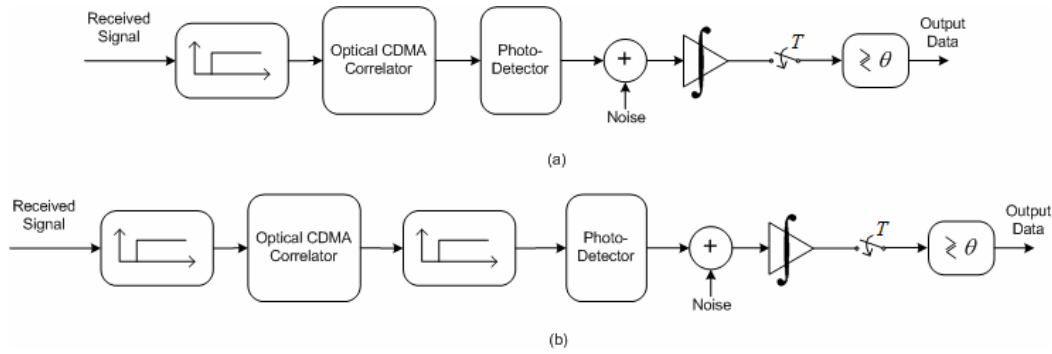


Fig.2.8. (a) Optical correlation receiver with hard-limiter, (b) Optical correlation receiver with double hard-limiters.

Both types of correlation receivers with hard-limiters are shown in Fig. 2.8. Correlation receivers with hard-limiters may be implemented either in a passive or an active structure.

## 2.4.2 Chip-Level Receivers

In [26], Shalaby proposed a new optical CDMA receiver, called the chip-level receiver. Both On-Off Keying (OOK) and pulse-position modulation (PPM) schemes, that utilize this receiver, were investigated. The key difference between chip-level and other receivers is that the chip-level receiver decision rule depends on the photon counts in each mark position, i.e., to decide data bit '1' the photon count in each mark position should exceed a certain threshold. Results demonstrated that significant improvement in the performance is gained when using the chip-level receiver in place of the correlation one. Nevertheless, the complexity of this receiver is independent of the number of users, and therefore, it is much more practical than the optimum receiver.

### 2.4.2.1 *High-Speed Chip-Level Receivers*

In this receiver, Fig. 2.9a, decision is based on  $w$  partial decision random variables. Signal will be sampled at each chip pulse interval and a '1' bit will be detected when at least one pulse is present at all chip pulse positions and a single missed chip pulse at the designated code pulse position is sufficient to detect '0' bit. It can be shown that if no noise is present, a hard-limiter receiver performs as well as a

chip-level detector. This receiver requires a fast electronic design, since the receiver needs to integrate  $w$  times the incoming signal on  $T_c$  intervals during a bit time. It has been shown that if only Poisson shot-noise is considered, the performance of this receiver rapidly approaches the performance of the ideal double hard-limiter receiver [26].

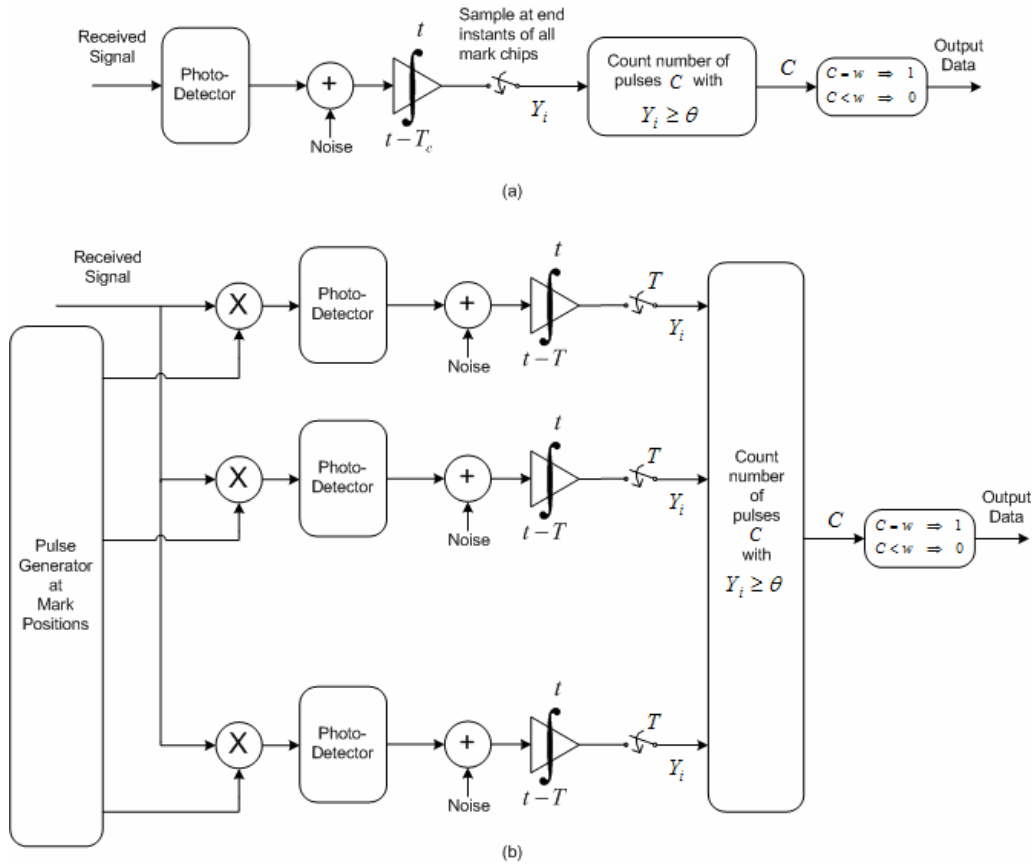


Fig. 2.9. (a) High-speed chip-level receiver, (b) All optical chip-level receiver.

### 2.4.2.2 All Optical Chip-Level Receivers

To make full use of the vast bandwidth available to the optical network, an equivalent all optical chip-level receiver that requires a lower speed electronic design (shown in Fig. 2.9b) was also presented by Shalaby, [26]. The received optical signal is sampled optically at the correct mark chips. Each sampled signal is then photodetected and integrated over the entire bit duration ( $T = LT_c$ ) and is further sampled electronically by the end of the bit duration. If each sampled signal is not less than  $\theta$ , a data bit '1' is declared to be transmitted. Otherwise a '0' is declared.



### 2.4.3 Comparison of Various Optical CDMA Receivers

Many researches were performed in order to compare the performance of various optical CDMA receivers. In this subsection, we focus on both the chip-level receivers and the correlation receivers with double optical hard-limiter. Zahedi and Salehi presented a comparison depending on the bit error probability [19], whereas Shalaby, in [18] has extended this comparison and considered the effect of the receiver complexity and the throughput capacity.

A comparison of the different receiver designs and their relative strengths and weaknesses is summarized in Table 2.1.

Table 2.1. Comparison of various optical CDMA receiver structures.

Receiver Design	Integration Time	Electronic Bandwidth	Receiver Complexity	Notes on Overall Usability and relative strength/weakness
(1) Passive Correlation	$T_c$	Large	Low	Low-speed applications, inefficient power consumption, inexpensive.
(2) Active Correlation	$T$	Low	Moderate	High-speed applications, relatively expensive design.
Optical Hard-limiter + (1)	$T_c$	Large	Moderate	Low-speed applications, depends on the availability of Hard-limiter.
Optical Hard-limiter + (2)	$T$	Low	Moderate	High-speed applications, depends on the availability of Hard-limiter.
Double Hard-limiter + (1)	$T_c$	Large	Moderate	Low-speed applications, Excellent performance, relatively inexpensive.
Double Hard-limiter + (2)	$\geq T_c, \leq T$	Medium	High	Medium to high-speed applications, inefficient power consumption.
High Speed Chip-level	$T_c$	Large	Low	Low-speed applications, efficient power consumption.
All-optical Chip-level	$\geq T_c, \leq T$	Medium	High	Unusable.

Now, we compare the performance in terms of the bit error probability and we present some results obtained by Shalaby [18]. It is important to mention that chip-level receivers are much simpler and their performances are competitive with that of traditional correlation receivers with double optical hard-limiters. Further, the throughput capacity of chip-level systems can be increased by almost a factor of 3.4 when increasing the code-correlation constraint from one to two [18].

The error probabilities for both receivers are plotted in Fig. 2.10, versus the average received photons per bit, for different system parameters. An optimum threshold has been used for the double-hard-limiters correlation receiver, whereas a suboptimum threshold has been used for the chip-level receiver. It is noticed that although the performance of the double-hard-limiter correlator is slightly better, it is expected to be worse than that of the chip-level receiver in practice, since the properties of the ideal sharp hard-limiter are impossible to practically realize. The error probabilities for the optimum receiver, and correlation receivers without hard-limiters and with a single hard-limiter, are also plotted in the same figure for convenience.

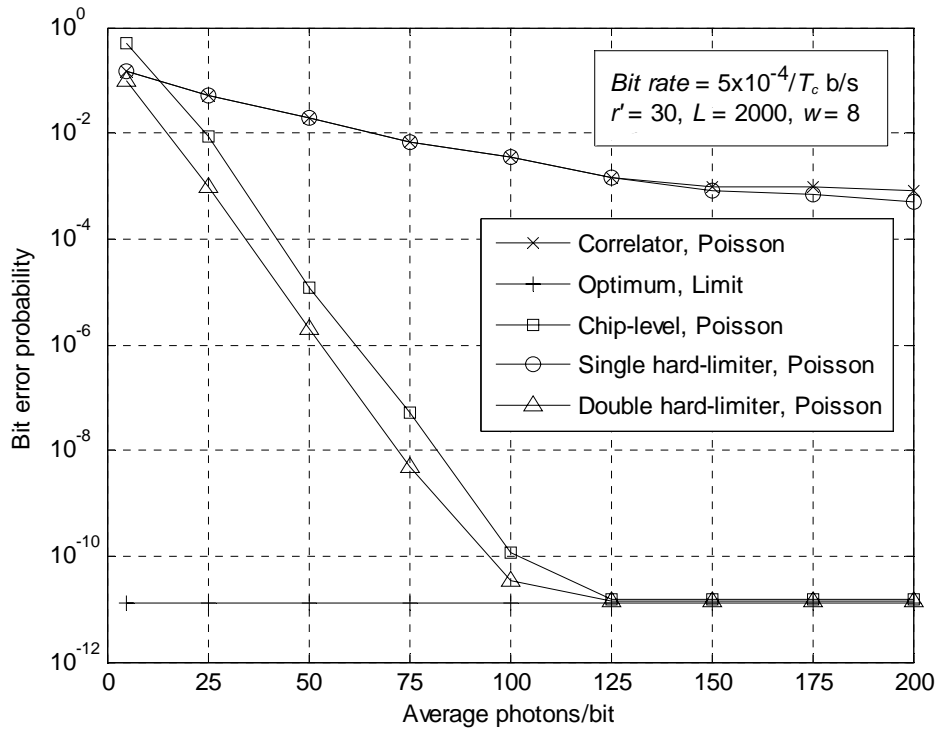


Fig. 2.10. Bit error probabilities for OOK-CDMA receivers, under a Poisson shot-noise-limited assumption, versus average photons/bit.

## 2.5 Performance of Optical CDMA Receivers

In this section, we will evaluate the performance of optical CDMA receivers in terms of packet success probability. For convenience and sake of comparison, we will evaluate the packet success probability for both chip-level receivers and correlation

receivers without optical hard-limiters. In this analysis, shot noise and thermal noise are taken to be of negligible power compared to the signal; we focus our attention on the influence of MAI. The effect of shot and thermal noise may be added in cases in which physical noise sources are expected to be of interest [27]. Optical beat noise among adjacent channels is also neglected. Optical orthogonal codes are used as the users' signature codes, with a correlation constraint of  $\lambda_a = \lambda_c = 1$ . That is, users of different codes interfere with each other by one chip at most. On the other hand, users of same code interfere with each other by 0, 1, or  $w$  chips. We consider the chip synchronous case which gives an upper bound of bit error probability [10].

### 2.5.1 Correlation Receivers without Hard-Limiter

Assuming that there are  $r' \in \{1, 2, \dots, N\}$  active users in the network at a given time slot, we define  $k \in \{0, 1, 2, \dots, r'-1\}$ , such that  $k = \sum_{i=1}^w k_i$ , and  $m \in \{0, 1, \dots, r'-1-k\}$  as the number of users that interfere with the desired user at exactly 1 chip and  $w$  chips, respectively;  $k_i$  denotes the number of users that interfere with the desired user at weighted chip  $i$ ,  $i \in \{1, 2, \dots, w\}$ .

Let  $p_1$  and  $p_w$  denote the probability of 1 and  $w$  chip-interferences, respectively, between two users, then [6]:

$$p_w = \frac{1}{L} \cdot \frac{1}{|C|} = \frac{1}{L} \cdot \left[ \frac{L-1}{w(w-1)} \right]^{-1} \quad (2.5)$$

$$p_1 = \frac{w^2}{L} - wp_w.$$

Assuming equally-likely binary data bits ( $\Pr\{0\} = \Pr\{1\} = 1/2$ ), the conditional bit-correct probability  $P_{bc}(m, k)$  is calculated as follows. The correlation receiver decides a data bit '1' was transmitted if the total received pulses  $Z$  from all weighted chips is greater than or equal to a threshold  $\theta = w$ . A data bit '0' is decided otherwise:

$$\begin{aligned} P_{bc}(m, k) &= \Pr\{\text{a bit success} \mid m, k\} \\ &= \frac{1}{2} \Pr\{\text{a bit success} \mid m, k, 1 \text{ was sent}\} \\ &\quad + \frac{1}{2} \Pr\{\text{a bit success} \mid m, k, 0 \text{ was sent}\} \end{aligned}$$

$$\begin{aligned}
&= \frac{1}{2} \Pr\{Z \geq w \mid m, k, 1 \text{ was sent}\} + \frac{1}{2} \Pr\{Z < w \mid m, k, 0 \text{ was sent}\} \\
&= \frac{1}{2} + \frac{1}{2} \Pr\{\text{all } m \text{ users send 0s and } Z < w \mid m, k, 0 \text{ was sent}\} \\
&= \frac{1}{2} + \frac{1}{2} \cdot \frac{1}{2^m} \cdot \frac{1}{2^k} \sum_{i=0}^{w-1} \binom{k}{i}.
\end{aligned} \tag{2.6}$$

Considering a packet of length  $K$  bits, the conditional packet success probability for the correlation receiver is thus

$$P_S(r' | m, k) = [P_{bc}(m, k)]^K = \left[ \frac{1}{2} + \frac{1}{2} \cdot \frac{1}{2^m} \cdot \frac{1}{2^k} \sum_{i=0}^{w-1} \binom{k}{i} \right]^K. \tag{2.7}$$

Since the interference can be modeled as a random variable having a multinomial distribution [18], the packet success probability given  $r'$  active users is

$$\begin{aligned}
P_S(r') &= \sum_{k=0}^{r'-1} \sum_{m=0}^{r'-1-k} \frac{(r'-1)!}{k!m!(r'-1-m-k)!} \cdot p_1^k p_w^m (1-p_1-p_w)^{r'-1-m-k} \\
&\quad \cdot \left[ \frac{1}{2} + \frac{1}{2} \cdot \frac{1}{2^m} \cdot \frac{1}{2^k} \sum_{i=0}^{w-1} \binom{k}{i} \right]^K.
\end{aligned} \tag{2.8}$$

### 2.5.2 Chip-Level Receivers

This case differs from that of the correlation receiver in the bit decision rule [26]. In our analysis, we select  $\theta = 1$  as a suboptimum threshold. Of course the obtained results form an upper bound (with respect to the bit error probability) of optimum chip-level receiver "with optimum  $\theta$ ". Let  $Y_i$ ,  $i \in \chi$ ,  $\chi \in \{1, 2, \dots, w\}$  be the photon count collected from marked chip  $i$ . Since we have  $r'$  active users, there are  $r'-1$  interfering users to the desired one. Out of these users, let  $m$  users interfere with the desired user at  $w$  chips and  $k$  users interfere with it at exactly 1 chip. Further, let  $\bar{k} = (k_1, k_2, \dots, k_w)$  be the interfering vector having a multinomial distribution. We evaluate the bit-correct probability as follows.

$$\begin{aligned}
P_{bc}(m, \bar{k}) &= \Pr\{\text{a bit success} \mid m, \bar{k}\} \\
&= \frac{1}{2} \Pr\{\text{a bit success} \mid m, \bar{k}, 1 \text{ was sent}\} \\
&\quad + \frac{1}{2} \Pr\{\text{a bit success} \mid m, \bar{k}, 0 \text{ was sent}\}
\end{aligned}$$

$$\begin{aligned}
&= \frac{1}{2} \Pr\{Y_i \geq 1 \forall i \in \mathcal{X} \mid m, \bar{k}, 1 \text{ was sent}\} \\
&\quad + \frac{1}{2} \Pr\{Y_i = 0, \text{some } i \in \mathcal{X} \mid m, \bar{k}, 0 \text{ was sent}\} \\
&= \frac{1}{2} + \frac{1}{2} \Pr\{\text{all } m \text{ users send 0s and } Y_i = 0, \text{some } i \in \mathcal{X} \mid m, \bar{k}, 0 \text{ was sent}\} \\
&= \frac{1}{2} + \frac{1}{2} \cdot \frac{1}{2^m} \left( \sum_{i=1}^w \frac{1}{2^{k_i}} - \sum_{i=1}^{w-1} \sum_{j=i+1}^w \frac{1}{2^{k_i+k_j}} + \dots + (-1)^{w-1} \frac{1}{2^k} \right),
\end{aligned} \tag{2.9}$$

where we have used the inclusion-exclusion property to justify last equality. The packet success probability given  $r'$  active users is thus expressed as follows

$$\begin{aligned}
P_S(r') &= \sum_{k=0}^{r'-1} \sum_{m=0}^{r'-1-k} \frac{(r'-1)!}{k!m!(r'-1-m-k)!} \cdot p_1^k p_w^m (1-p_1-p_w)^{r'-1-m-k} \\
&\quad \cdot \sum_{\substack{k_1, k_2, \dots, k_w: \\ k_1 + \dots + k_w = k}} \frac{k!}{k_1! \dots k_w!} \cdot \left(\frac{1}{w}\right)^k \\
&\quad \cdot \left[ \frac{1}{2} + \frac{1}{2^{m+1}} \left( \sum_{i=1}^w \frac{1}{2^{k_i}} - \sum_{i=1}^{w-1} \sum_{j=i+1}^w \frac{1}{2^{k_i+k_j}} + \dots + (-1)^{w-1} \frac{1}{2^k} \right) \right]^K
\end{aligned} \tag{2.10}$$

### 2.5.3 Simulation Results

The packet success probability has been evaluated for both correlation receivers without hard-limiters and chip-level receivers for different network parameters. Our results are plotted in Figs. 2.11-2.13. We have used OOCs having a unity correlation constraint and a code weight  $w = 3$  in all figures. Table 2.2 shows examples of these codes [9].

In Fig. 2.11, the packet success probability has been plotted against the number of active users for different packet lengths,  $K \in \{20, 500\}$  bits. A code length of  $L = 31$  was selected. A general trend for the curves can be noticed; as the number of active users in the network increases, the effect of the MAI also increases and hence the packet success probability decreases. It can also be seen that the performance of chip-level receivers is not affected seriously when changing the packet length, whereas for correlation receivers, for longer packets there will be higher risks of errors. Finally, chip-level receivers perform better than correlation receivers irrespective of the packet length.

Table 2.2. Examples of optimal  $(L,3,1,1)$  optical orthogonal codes.

$L$	Optimal $(L,3,1,1)$ codes
7	{0, 1, 3}
13	{0, 1, 4}, {0, 2, 7}
19	{0, 1, 5}, {0, 2, 8}, {0, 3, 10}
25	{0, 1, 6}, {0, 2, 9}, {0, 3, 11}, {0, 4, 13}
31	{0, 1, 7}, {0, 2, 11}, {0, 3, 15}, {0, 4, 14}, {0, 5, 13}
37	{0, 1, 11}, {0, 2, 9}, {0, 3, 17}, {0, 4, 12}, {0, 5, 18}, {0, 6, 12}
43	{0, 1, 19}, {0, 2, 22}, {0, 3, 15}, {0, 4, 13}, {0, 5, 16}, {0, 6, 14}, {0, 7, 17}

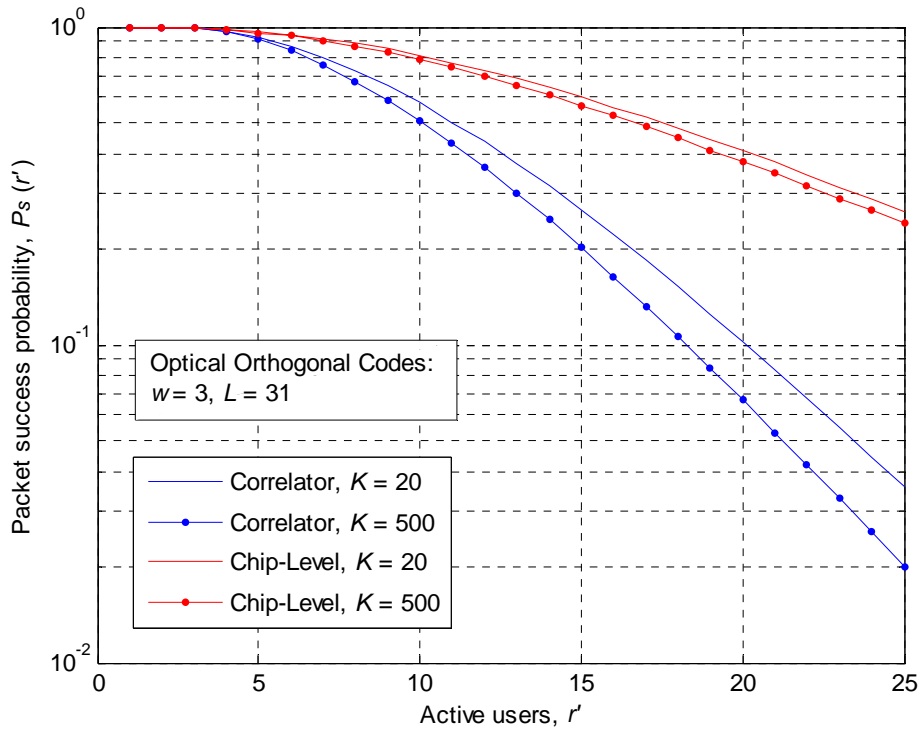


Fig. 2.11. Packet success probability versus number of active users for different packet sizes.

We have plotted the packet success probability versus the number of active users and the code length for both types of receivers in Figs. 2.12 and 2.13. A packet length of  $K = 127$  bits is imposed in the simulation [7]. The results show that the performance of both receivers is better for longer codes and for small population networks. Also it can be inferred that the chip-level receivers can tolerate the effect of MAI more than correlation receivers without hard-limiters.

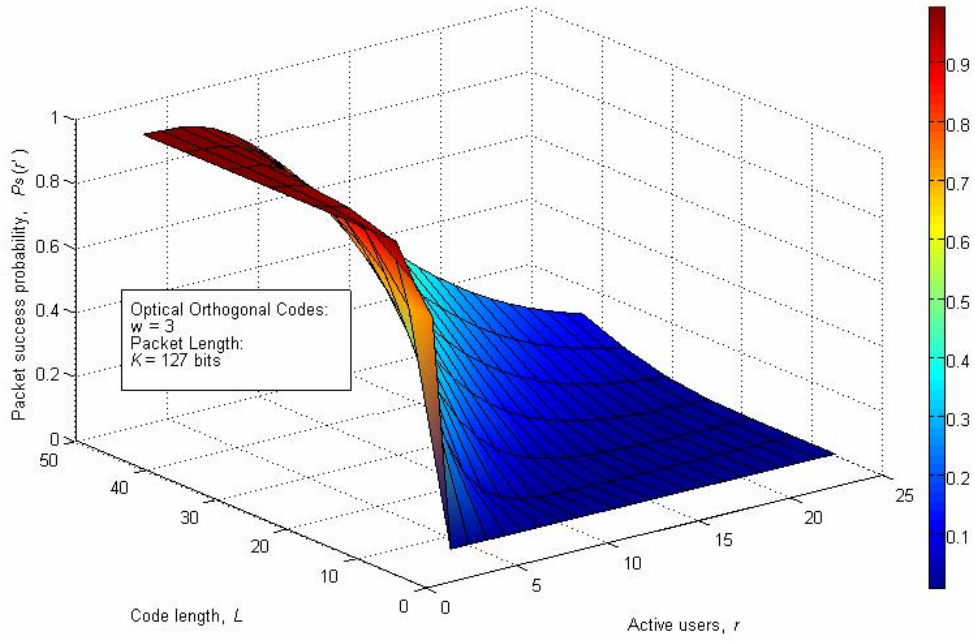


Fig. 2.12. Packet success probability versus number of active users and code length for correlation receivers.

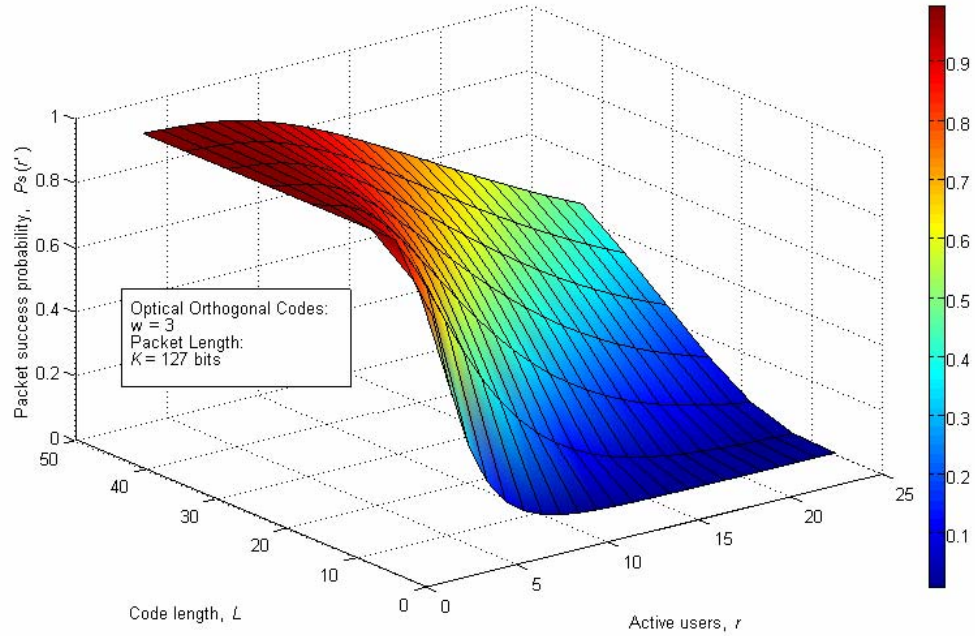


Fig. 2.13. Packet success probability versus number of active users and code length for chip-level receivers.

#### **2.5.4 Conclusions**

We have presented in this section the performance of various optical CDMA receivers. We have considered the effect of MAI and derived the packet success probability for both correlation receivers without optical hard-limiters and chip-level receivers, and then we have compared the results. The following concluding remarks can be extracted from the results:

- 1- Chip-level receivers are preferred over conventional correlation receivers. They have better ability to overcome the effect of MAI, and thus can be used in larger population networks.
- 2- The performance of both chip-level receivers and correlation receivers decreases significantly as the number of active users in the network increases and for short codes.
- 3- There emerges a high need to design a robust data link layer and MAC protocols for optical CDMA networks that ensure a fair access to the network.



# CHAPTER 3

## OPTICAL CDMA RANDOM ACCESS PROTOCOLS FOR FUTURE LOCAL AREA NETWORKS

### Outline:

- Introduction
- Background and Basic Information
- Optical CDMA Protocols with & without Pretransmission Coordination
- Round Robin Receiver/Transmitter ( $R^3T$ ) Protocol

## CHAPTER 3

# OPTICAL CDMA RANDOM ACCESS PROTOCOLS FOR FUTURE LOCAL AREA NETWORKS

### **3.1 Introduction**

Optical fibers have a huge transmission capacity. On the other hand optical technology is still in its infancy, and conversions between electrical and optical environment are relatively slow compared to the transmission capacity. Thus, in optical networks the processing power, instead of bandwidth, is the limiting factor. Therefore, the requirements for the media access control (MAC) protocol are different in the optical network than in the traditional electronic network.

In this chapter, we start by giving a quick review for the different MAC protocols that were proposed in literature [28]-[32]. The link layer of an optical direct-detection CDMA packet network is then considered. We present the previous work concerning optical CDMA networks and analyze several random access protocols. In [6], Shalaby proposed two different protocols (Pro 1 and Pro 2), that need pretransmission coordination. A variation of the second protocol, that does not need pretransmission coordination, is also discussed. These protocols are concerned with different techniques for assigning spreading codes to users. However, the effect of multi-packet messages, connection establishment and corrupted packets haven't been taken into account. Recently, Shalaby [7] has developed a new protocol called round robin receiver/transmitter ( $R^3T$ ) protocol that has solved some of the above problems. The main issue in this chapter is concerned with the work in [7]; we will extend this work and derive an expression for calculating the blocking probability (The probability that an arrival is blocked).

### **3.2 Background and Basic Information**

The MAC layer exists just above the physical layer in the Open Systems Interconnection (OSI) model and the IEEE 802 reference model. It is designed to

ensure orderly and fair access to a shared medium. It manages the division of access capacity among the different stations on the network. A good MAC protocol should be:

- Efficient: There should be high data throughput and packets should not experience large transfer delays.
- Fair: Each station should have equal access to the medium.
- Simple: The implementation of the MAC protocol should not be so complex that it requires powerful hardware or long processing times that impair performance.

These conflicting requirements have been a challenge to MAC protocol designers ever since the development of the ALOHA protocol in the 1960s. A large amount of research has been performed in this area, which has led to many solutions, implementations and standards. Despite this extensive research effort, there is still a strong need for MAC research [29], and [30].

### **3.2.1 Traditional Random Access Protocols**

The original single channel random access protocol is the ALOHA protocol, where transmission is done with no regard to other nodes. If two messages from different nodes overlap in time, both are corrupted. Systems in which multiple users share a common channel in a way that can lead to conflicts are widely known as contention systems. Several protocols are more or less pure improvements of the ALOHA protocol, e.g., Slotted ALOHA, CSMA (Carrier-Sense Multiple-Access), and CSMA/CD (CSMA with Collision Detection). Common to the random access protocols is that they do not perform well at high traffic loads owing to the increased probability of collision.

#### **3.2.1.1 Pure ALOHA**

This is the conventional form of access in networks. There is no explicit media access protocol. The stations are transmitting their messages asynchronously without any observation of the channel traffic. There will be collisions of course and faulty packets must be retransmitted until error free reception. Retransmissions occur after the stations wait a random amount of time to avoid repeated collisions.

### 3.2.1.2 Slotted ALOHA

In slotted ALOHA, all nodes are synchronized and transmissions are allowed to be started only at the beginning of a time slot. The vulnerable period will be reduced from twice the packet length for the case of pure ALOHA to exactly the packet length. In this way, the probability of collision is reduced and the throughput is doubled at the expense of system complexity.

The relation between the throughput (normalized to the channel capacity) and the offered traffic (transmission attempts per packet time) is shown in Fig. 3.1 for both pure ALOHA systems and slotted ALOHA systems [33].

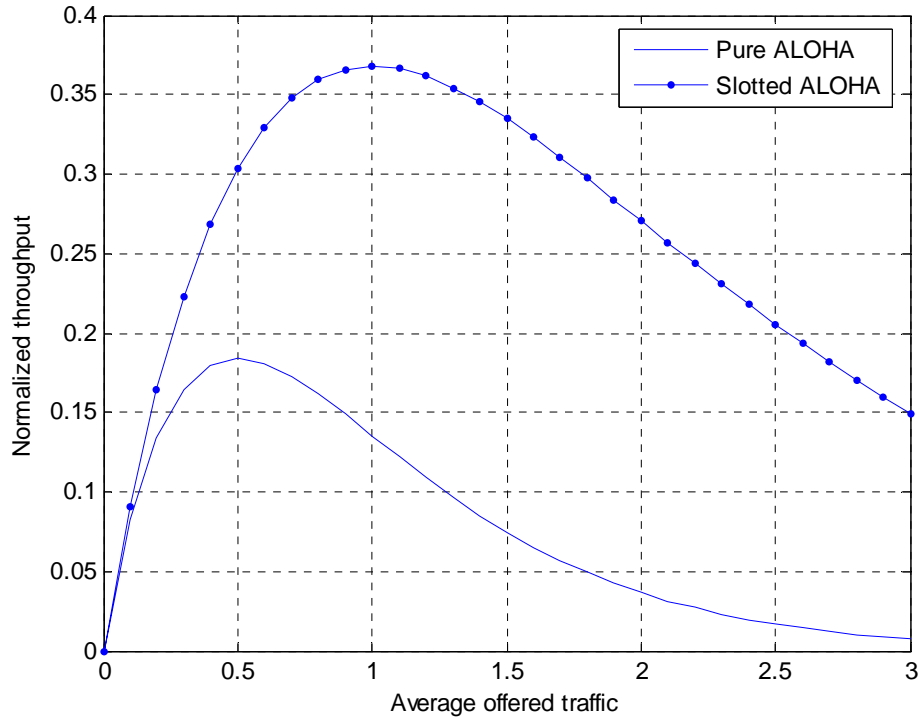


Fig. 3.1. Normalized throughput versus offered traffic for ALOHA systems.

It can be inferred that the best we can hope for is a channel utilization of 18 percent for pure ALOHA systems and 37 percent for slotted ALOHA systems. This result is not very encouraging, but with everyone transmitting at will, we could hardly have expected a 100 percent success rate.

### **3.2.1.3 CSMA and CSMA/CD**

In both pure and slotted ALOHA, a node's decision to transmit is made independently of the activity of the other nodes attached to the broadcast channel. In particular, a node neither pays attention to whether another node happens to be transmitting when it begins to transmit, nor stops transmitting if another node begins to interfere with its transmission.

In CSMA, the transmission medium is sensed before transmission starts, if the channel load is below a certain threshold the transmission starts with different (persistent) strategies [32]. Otherwise, the transmitter waits until the load falls below the threshold. If a collision occurs, the medium is busy for the whole duration of the corrupted transmissions. This is avoided in the CSMA/CD protocol, where a collision can be detected during transmission. If a collision is detected by two nodes, both nodes stop and wait for a random time before trying again, beginning with the carrier-sense mechanism. Many variations on CSMA and CSMA/CD have been proposed, with the difference being primarily in the manner in which nodes perform back-off. It is obvious that with this coordination, CSMA and CSMA/CD can achieve a much better utilization than ALOHA systems.

### **3.2.2 The Need for MAC Protocols for Optical Networks**

Because optical environment differs from traditional electronic environment, the requirements for MAC protocols are also different. The main difference is that in electronic networks the limiting factor is the bandwidth, while in optical networks there is enough bandwidth and the processing power is the scarce source. Thus, in optical environment the packets compete rather for processing time in the nodes than for the transmission channels. The most important factors of the performance of the MAC protocols in optical networks are:

- Throughput
- Delay
- Fairness
- Buffer requirements
- Number and cost of components needed

### **3.3 Optical CDMA Protocols with and without Pretransmission Coordination**

In this section we discuss two different protocols for slotted optical CDMA packet networks that were proposed by Shalaby [6]. These protocols, called Pro 1 and Pro 2, need pretransmission coordination; and a control packet is sent by a transmitter before launching its data. Of course in order to implement these protocols, we need both transmitter and receiver be tunable. That is they should be able to tune their signature codes to the one assigned in the control packet. Furthermore, we present a variation of Pro 2 that does not need pretransmission coordination. Of course the implementation of this variant protocol does not require any receiver tunability, and is thus simpler. Since under normal situations the network users send their data in a burst mode (peak traffic to mean traffic ratios of 1000:1 are common), we will allow the total number of users to exceed the number of available codes. System performance is measured in terms of the system throughput and the average packet delay. Both correlation receivers and chip-level receivers are considered.

#### **3.3.1 System Architecture**

The hardware architecture of the network is shown in Fig. 3.2. There are  $N$  users in the network. Users are connected to input and output ports of a central passive star coupler. The star coupler is the main communication medium, and it is basically a power divider which acts as a multi-access broadcast channel.

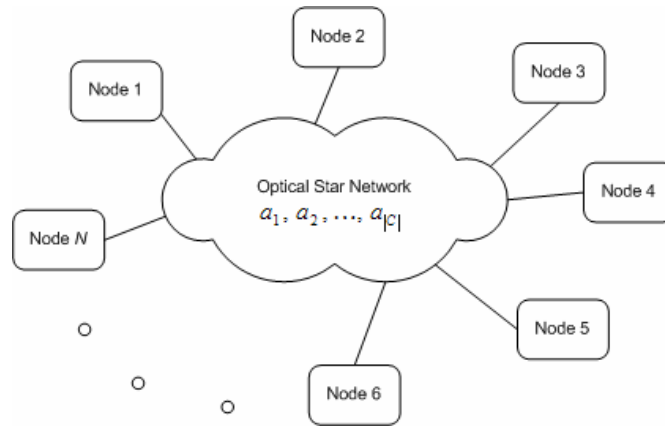


Fig. 3.2. Optical CDMA network architecture.

A set of direct-sequence OOCs  $C = \{a_1, a_2, a_3, \dots, a_{|C|}\}$ , with cardinality  $|C|$  and with auto- and cross-correlation constraints  $\lambda_a = \lambda_c = 1$  is used as the users' signature sequences.

### **3.3.2 Optical CDMA Protocols' Description**

In this subsection, we present a brief description for the different optical CDMA random access protocols according to which codes are assigned to users. We will only stress on the major differences between these protocols.

#### ***3.3.2.1 First Protocol: Pro 1***

In this protocol, we assume that all codes are available in a pool. When a node wants to transmit a packet, it is assigned a code at random. Used codes are removed from the pool and cannot be used by other users. This assumption ensures minimal interference between users. On the other hand, if the number of active users exceeds the number of available codes, some users might be blocked temporary and they should try to transmit their packets later. Of course this adds to the latency in the network and limits the throughput significantly.

#### ***3.3.2.2 Second Protocol: Pro 2***

The key difference between this protocol and Pro 1 is that once codes are assigned to active users, they are not removed from the pool. That is, any active user can always find a code to transmit its data. Of course more interference is possible in this case since a code can be used more than once. In order to reduce the probability of interference among different users, a code is randomly cyclic shifted around itself once assigned. Thus, higher throughputs can be achieved with lower delays.

#### ***3.3.2.3 Variation of Pro 2***

A variation of Pro 2 that avoids the receiver tunability, and hence does not require any pretransmission coordination, can be achieved by distributing the codes to

all receivers a priori. That is, when a user logs onto the network, it is given a code randomly that might possibly be used by another user. Further, the codes are randomly cyclic shifted around themselves for interference control purpose.

### 3.3.3 Optical CDMA Protocols' Performance

Users in the network can be classified as either thinking users or backlogged users. Thinking users are the ones that are transmitting new packets with average activity  $A \in [0, 1]$ . While, users in the backlog mode are waiting a random delay time with average  $d > 0$  time slots before retransmitting corrupted packets. Assuming that at a given slot the number of backlogged users is  $n \in \{0, 1, \dots, N\}$ , the probabilities of  $i \in \{0, 1, \dots, n\}$  backlogged users and  $j \in \{0, 1, \dots, N - n\}$  thinking users are

$$P_{bl}(i | n) = \binom{n}{i} \left(\frac{1}{d}\right)^i \left(1 - \frac{1}{d}\right)^{n-i} \quad \text{and} \quad P_{th}(j | n) = \binom{N-n}{j} A^j (1-A)^{N-n-j}, \quad (3.1)$$

respectively. The offered traffic and system throughput are

$$G(n) = (N - n)A + \frac{n}{d} \quad (3.2)$$

and

$$\beta(n) = \begin{cases} \sum_{j=0}^{N-n} \sum_{i=0}^n ((i+j) \wedge |C|) P_S((i+j) \wedge |C|) P_{bl}(i | n) P_{th}(j | n); & \text{for Pro 1} \\ \sum_{j=0}^{N-n} \sum_{i=0}^n (i+j) P_S(i+j) P_{bl}(i | n) P_{th}(j | n); & \text{for Pro 2} \end{cases}, \quad (3.3)$$

respectively [6], where  $x \wedge y$  denotes the minimum of the two numbers  $x$  and  $y$ . At a given time slot and for  $r'$  active users, the packet success probability  $P_S(r')$  for both correlation receivers and chip-level receivers are given by equations (2.8) and (2.10), respectively.

#### 3.3.3.1 *The Effect of MAI*

Since we are using OOCs with correlation constraints equal 1, users of different codes (Pro 1 and Pro 2) interfere with each other by one chip at most. On the other hand, users of same code (Pro 2) interfere with each other by 0, 1, or  $w$  chips. Assuming chip-synchronous interference model among users, the probabilities  $P_1$  and



$P_w$  of one chip and  $w$  chips interferences, respectively, can be expressed as follows [6]:

$$P_1 = \begin{cases} \frac{w^2}{L}; & \text{for Pro 1} \\ \frac{w^2}{L} \cdot \frac{|C|-1}{|C|} + \frac{w(w-1)}{L} \cdot \frac{1}{|C|}; & \text{for Pro 2} \end{cases} \quad (3.4)$$

and

$$P_w = \begin{cases} 0; & \text{for Pro 1} \\ \frac{1}{L} \cdot \frac{1}{|C|}; & \text{for Pro 2} \end{cases} .$$

### 3.3.3.2 Performance Metrics

To obtain the steady state system throughput and the average packet delay, the above system can be described by a discrete Markov chain composed of  $N + 1$  states depending on the number of backlogged users  $n \in \{0, 1, \dots, N\}$ . The transition between any two states occurs on a slot-by-slot basis. The transition probabilities between any two states and the stationary probabilities  $\pi_n$  for both systems with Pro 1 and Pro 2 can be obtained as in [6]. Finally, the steady state system throughput  $\beta$ , and the average packet delay  $D$  can be computed from the following relations.

$$\beta = \sum_{n=0}^N \beta(n) \pi_n, \quad \text{and} \quad D = 1 + \frac{1}{\beta} \sum_{n=0}^N n \pi_n. \quad (3.5)$$

### 3.3.4 Results and Conclusions

We present some results for the steady state system throughput and the average packet delay for both protocols in Figs. 3.3 and 3.4. OOCs with code length  $L = 31$  and code weight  $w = 3$  are used. A packet size of  $K = 127$  bits is imposed in both figures. The number of users in the network is  $N = 30$ . The same thinking and backlog activities ( $1/d = A$ ) are used in Fig. 3.3, while in Fig. 3.4 the backlogged delay is maintained constant ( $d = 2$ ). The following conclusions can be noticed:

- 1- When using the first protocol (Pro 1) the maximum achievable throughput cannot exceed the number of available codes, while for the second protocol (Pro 2) the throughput can reach higher values.

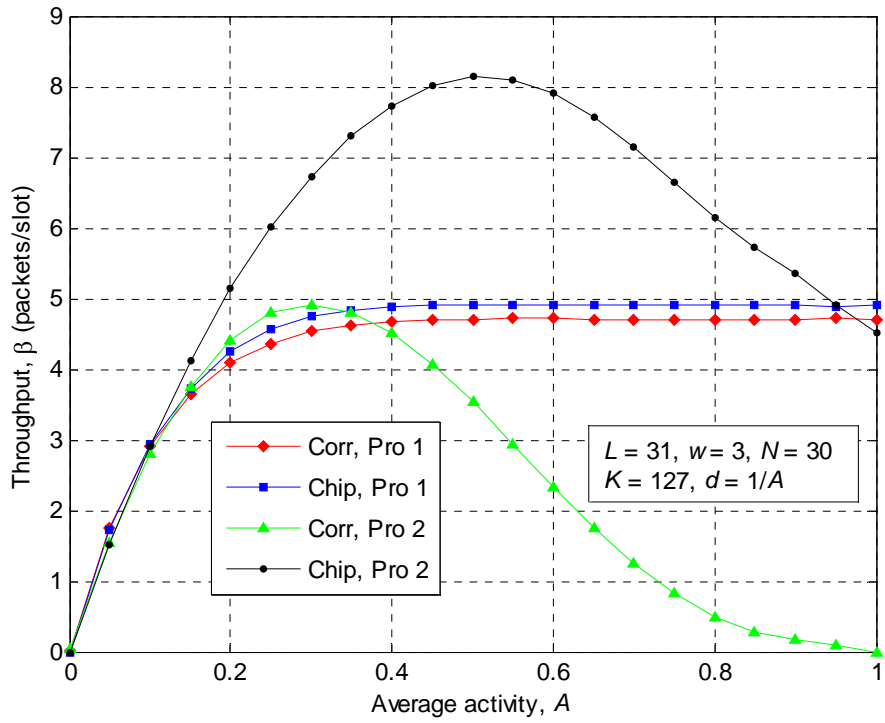


Fig. 3.3. Throughput versus average activity for different protocols.

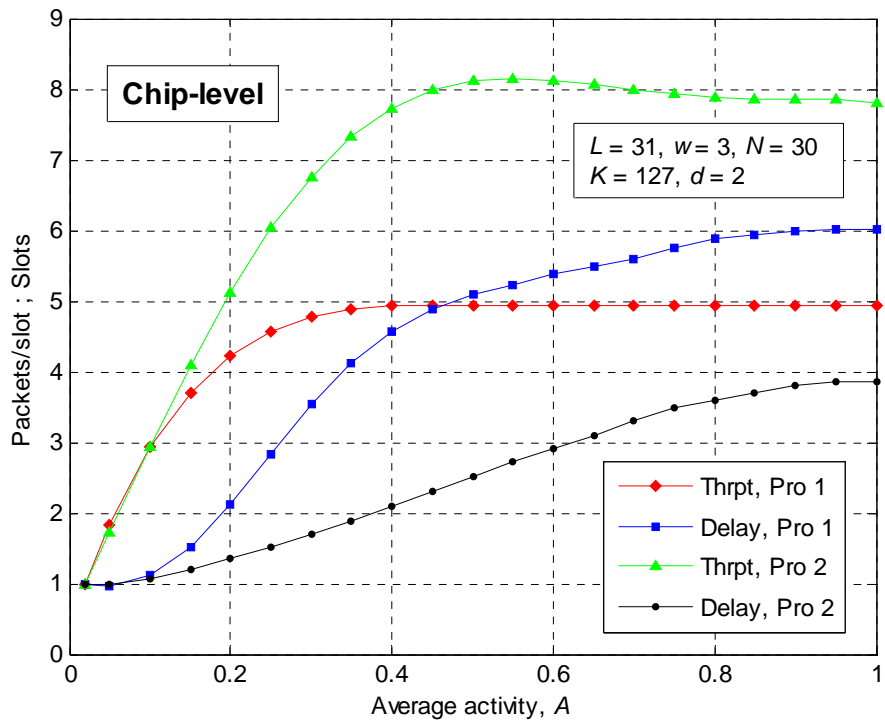


Fig. 3.4. Throughput and delay versus average activity for different protocols.

- 2- The performance of Pro 1 is almost the same for both types of receivers, whereas the performance of Pro 2 is better if chip-level receivers are used because of their higher ability to overcome the effect of MAI.
- 3- The average packet delays of Pro 2 significantly outperform that of Pro 1, because for the former active users can always find a CDMA code to transmit their data.
- 4- For a fixed backlogged delay  $d$ , the throughput of the second protocol (Pro 2) will saturate after it reaches its peak and it won't decay that fast, Fig. 3.4.
- 5- It seems that Pro 1 is the choice for correlation receivers, while Pro 2 with constant backlogged delay is the choice for chip level receivers.

### **3.4 Round Robin Receiver/Transmitter ( $R^3T$ ) Protocol**

The two aforementioned protocols have focused upon the problem of assigning codes for different users [6]. In the analysis of these protocols, we have over-simplified the system in order to get some insight on the problem. However, some important problems have not been considered, such as:

- How the system deals with multi-packet messages.
- How the transmitter respond to an arrived message.
- How the receiver responds to a request for connection.
- How the system deals with lost packets and erroneous packets.
- How the propagation delay affects the network performance.

In [7], Shalaby has developed a new protocol called round robin receiver/transmitter  $R^3T$  protocol which has solved some of the above problems. In his analysis, focus was oriented towards the MAI only, where the effect of both receiver's shot and thermal noises was neglected. The performance of this protocol was measured in terms of the steady state system throughput, the average packet delay and the protocol efficiency.

In this section, we present briefly the basic concept of the  $R^3T$  protocol as well as the main results obtained by Shalaby. We will also extend this work by adding the blocking probability (The probability that an arrival is blocked) as a new metric for the performance of the  $R^3T$  protocol.

### **3.4.1 Network and System Design**

#### ***3.4.1.1 Physical Layer Implementation***

Concerning the network topology at the physical level, we have a passive optical star network connecting  $N$  users (Fig. 3.2). Each node is equipped with a fixed on-off keying CDMA (OOK-CDMA) encoder and a tunable CDMA decoder. A set of OOCs having a unity correlation constraint and with a cardinality  $|C|$  is used for the spreading operation and serves as the user's addresses. Because of its superiority over the correlation model, chip-level receivers are selected at the physical layer.

#### ***3.4.1.2 Optical Link Layer***

The  $R^3T$  protocol is based on a go-back  $n$  automatic repeat request (ARQ), that is when a packet gets corrupted, the transmitter retransmits it and all sub-sequent packets. Many assumptions were imposed in the  $R^3T$  protocol stack [7]:

- Time is slotted with a slot size  $T_s$ ; a packet must fit in a time slot.
- A message is composed of  $\ell$  packets each having  $K$  bits.
- Messages arrive to a station with a probability  $A$ , also called user activity.
- Each node has a single buffer to store only the message being served, any arrival to a non empty buffer is disregarded (No queuing system available).
- Connection requests and acknowledgements are exchanged between stations in order to establish a connection.
- A two-way propagation time which is assumed to be equal to  $t$  time slots and a timeout duration of  $\tau$  time slots, such that  $\tau \leq t$ .
- With the aid of a cyclic redundancy check (CRC) codes, a receiver can determine erroneous packets and can ask for retransmission.

### **3.4.2 Mathematical Model and Theoretical Analysis**

Because of the complexity of the model and the prohibitively large number of states in the  $R^3T$  protocol, the equilibrium point analysis (EPA) technique will be used in our analysis for simplification. In this technique, the system is always assumed to

be operating at an equilibrium point [7]. That is, at any time slot, the average number of users entering any state must be equal to that departing from the state.

### 3.4.2.1 State Diagram and Protocol Description

The detailed state diagram of the  $R^3T$  protocol is shown in Fig. 3.5. Each state is labeled by its number of users. The different modes of operation and states are briefly described in Table 3.1.

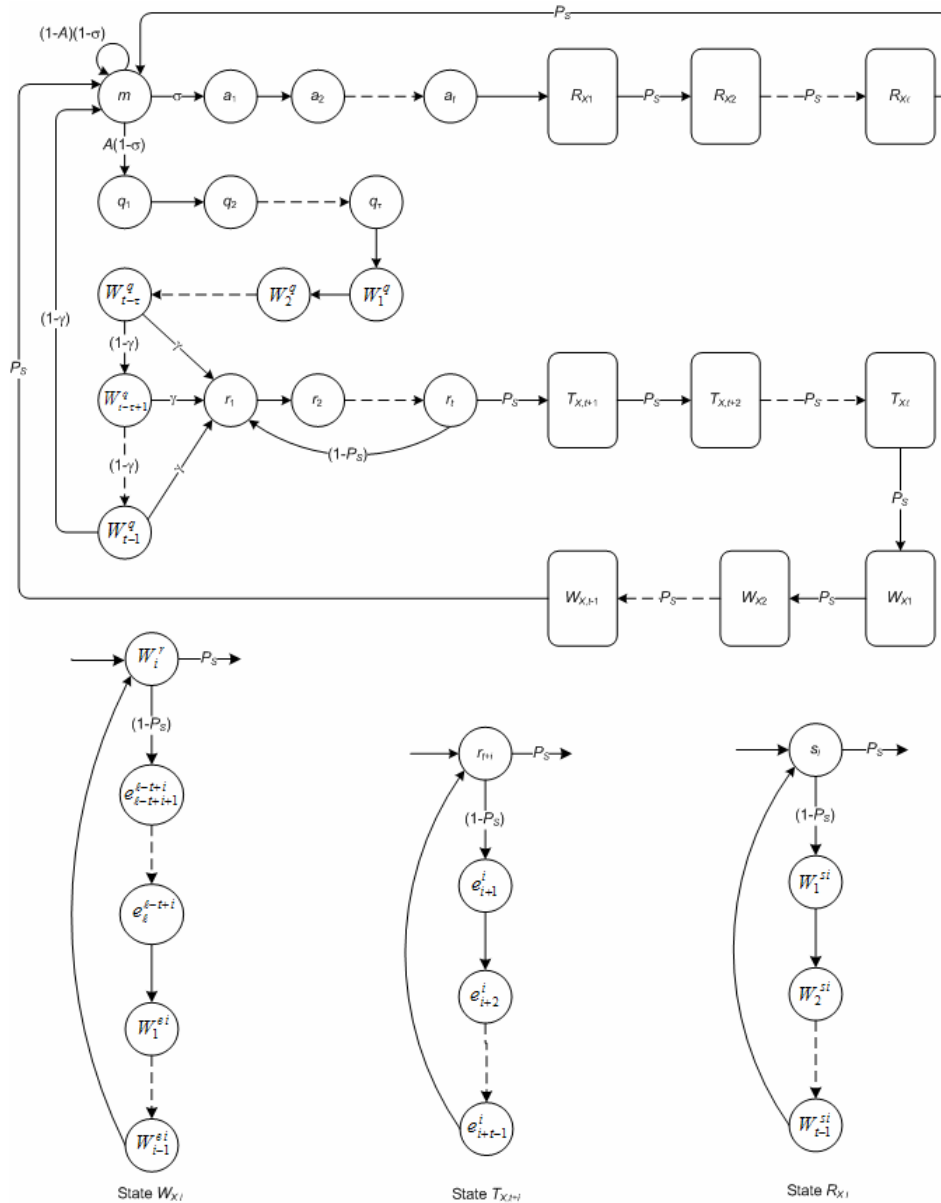


Fig. 3.5. Complete state diagram of the  $R^3T$  optical CDMA protocol.

A user in the initial state scans across the codes in a round robin method, when a connection request is found, an event which happens with a probability  $\sigma$ , the user proceeds to send an acknowledgement and enters the reception mode. When all packets are received successfully, event happening with a probability  $P_s$ , the user returns to the initial state again. The station moves to the requesting mode from the initial state if no requests are found and if there is a message arrival, event that happens with a probability  $A$ . After asking for a connection request, the station enters a waiting mode till it receives an acknowledgement, event which occurs with a probability  $\gamma$ , if timed-out (after  $\tau$  time slots), the station returns to the initial state, otherwise it enters the transmission mode.

Table 3.1. Notations and description for states in the  $R^3T$  protocol state diagram.

Mode of Operation	State Notation	State Description
Idle Mode	$m$	Initial state.
Transmission Mode	$r$	Transmission states.
	$e$	Retransmission states.
	$W^r$	Waiting after transmission states.
	$W^e$	Waiting after retransmission states.
Reception Mode	$s$	Reception states.
	$W^s$	Waiting after reception states.
Acknowledgement Mode	$a$	Acknowledgement states.
Requesting Mode	$q$	Requesting states.
	$W^q$	Waiting after request states.

After transmission is done, the station goes to the waiting mode to collect the acknowledgements for the last  $t - 1$  packets sent, and then returns to the initial state again. The station remains in the initial state if there is no message arrival and if no connection requests are found.

### 3.4.2.2 Performance Evaluation

We start our analysis by assuming that  $\ell \geq t$ , where  $t \geq \tau \geq 1$ . It is evident that the number of users transmitting the packet  $i$  must be equal to that receiving the same packet. Considering only the first packet, we can directly write  $r_1 = s_1$ . By writing the flow equations into states  $s_i$ ,  $i \in \{1, 2, \dots, \ell\}$  in the reception mode we get:

$$s_1 = s_2 = \dots = s_\ell = r_1. \quad (3.6)$$

The probability that a request is found by a scanning user is equal to the probability that another user is in the requesting states [7]:

$$\sigma = \frac{1}{N} \sum_{i=1}^{\tau} q_i = \frac{1-\sigma}{\sigma} AP_S \tau \frac{r_1}{N}. \quad (3.7)$$

The steady-state system throughput  $\beta(N, A, t, \tau, \ell)$  is defined as the average number of successfully received packets per slot:

$$\beta(N, A, t, \tau, \ell) = \sum_{i=1}^{\ell} s_i P_S = P_S(r') \ell r_1, \quad (3.8)$$

where we have used equation (3.6) to carry out the summation. Here,  $r'$  denotes the number of active users in a given slot and is expressed as follows:

$$r' = \sum_{i=1}^{\ell} r_i + \sum_{i=1}^{\ell-t} \sum_{j=i+1}^{i+t-1} e_j^i + \sum_{i=1}^{t-1} \sum_{j=\ell-t+i+1}^{\ell} e_j^{\ell-t+i}. \quad (3.9)$$

By writing down the flow equations of the transmission states and retransmission states in the transmission mode and carrying out summations which involve mathematical series we obtain [7]:

$$r' = [\ell + (1 - P_S(r'))(t-1)(\ell - t/2)] r_1. \quad (3.10)$$

Substituting back in equation (3.8), the throughput can be rewritten as follows:

$$\beta(N, A, t, \tau, \ell) = \frac{P_S(r') \ell \cdot r'}{\ell + (1 - P_S(r')) \cdot (t-1) \cdot (\ell - t/2)}. \quad (3.11)$$

Here,  $r'$  is determined so as the number of users in all states is equal to  $N$ :

$$\begin{aligned} N = m &+ \sum_{i=1}^{\ell} r_i + \sum_{i=1}^{\ell-t} \sum_{j=i+1}^{i+t-1} e_j^i + \sum_{i=1}^{t-1} \sum_{j=\ell-t+i+1}^{\ell} e_j^{\ell-t+i} + \sum_{i=1}^{t-1} W_i^r + \sum_{i=1}^{t-1} \sum_{j=1}^{i-1} W_j^{e_i} \\ &+ \sum_{i=1}^{\ell} s_i + \sum_{i=1}^{\ell} \sum_{j=1}^{t-1} W_j^{s_i} + \sum_{i=1}^t a_i + \sum_{i=1}^{\tau} q_i + \sum_{i=1}^{t-1} W_i^q \end{aligned} \quad (3.12)$$

The blocking probability is defined as the probability of an arrival being blocked. In this case, it is equal to the probability that the station is not in the initial

state  $m$  and there is a message arrival  $A$  or the station is in the initial state  $m$  but there is a request for connection  $\sigma$  and at the same time there is a message arrival  $A$ . Thus, we can write:

$$P_B = \frac{m}{N} \sigma A + \left(1 - \frac{m}{N}\right) A = A \left[1 - (1 - \sigma) \frac{m}{N}\right]. \quad (3.13)$$

Next, we write the flow equations for states in the acknowledgement mode and requesting states in the requesting mode, respectively:

$$\begin{aligned} s_1 &= a_t + (1 - P_s) s_1 \quad \Rightarrow \quad a_t = P_s s_1 = P_s r_1, \\ a_1 &= a_2 = \dots = a_t = \sigma m = P_s r_1 \end{aligned} \quad (3.14)$$

and,

$$q_1 = q_2 = \dots = q_\tau = A(1 - \sigma)m. \quad (3.15)$$

Thus,

$$m = \frac{P_s}{\sigma} r_1.$$

Substituting back in equation (3.13) and using equation (3.7) we get

$$P_B = A \left[1 - \frac{\sigma}{A\tau}\right]. \quad (3.16)$$

Solving equation (3.7) to get  $\sigma$  and then using equation (3.8), the blocking probability can be evaluated as:

$$P_B = A \left[1 - \frac{1}{2N\ell} \left( \sqrt{\beta^2 + 4 \frac{N\ell}{A\tau} \beta} - \beta \right) \right]. \quad (3.17)$$

We finally define two more performance measures that are variants of the steady state throughput and the blocking probability:

- Protocol efficiency: It is defined as the ratio between the number of successfully received packets and the number of packets available for transmission.

$$\eta = \frac{\beta(N, A, t, \tau, \ell)}{r'}. \quad (3.18)$$

- Average delay: For an average offered traffic  $G = NA \cdot (1 - P_B)$  and using Little's theorem, the average packet delay  $D$  is given by

$$D = \frac{NA \cdot (1 - P_B)}{\beta(N, A, t, \tau, \ell)} \quad \text{slots.} \quad (3.19)$$

Note that in his analysis, Shalaby assumed that the blocking probability is



equal to zero in equation (3.19). He also defined the protocol efficiency as the fraction of successfully received packets (the ratio between the number of successfully received packets and the maximum number of packets available for transmission, which is  $N/2$ ); which is not quiet fair because at a given time slot and for the same throughput there may be fewer packets available for transmission, which yields a higher efficiency.

### 3.4.3 Simulation Results

In this subsection, we present and discuss some numerical results for the steady state throughput, the average packet delay and the blocking probability obtained in the previous subsection. Chip-level receivers and OOCs are implemented at the physical layer of our optical CDMA network. Our results are plotted in Figs. 3.6-3.8. A message length of  $\ell = 15$  and a packet size of  $K = 127$  bits are imposed in all figures. A timeout duration of  $\tau = 1$  is used in all figures but Fig. 3.8. Different parameters of interest are considered.

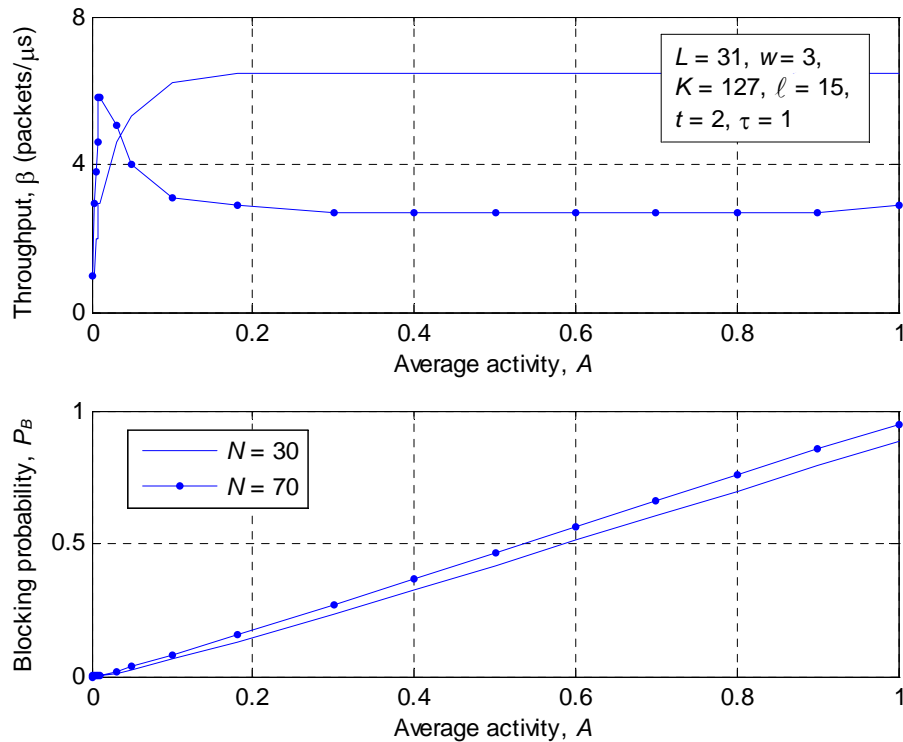


Fig. 3.6. Throughput and blocking probability versus average activity for different number of users.

In Fig. 3.6, the throughput and the blocking probability have been plotted versus the average activity for different number of users  $N \in \{30, 70\}$ . It can be inferred that as the user activity increases, the throughput increases till it reaches saturation for the case of small number of users,  $N = 30$ . For larger population networks, the throughput will fall after reaching a peak value as the user activity increases till it saturates at a lower value. It is noticed that the blocking probability increases rapidly as the activity increases regardless of the number of users in the network. Also for the same value of average activity, the blocking probability is higher for high population networks.

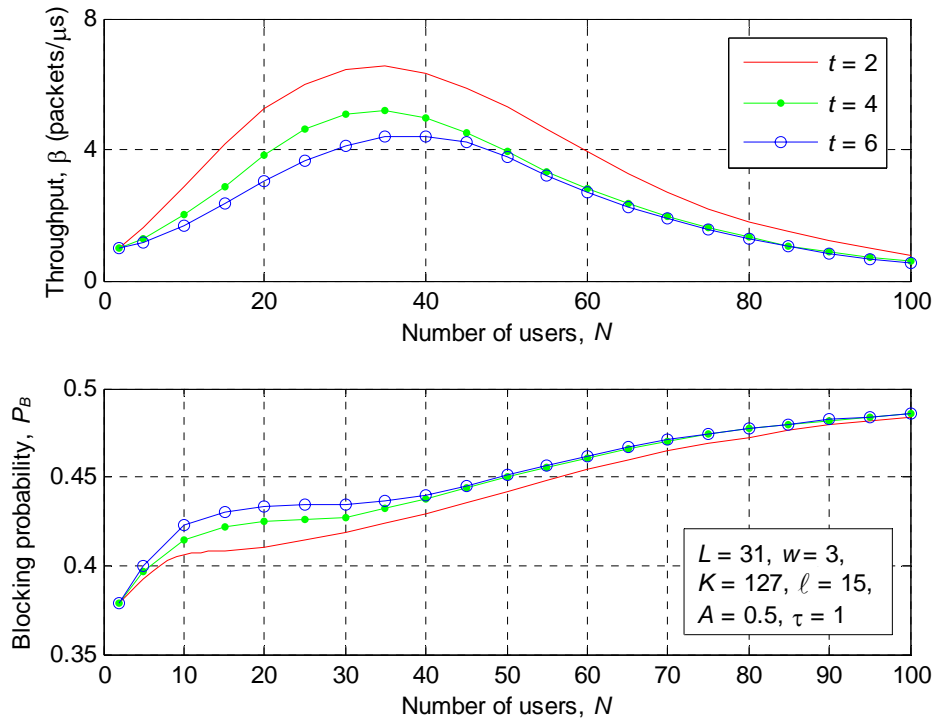


Fig. 3.7. Throughput and blocking probability versus number of users for different propagation delays.

In Fig. 3.7, we have plotted the throughput versus the number of users  $N$  for different propagation delays (different interstation distances) and same average activity  $A = 0.5$ . General trends can be noticed. There is always an optimum value of  $N$  that maximizes the throughput. In the case of long propagation delays, there is a little degradation in the performance of the  $R^3T$  protocol. This is because for longer propagation delays, users are busy transmitting their messages over long distances.

The interference would thus increase rapidly and packet failures become more probable. It can also be inferred from this figure that the blocking probability increases as the number of users in the network increases and for longer propagation delays. This can be explained in a similar way; that is in large population networks and for longer interstation distances users are always busy retransmitting corrupted packets and thus any message arrival will be blocked. Comparing these results to the ones obtained in Fig. 3.6, we conclude that the main parameter affecting the blocking probability is the average user activity, not the size of the network population.

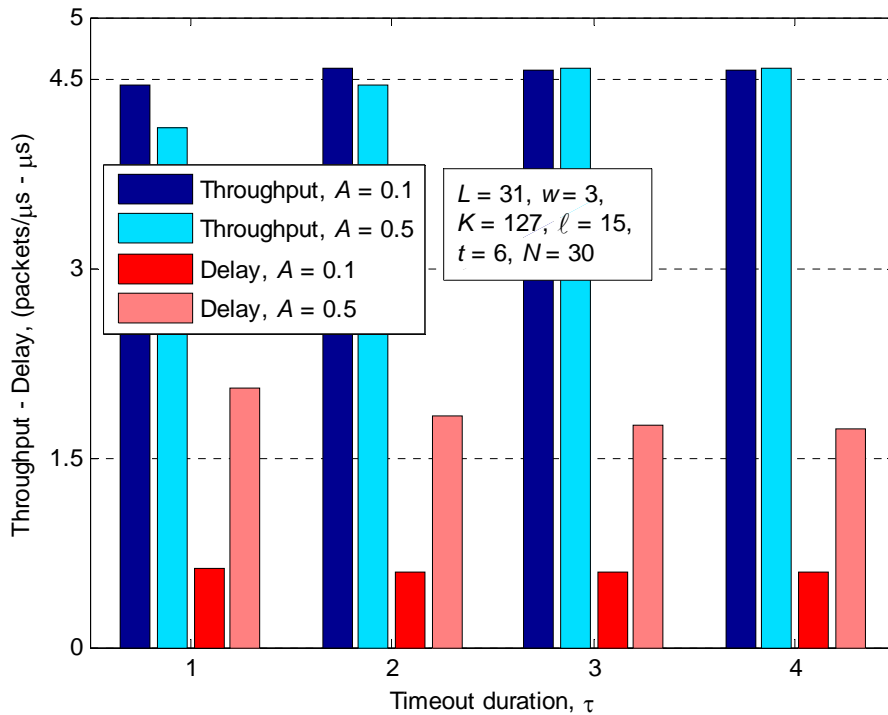


Fig. 3.8. Throughput and delay versus timeout duration for different activities.

Finally, the steady state system throughput and the average packet delay have been plotted against the timeout duration  $\tau$  in Fig. 3.8 for various arrivals,  $A \in \{0.1, 0.5\}$ . It can be seen that as  $\tau$  increases, the throughput increases and thus the delay is reduced, which verifies equation (3.19). Indeed as  $\tau$  increases, more requests can be acknowledged and thus the throughput increases, which causes the delay to decrease. As the user activity increases, more packets are available in the network yielding to a major increase in the interference. Packets are thus damaged and must be retransmitted, which causes the average delay to increase significantly.

### **3.4.4 Summary and Conclusions**

Four main performance measures have been derived based on the EPA techniques. These measures are the steady state system throughput, the blocking probability, the average packet delay, and the protocol efficiency. In order to have some insight on the problem under consideration, focus has been given to MAI only and other sources of noise have been neglected. The following conclusions can be extracted from this work:

- 1- The  $R^3T$  protocol exhibits an acceptable throughput and average packet delay only for small population networks.
- 2- The achievable throughput exceeds the number of available codes  $|C|$  for small propagation delays, Figs. 3.6 and 3.7.
- 3- Although the steady state throughput is acceptable, the blocking probability is still high even for small user activities. The blocking probability can reach up to 95 % at very high activities.
- 4- The throughput obtained represents an upper bound because only the effect of MAI was considered. Other performance degradation parameters such as the receiver's shot and thermal noises are neglected.
- 5- The delay obtained represents a lower bound because queuing systems are not considered. Delay is only due to the service time, queuing delay is neglected.
- 6- An asymptotic efficiency of 100 % can be reached easily with suitable choices of code weight and code length, [7].
- 7- Of course, there exists a tradeoff between the throughput, the average delay and the blocking probability.
- 8- The  $R^3T$  protocol is an optimum solution for small population LANs and for relatively small user activity.

# CHAPTER 4

## IMPAIRMENTS IN THE $R^3T$ OPTICAL RANDOM ACCESS CDMA PROTOCOL

### Outline:

- Introduction
- Impairments in Fiber Optic Communication Systems
- Performance of the  $R^3T$  Protocol in a Noisy Environment
- Conclusions

# CHAPTER 4

## IMPAIRMENTS IN THE $R^3T$ OPTICAL RANDOM ACCESS CDMA PROTOCOL

### **4.1 Introduction**

Fiber optic transmission and communication are technologies that are constantly growing and becoming more modernized and increasingly being used in the modern day industries. However, the effects of noise and dispersion cause a marked decrease in transmitted power, and therefore, have limited progress in areas of high-speed transmission and signal efficiency over long distances [34], and [35]. However, new advances are continually being made to combat these losses and improve the reliability of fiber systems. In this chapter, we discuss the major sources of noise and dispersion in optical CDMA systems, showing their impact on the performance of the  $R^3T$  protocol [7].

### **4.2 Impairments in Fiber Optic Communication Systems**

A complete description of all impairments in fiber optic communication systems would be very long. In this section, we will describe only two noise sources often encountered in connection with optical detectors, also we will present the major sources of light dispersion in optical fibers.

#### **4.2.1 Receiver Noise**

Noise corrupts the transmitted signal in a fiber optic system. This means that noise sets a lower limit on the amount of optical power required for proper receiver operation. There are many sources of noise in fiber optic systems. Shot noise and thermal noise are the two fundamental noise mechanisms responsible for current fluctuations in optical receivers even when the incident optical power is constant. Of course, additional noise is generated if the incident power itself is fluctuating because

of noise produced by optical amplifiers. This subsection considers only the noise generated at the receiver.

#### **4.2.1.1 Shot Noise**

Shot noise is a manifestation of the fact that an electric current consists of a stream of electrons that are generated at random times. Dark current and quantum noises are two types of noises that manifest themselves as shot noise. Dark current noise results from dark current that continues to flow in the photodiode when there is no incident light. Dark current noise is independent of the optical signal. In addition, the discrete nature of the photodetection process creates a signal dependent shot noise called quantum noise. Quantum noise results from the random generation of electrons by the incident optical radiation. Mathematically, shot noise is modeled as a stationary process with Poisson statistics. Shot noise may be minimized by keeping any DC component to the current small, especially the dark current, and by keeping the bandwidth of the amplification system small.

#### **4.2.1.2 Thermal Noise**

At a finite temperature, electrons move randomly in a conductor. Random thermal motion of electrons in a resistor manifests as a fluctuating current even in the absence of an applied voltage. The load resistor  $R_L$  in the front end of an optical receiver adds such fluctuations to the current generated by the photodiode. This additional noise component is referred to as thermal noise. Mathematically, thermal noise can be treated as a stationary Gaussian random process. A reduction in thermal noise is possible by increasing the value of the load resistor. However, increasing the value of the load resistor significantly reduces the receiver bandwidth. Thus, one may cool the system, especially the load resistor.

#### **4.2.2 Light Dispersion in Fibers**

Dispersion is the widening of a pulse as it travels through a fiber. As a pulse widens, it can broaden enough to interfere with neighboring pulses, leading to intersymbol interference. Dispersion thus limits the maximum transmission rate on a

fiber-optic channel. Dispersion can potentially be a significant problem for optical CDMA because of the large bandwidth of the signal. Fortunately the propagation distance is not long in LANs and access networks, so intersymbol interference is usually not a problem. For frequency hopping systems, the dispersion can be compensated by introducing a time offset between the chips at the different frequencies [36]. New fiber designs, such as reduced-slope fibers, have low dispersion over a very wide range because the slope of dispersion is less than  $0.05 \text{ ps/nm}^2 \cdot \text{km}$ , which is significantly lower than standard fibers [34].

In this subsection, we present the major sources of dispersion encountered in optical communication systems.

#### ***4.2.2.1 Modal Dispersion***

This type of dispersion is very significant and is related to the fact that a pulse of light transmitted through a fiber optic cable is composed of several modes, or rays, of light instead of only one single beam; therefore, it is called modal or intermodal dispersion. Each mode of light travels a different path, as a result the modes will not be received at the same time, and the signal will be distorted or even lost over long distances. This type of dispersion is negligible in single mode fibers. New concepts and designs are continually being developed to reduce dispersion in optical fibers.

#### ***4.2.2.2 Chromatic Dispersion***

Chromatic dispersion can be viewed as a combination of both material dispersion and waveguide dispersion. It is also known as intramodal dispersion. Material dispersion results from the fact that the refractive index of the fiber medium varies as a function of the wavelength [34]. Since neither the light source nor the fiber optic cable is 100 percent pure, the pulse being transmitted becomes less and less precise as the light's wavelengths are separated over long distances. Waveguide dispersion is very similar to material dispersion in that they both cause signals of different wavelengths or frequencies to separate from the light pulse. However, waveguide dispersion depends on the shape, design, and chemical composition of the fiber core. Light which is not coupled into the core of the fiber propagates through the



inner layer of the cladding. It travels at a faster velocity because the refractive index of the cladding is lower than that of the core. An increase in the waveguide dispersion in an optical fiber can be used in order to counterbalance material dispersion and shift the wavelength of zero chromatic dispersion to 1550 nm, Fig. 4.1. Engineers used this concept to develop zero-dispersion-shifted fibers designed to have larger waveguide dispersion. Developers doped the core with germanium oxide in order to increase the difference between the refractive indices of the cladding and the core, thus enlarging waveguide dispersion [34].

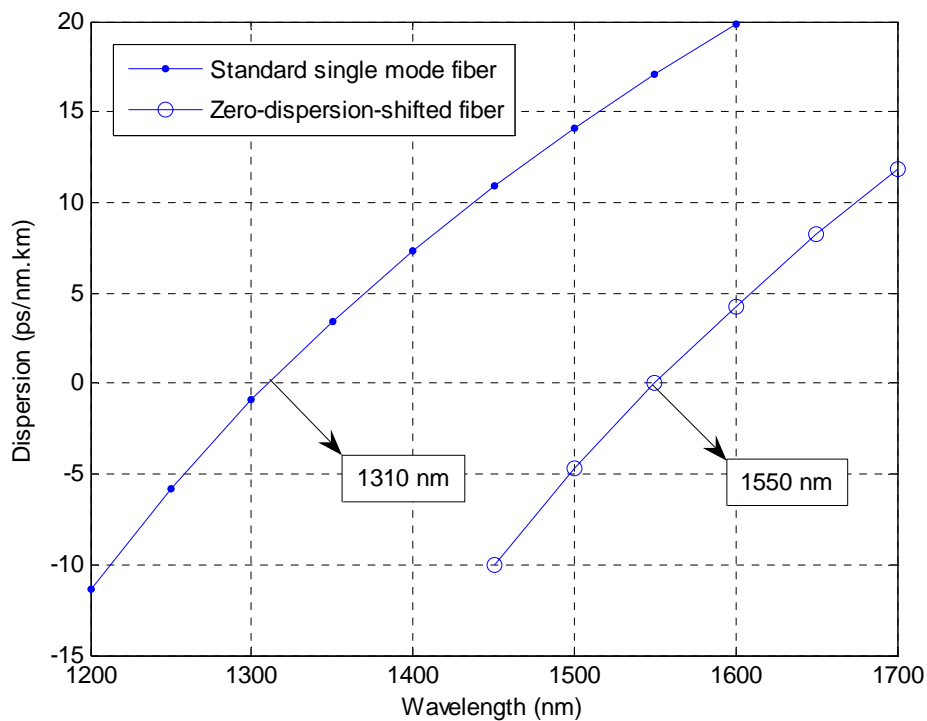


Fig. 4.1. Typical dispersion versus wavelength curves.

### **4.3 Performance of the $R^3T$ Protocol in a Noisy Environment**

In [7], Shalaby proposed the so called  $R^3T$  protocol. We have presented an overview of this protocol in the previous chapter and discussed its performance in terms of the steady state system throughput, the average packet delay and the protocol efficiency. In his analysis, Shalaby neglected both the receiver's noise and the light dispersion. In this section, we will study the effect of thermal noise and its impact on

the performance of the  $R^3T$  protocol. Then, we will consider the effect of dispersion.

### **4.3.1 System Architecture and Hardware Implementation**

Recall that the basic architecture of our optical CDMA network is a passive star network connecting  $N$  nodes (Fig. 3.2). Users produce OOK-CDMA signals that represent their data. Because of the broadcast nature of the star topology and the lack of coordination between users, the effect of MAI will be considered in our analysis. Optical orthogonal codes are used as the user signature codes because of their good out-of-phase autocorrelation and cross-correlation properties [9]. Chip-level receivers are implemented at the physical layer because of their high ability to overcome the effect of multiple-access interference (MAI). The complete model for this receiver can be found in [26]. The packet success probability  $P_s(r')$  given  $r'$  active users for chip-level receiver has been derived in Subsection 2.5.2, where we have considered only the effect of MAI. In our analysis in this chapter, we will use avalanche photodiodes (APDs), because optical receivers that employ an APD generally provide a higher signal to noise ratio (SNR) for the same amount of incident optical power. The improvement is due to the internal gain that increases the photocurrent significantly.

### **4.3.2 Effect of Thermal Noise**

In most cases of practical interest, thermal noise dominates the receiver performance. Accordingly, in our analysis we will study only the effect of thermal noise and its impact on the performance of the  $R^3T$  protocol. In this subsection, we start by deriving a corresponding new expression for the packet success probability for chip-level receivers, which accounts for both the effect of thermal noise and MAI. Finally, we apply this expression to the  $R^3T$  protocol and discuss the results obtained.

#### ***4.3.2.1 Mathematical Analysis***

In our model we assume that the decision variable  $Y_j$ , for chip-level receivers; which indicates the photon count per marked chip positions  $j \in x = \{1, 2, \dots, w\}$  to

have a Gaussian distribution. We consider  $u$  users out of  $m$  users interfering in  $w$  chips and  $v_j$  users out of  $k_j$  users making interference at weighted chip  $j$ . The conditional mean  $m_{b_j}$  and variance  $\sigma_{b_j}^2$  for the decision variable  $Y_j$  can be expressed as follows:

$$\begin{aligned} m_{b_j} &= G_{APD} \left[ (u + b + v_j) \cdot Q + Q_d \right] \\ \sigma_{b_j}^2 &= F G_{APD} \cdot m_{b_j} + \sigma_n^2 \end{aligned} \quad (4.1)$$

Here  $b \in \{0, 1\}$  is the user data bit and  $G_{APD}$  is the average APD gain. The average number of absorbed photons per received single-user pulse and the number of absorbed photons due to the APD dark current within a chip interval  $T_c$ , denoted by  $Q$  and  $Q_d$  respectively, are given by [18]:

$$Q = \frac{R_{APD} P_{av} T}{q_e w}, \quad Q_d = \frac{I_d T_c}{q_e}, \quad (4.2)$$

where,  $P_{av}$  is the received average peak laser power (of a single user),  $T$  is the bit duration,  $R_{APD}$  is the APD responsivity at unity gain,  $I_d$  is the APD dark current,  $w$  is the code weight and  $q_e = 1.6 \times 10^{-19}$  C is the magnitude of the electron charge. The variance of the thermal noise within a chip interval  $\sigma_n^2$  is expressed as follows:

$$\sigma_n^2 = \frac{2K_B T^o}{q_e^2 R_L} T_c, \quad (4.3)$$

where,  $K_B = 1.38 \times 10^{-23}$  J/K is Boltzmann's constant,  $T^o$  is the receiver noise temperature, and  $R_L$  is the receiver load resistor. Defining  $k_{eff}$  as the APD effective ionization ratio, the APD excess noise factor  $F$  can be given by [37]:

$$F = k_{eff} G_{APD} + \left( 2 - \frac{1}{G_{APD}} \right) (1 - k_{eff}). \quad (4.4)$$

As mentioned in Chapter 2, the decision rule of the chip-level receiver depends on the photon count  $Y_j$  collected from marked chip positions [26] such that

$$\text{Decide} \begin{cases} 1; & \text{if } Y_j \geq \theta \\ 0; & \text{otherwise} \end{cases} \quad \forall j \in x. \quad (4.5)$$

The decision threshold  $\theta$  (photons/chip) must be optimized in order to achieve good performance [18]. The threshold dependence of the OOK-CDMA chip-level receivers is illustrated in Fig. 4.2. We have plotted the bit error probability versus the decision

threshold for different power levels. It can be seen that when the optical power is large enough (so that the error probability floor is reached), the optimum threshold is not unique and covers a wide range. However, when the optical power is not that large, then there is only one unique optimum threshold [18].

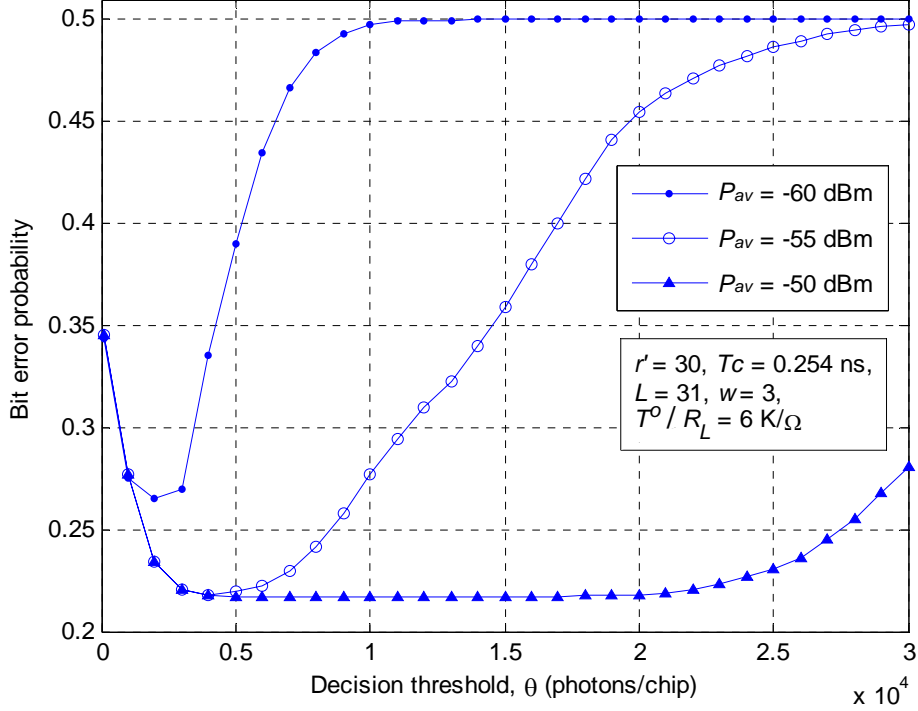


Fig. 4.2. Bit error probabilities for OOK-CDMA chip-level receivers versus the decision threshold.

This curve has been plotted for an APD having an average gain  $G_{APD} = 100$ , its unit gain responsivity  $R_{APD} = 0.84$  A/W, its effective ionization ratio  $k_{eff} = 0.02$  and its dark current  $I_d = 1$  nA.

We start by deriving the bit correct probability as follows:

$$\begin{aligned}
 P_{bc}(m, \bar{k}) &= \frac{1}{2} \Pr\{\text{a bit success} \mid m, \bar{k}, 1 \text{ was sent}\} \\
 &\quad + \frac{1}{2} \Pr\{\text{a bit success} \mid m, \bar{k}, 0 \text{ was sent}\} \\
 P_{bc}(m, \bar{k}) &= \frac{1}{2} \Pr\{Y_j \geq \theta \text{ for all } j \in x \mid m, \bar{k}, 1 \text{ was sent}\} \\
 &\quad + \frac{1}{2} \Pr\{Y_j < \theta \text{ for some } j \in x \mid m, \bar{k}, 0 \text{ was sent}\}
 \end{aligned} \tag{4.6}$$

Here,  $\bar{k} = \{k_1, k_2, \dots, k_w\}$  denotes the interference vector and is modeled as a multinomial random variable [18]. Using the inclusion–exclusion property yields:

$$\begin{aligned} P_{bc}(m, \bar{k}) &= \frac{1}{2} + \frac{1}{2} \sum_{b=0}^1 (-1)^b \times \Pr\{Y_j < \theta \text{ for some } j \in x \mid m, \bar{k}, b\} \\ &= \frac{1}{2} - \frac{1}{2} \sum_{b=0}^1 (-1)^b \sum_{i=1}^w (-1)^i \binom{w}{i} \Pr\{Y_t < \theta, t \in \{1, 2, \dots, j\} \mid m, \bar{k}, b\}. \end{aligned} \quad (4.7)$$

The last probabilities can be expressed as follows:

$$\begin{aligned} &\Pr\{Y_t < \theta, t \in \{1, 2, \dots, j\} \mid m, \bar{k}, b\} \\ &= \sum_{u=0}^m \binom{m}{u} \left(\frac{1}{2}\right)^m \cdot \sum_{v_1=0}^{k_1} \binom{k_1}{v_1} \left(\frac{1}{2}\right)^{k_1} \cdot \sum_{v_2=0}^{k_2} \binom{k_2}{v_2} \left(\frac{1}{2}\right)^{k_2} \cdots \cdot \sum_{v_i=0}^{k_i} \binom{k_i}{v_i} \left(\frac{1}{2}\right)^{k_i} \\ &\quad \cdot \Pr\{Y_1 < \theta \mid u, v_1, b\} \cdot \Pr\{Y_2 < \theta \mid u, v_2, b\} \cdots \Pr\{Y_i < \theta \mid u, v_i, b\} \\ &= \sum_{u=0}^m \binom{m}{u} \left(\frac{1}{2}\right)^m \prod_{j=1}^i \sum_{v_j=0}^{k_j} \binom{k_j}{v_j} \left(\frac{1}{2}\right)^{k_j} Q\left(\frac{m_{bj} - \theta}{\sigma_{bj}}\right), \end{aligned} \quad (4.8)$$

where  $Q(x)$  is the normalized Gaussian tail probability, given by

$$Q(x) = \frac{1}{\sqrt{2\pi}} \int_x^\infty e^{-s^2/2} ds. \quad (4.8)$$

Combining the last equations, the bit correct probability can be rewritten as follows:

$$\begin{aligned} P_{bc}(m, k, b) &= \frac{1}{2} - \frac{1}{2} \sum_{b=0}^1 (-1)^b \sum_{i=1}^w (-1)^i \binom{i}{w} \sum_{u=0}^m \binom{m}{u} \left(\frac{1}{2}\right)^u \left(\frac{1}{2}\right)^{m-u} \\ &\quad \cdot \prod_{j=1}^i \sum_{v_j=0}^{k_j} \binom{k_j}{v_j} \left(\frac{1}{2}\right)^{k_j} Q\left(\frac{m_{bj} - \theta}{\sigma_{bj}}\right) \end{aligned} \quad (4.9)$$

Finally, the packet success probability for a packet of  $K$  bits can be given by:

$$\begin{aligned} P_s(r', P_{av}, \theta) &= \sum_{k=0}^{r'-1} \sum_{m=0}^{r'-1-k} \frac{(r'-1)!}{k!m!(r'-1-m-k)!} \cdot p_1^k p_w^m (1-p_1-p_w)^{r'-1-m-k} \\ &\quad \cdot \sum_{\substack{k_1, k_2, \dots, k_w: \\ k_1 + \dots + k_w = k}} \frac{k!}{k_1! \cdots k_w!} \left(\frac{1}{w}\right)^k \cdot \left[ \frac{1}{2} - \frac{1}{2} \sum_{b=0}^1 (-1)^b \sum_{i=1}^w (-1)^i \binom{i}{w} \right. \\ &\quad \cdot \left. \sum_{u=0}^m \binom{m}{u} \left(\frac{1}{2}\right)^u \left(\frac{1}{2}\right)^{m-u} \cdot \prod_{j=1}^i \sum_{v_j=0}^{k_j} \binom{k_j}{v_j} \left(\frac{1}{2}\right)^{k_j} Q\left(\frac{m_{bj} - \theta}{\sigma_{bj}}\right) \right]^K. \end{aligned} \quad (4.10)$$

#### 4.3.2.2 Numerical Results

The result obtained in equation (4.10) will be applied to equations (3.11), (3.17)-(3.19) in order to calculate the steady state system throughput, the blocking

probability, the protocol efficiency, and the average packet delay, respectively. Typical values of the simulation parameters are shown in Table 4.1. Users are assumed to transmit fixed size messages, composed of  $\ell$  packets. A packet must fit in a time slot such that  $T_s = K L T_c$ . Here,  $T_s$  is the slot duration,  $K$  is number of bits per packet,  $L$  is the code length and  $T_c$  is the chip duration. The selection of these parameters ensures a slot size constraint of  $T_s = 1\mu\text{s}$  in our simulation. A timeout duration of  $\tau = 1$  is imposed in all figures and a two way propagation delay time of  $t \in \{2, 4, 6\}$  time slots is selected.

Table 4.1. Typical values of simulation parameters.

CDMA Encoding Parameters		Photo-detector	
<u>Data</u>	<u>OOCs</u>	<u>APD</u>	
$\ell = 15$ packets	$L = 31$	$R_{APD} = 0.84$ A/W	$I_d = 1$ nA
$K = 127$ bits	$w = 3$	$G_{APD} = 100$	$k_{eff} = 0.02$
	$\lambda_a = \lambda_c = 1$	$T^o/R_L = [0, 10]$	

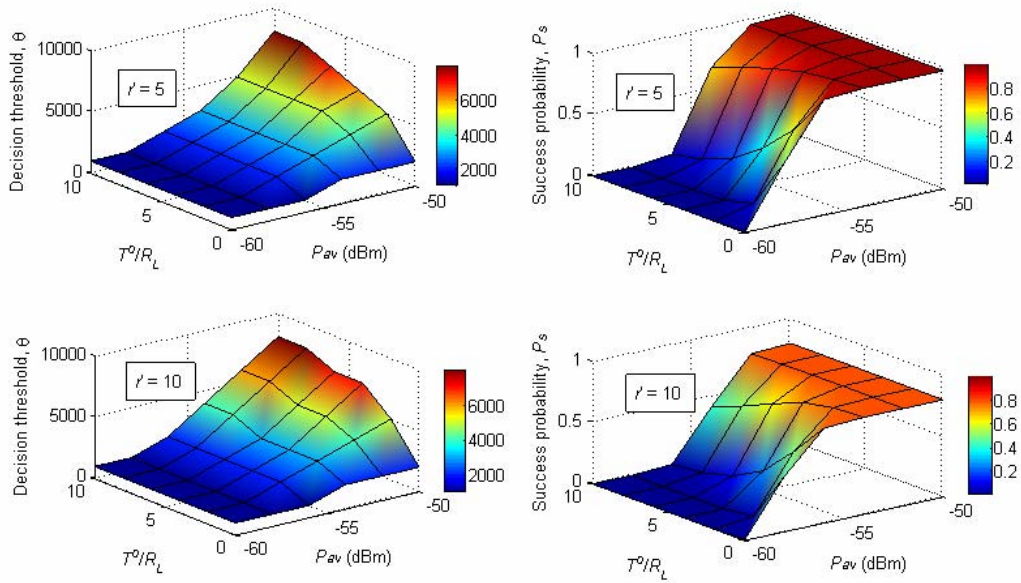


Fig. 4.3. Packet success probability and decision threshold versus the average peak laser power and the receiver noise temperature for different number of active users.

In Fig. 4.3, the packet success probability has been plotted versus the average peak laser power and the receiver noise temperature ( $\sim T^o/R_L$ ) for different number of active users in the network. Also the optimum decision threshold  $\theta$  has been investigated. It can be inferred that the packet success probability is significantly affected for smaller amounts of power and for higher noise temperatures. The performance also depends on the number of active users, because as more users start transmitting packets the effect of MAI will add to the effect of thermal noise, thus we note a dramatically performance degradation in the system. In order to achieve the optimum performance, the threshold must be increased when operating at higher power levels. Also to compensate for the effect of thermal noise the decision threshold must be increased for higher noise temperatures.

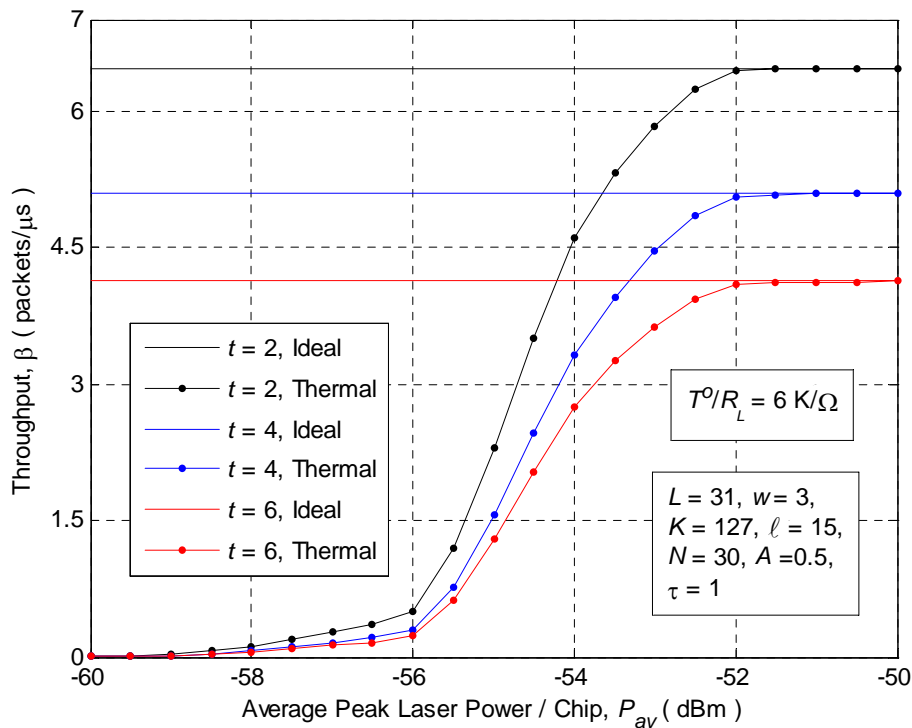


Fig. 4.4. Throughput versus average peak laser power for different propagation delays.

We have plotted the relation between the steady state system throughput and the average peak laser power for different propagation delays in Fig. 4.4. General trends of the curves can be noticed. The throughput falls down as the propagation delay is increased as in [7]. It can be noticed that for relatively small power levels,

there is a limitation in the performance of the  $R^3T$  protocol. By increasing the average peak laser power up to -52 dBm, the effect of thermal noise becomes marginal, and regardless of the propagation delay and other link parameters, the receiver can tolerate this degradation and achieves the same throughput as the ideal case (when considering only the effect of MAI).

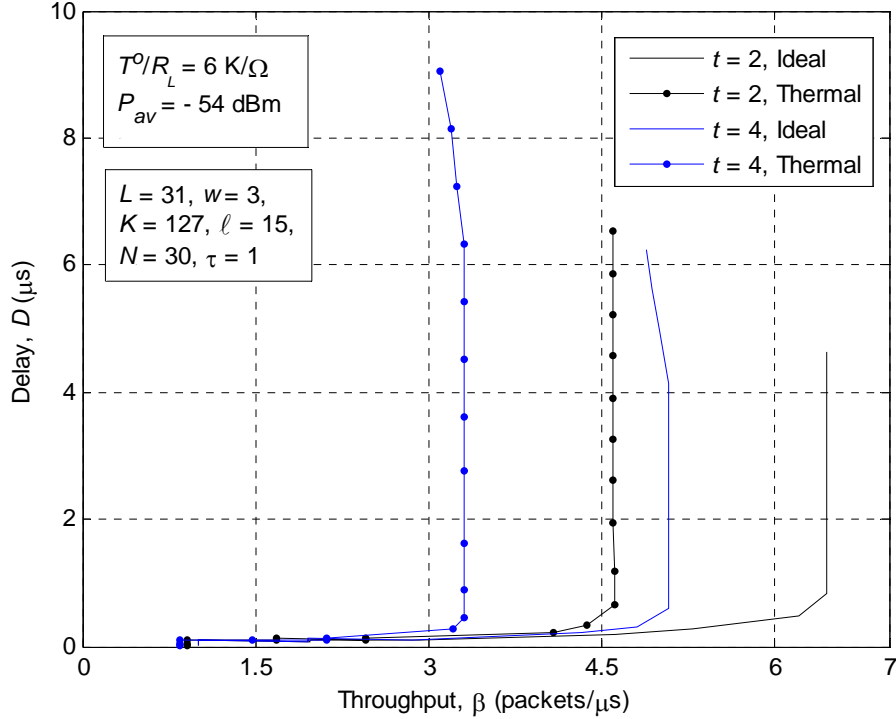


Fig. 4.5. Packet delay versus throughput for different propagation delays.

Figure 4.5, depicts the relation between the average packet delay and the throughput. It has been plotted for different propagation delays. For convenience and sake of comparison, we have neglected the blocking probability when computing the average packet delay;  $P_b = 0$  in equation (3.19). It can be seen that, in order to obtain a negligible delay, the throughput will not be that high, so that a trade off must be considered. It can be inferred that because of the increase in the user activity, the throughput saturates [7] and the delay will grow rapidly. Also it is noticed that the average packet delay becomes significant for longer propagation delays. The degradation in the performance can also be compensated by reasonably increasing the average peak laser power as demonstrated in Fig. 4.3.



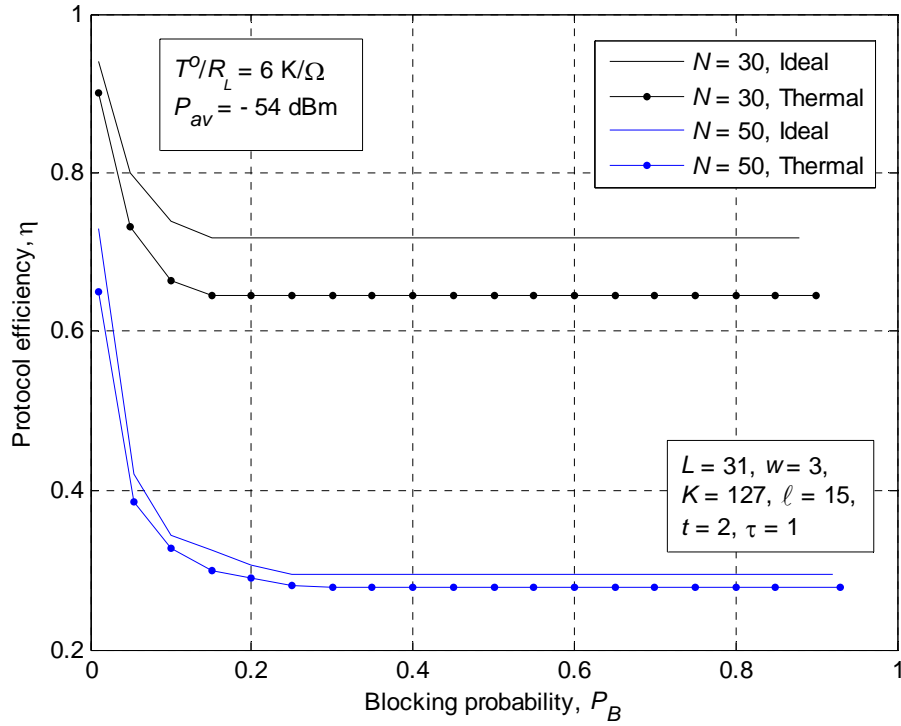


Fig. 4.6. Protocol efficiency versus blocking probability for different number of users.

In Fig. 4.6, we have plotted the protocol efficiency against the blocking probability for different number of users in the network,  $N \in \{30, 50\}$ . General trends of the curves can be noticed. As the users start to send more packets (arrival rate increases), the blocking probability increases and thus the protocol efficiency starts to fall till it reaches its floor. This is because for small propagation delays ( $t = 2$ ), as the user activity is increased the throughput also increases till it reaches a saturation value [7]. At this instant the number of active users is considered also to be constant because of the relatively small delays and thus the efficiency saturates. For small population networks the efficiency can reach as high as 95%. Finally, it can be noticed that the effect of thermal noise is dominant for a relatively small number of users in the network. For larger population networks, the effect of thermal noise is negligible with respect to the MAI.

#### 4.3.3 Effect of Light Dispersion

One of the main performance degradation factors in long-haul fiber optic

communication systems is the dispersion effect, which results in a temporal widening of optical pulses. In particular, intersymbol interference (ISI), pulse width and peak power limitation, and pulse distortion [38], [39] have previously been examined. We focus our analysis upon the traditional pulse-distorting impact of the dispersion, which shows to be vital and severe in limiting the user bit rate. Modal dispersion and chromatic dispersion are the two mechanisms causing pulse spreading when selecting a graded index-multimode fiber.

#### 4.3.3.1 Mathematical Analysis

Starting first with the modal dispersion, which is the main part that contributes to the light dispersion, the pulse spreading is

$$\Delta t_{\text{modal}} = \frac{(NA)^4}{32 c n_1^3} \cdot z, \quad (4.11)$$

where  $NA$  denotes the numerical aperture of the fiber,  $n_1$  is the refractive index of its core,  $c = 3 \times 10^8$  m/s is the speed of light in free space and  $z$  is the fiber length or more precisely the interstation distance and is given by:

$$z = \frac{v \cdot t}{2} \times T_s. \quad (4.12)$$

Here,  $v$  is the velocity of light inside the fiber core and is related to its refractive index. Then, we consider the effect of the chromatic dispersion, which is the combination of both material dispersion and waveguide dispersion, we define the chromatic dispersion parameter as follows:

$$D_{\text{chrom}}(\lambda) = \frac{S_o}{4} \times \left[ \lambda - \frac{\lambda_o^4}{\lambda^3} \right], \quad (4.13)$$

where  $\lambda$  is the operating wavelength,  $\lambda_o$  is the zero dispersion wavelength and  $S_o$  is the zero dispersion slope. Let  $\Delta\lambda$  be the spectral line width of the used light source. The pulse spreading can be written as:

$$\Delta t_{\text{chrom}} = D_{\text{chrom}}(\lambda) \cdot \Delta\lambda \cdot z. \quad (4.14)$$

We finally, extended the slot duration to  $T_s'$  as depicted in equation (4.15) by including guard bands, to compensate for the ISI effect.

$$T_s' = KL \sqrt{T_c^2 + \Delta t_{\text{modal}}^2 + \Delta t_{\text{chrom}}^2}. \quad (4.15)$$

### 4.3.3.2 Numerical Results

To reduce the complexity and the cost of our optical CDMA network, we have selected an LED as the light source in the transmitter side and a multimode graded index fiber as the channel connecting users to the star coupler. This selection is suitable for typical LANs because of the small distances they cover. Table 4.2 illustrates the optical link specifications.

Table 4.2. Light source and optical fiber specifications.

Light Source	Optical Fiber
<i>LED</i>	<i>Multimode – Graded Index</i>
$\lambda = \{850, 1300, 1550\}$ nm	NA = 0.257, $n_1 = 1.478$
$\Delta\lambda = 50$ nm	$S_o = 0.097$ ps/nm <sup>2</sup> .km
	$\lambda_o = 1343$ nm

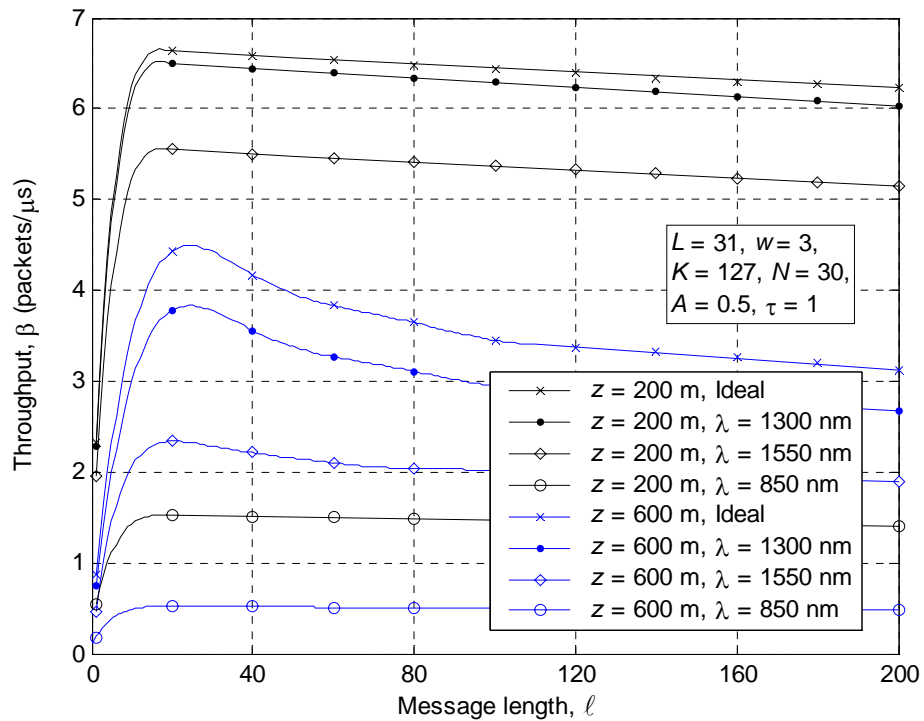


Fig. 4.7. Throughput versus message length for different interstation distances and wavelengths.

The impact of the light dispersion on the performance of the  $R^3T$  protocol is shown in Fig. 4.7, the throughput has been plotted against the message length for various operating wavelengths  $\lambda \in \{1550, 1300, 850\}$  nm, for two different interstation distances  $z = \{200, 600\}$  m. As the message length is increased, the effect of MAI is also increased, and thus the throughput starts to fall as in [7], similar trends are noticed when the dispersion is considered but with lower values of throughput. When operating in the 2<sup>nd</sup> window around the 1300 nm, the effect of the dispersion will be relatively small. There is a performance degradation for longer interstation distances; which verifies equations (4.11) and (4.14).

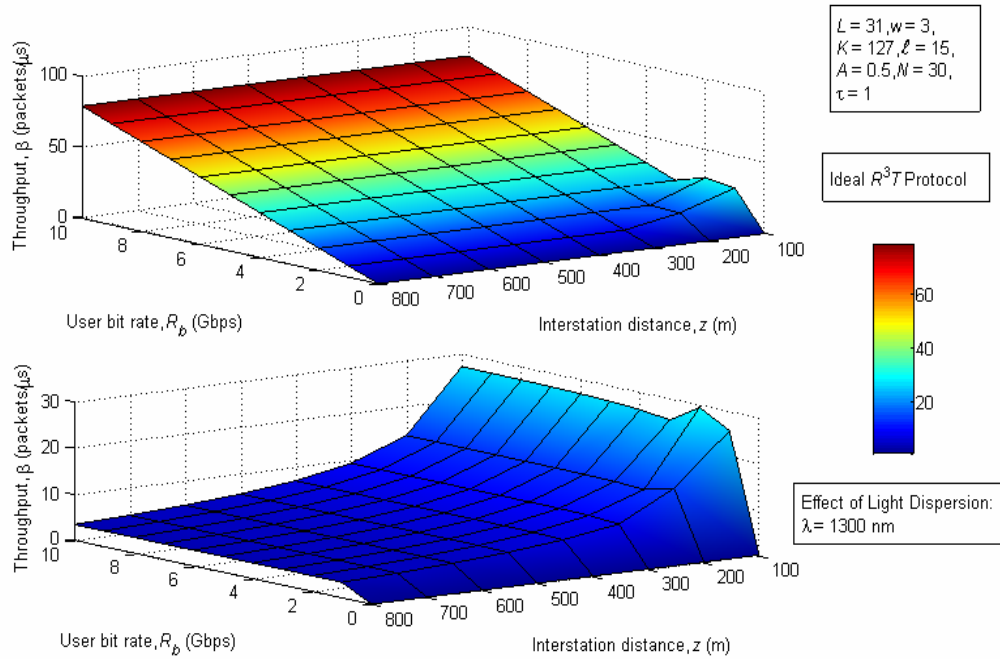


Fig. 4.8. Throughput versus user bit rate for different interstation distances.

Finally the effect of the dispersion in limiting the user bit rate ( $R_b = 1/LT_c$ ) is investigated in Fig. 4.8, where we have plotted the throughput versus the user bit rate for different interstation distances. An operating wavelength  $\lambda = 1300$  nm is selected to ensure minimal effect of dispersion. At lower bit rates, the effect of dispersion is negligible, whereas at higher rates there is an absurd degradation in the performance of the  $R^3T$  protocol.

## 4.4 Conclusions

In this chapter, we presented a brief description of the major limitations in optical communication systems. Focus was oriented towards the receiver's noise and the dispersion in optical fibers. The performance of the  $R^3T$  protocol has been studied in such noisy environments. The Gaussian approximation has been employed in our derivation of the performance of this protocol taking into account the effect of thermal noise. Finally, the dispersion effect was considered. The throughput, the average packet delay and the efficiency of the  $R^3T$  protocol have been derived, simulated and compared with the previous work in [7]. The following concluding remarks can be extracted from our work:

- 1- For a practical value of the receiver's noise temperature ( $T^o/R_L = 6 \text{ K}/\Omega$ ), we can tolerate the effect of thermal noise by reasonably increasing the transmitted power so that the received average peak power reaches a minimum value of -52 dBm.
- 2- A cooling system may be used at the receiver in order to compensate for the effect of thermal noise, Fig. 4.3.
- 3- For small population networks, the effect of noise will be dominant, while for larger networks; the MAI is the main limiting factor.
- 4- The  $R^3T$  protocol exhibits an acceptable average packet delay under the effect of both MAI and thermal noise.
- 5- An asymptotic efficiency of  $\sim 95 \%$  can be reached with suitable selection of link parameters.
- 6- It is clear that when operating in the 2<sup>nd</sup> window and for relatively small interstation distances (LAN), the dispersion effect will be negligible.
- 7- At relatively small user bit rates ( $R_b < 3 \text{ Gbps}$ ), the effect of dispersion is marginal, Fig. 4.8. There also exist optimum values of rates that maximize the system throughput.

# CHAPTER 5

## THE $R^3T$ OPTICAL RANDOM ACCESS CDMA PROTOCOL WITH QUEUING SUBSYSTEM

### Outline:

- **Scope and Motivation**
- **System Architecture**
- **Mathematical Model**
- **Theoretical Analysis**
- **Simulation Results**
- **Conclusions**

## CHAPTER 5

# THE $R^3T$ OPTICAL RANDOM ACCESS CDMA PROTOCOL WITH QUEUING SUBSYSTEM

### **5.1 Scope and Motivation**

Most of the research in the field of optical CDMA has focused on the physical layer [9]-[11], and [18]-[26]. However, a few authors have examined the data link layer of optical CDMA networks [4]-[7], and [40]. In [7], Shalaby has introduced a new protocol called round robin receiver/transmitter ( $R^3T$ ) protocol, which was based on a go-back  $n$  automatic repeat request (ARQ). In his model, Shalaby has assumed that each node is equipped with a single buffer to store only a single message (the message that is being served); any arrival to a nonempty buffer was discarded. This of course gives rise to a blocking probability and thus limits the system throughput.

In this chapter, we aim at enhancing the performance of the  $R^3T$  model by introducing a queuing subsystem, namely increasing the number of available buffers. A detailed state diagram is outlined and a mathematical model based on the equilibrium point analysis (EPA) is presented. In addition, the steady state system throughput, the protocol efficiency, and the timeout probability are derived and evaluated under several network parameters. We proved by numerical analysis that a significant improvement in the protocol performance can be achieved by only adding a single buffer to the system.

### **5.2 System Architecture**

In this section, we discuss the hardware implementation of our optical CDMA network and investigate the optical link layer of the proposed model.

#### **5.2.1 Optical CDMA Network**

In a typical optical CDMA network there would be  $N$  transmitter and receiver pairs (nodes or users). Figure 5.1 shows one such network in a star configuration.

Each node is equipped with a queuing system followed by a fixed CDMA encoder and a tunable CDMA decoder; that is a fixed transmitter-tunable receiver (FT-TR). The transmitter generates an optical ON-OFF keying CDMA (OOK-CDMA) signal (according to its signature sequence) that represents its data. Users are assigned these signature codes randomly from a set of direct-sequence optical-orthogonal codes (OOCs); denoted by  $\phi(L, w, \lambda_a, \lambda_c)$ , where  $L$  is the code length,  $w$  is the code weight, and  $\lambda_a$  and  $\lambda_c$  are the auto-correlation and cross correlation constraints, respectively. A code may be given to more than one user. Further, a code is randomly cyclic shifted around itself upon assignment in order to reduce the effect of MAI.

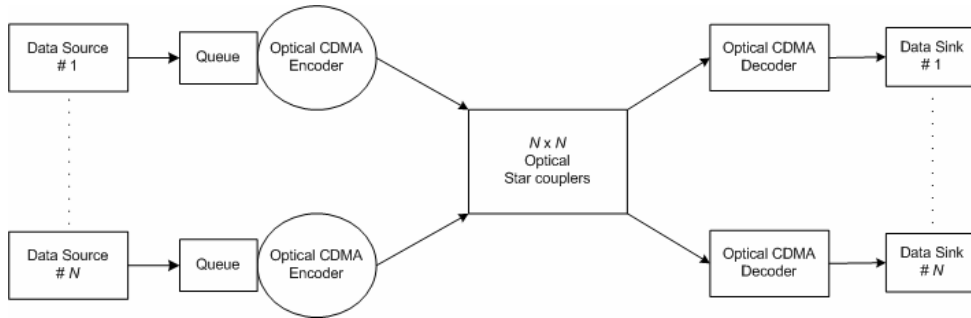


Fig. 5.1. An optical CDMA network in a star configuration

Chip-level receivers [26] are used because of their high ability to overcome the effect of multiple-access interference (MAI). The packet success probability  $P_s(r')$  given  $r'$  active users for this receiver has been derived in Subsection 2.5.2, where we have considered only the effect of MAI. In our analysis, both receiver shot noise and thermal noise are neglected in order to be able to compare our results with [7]. The impact of noise and dispersion on the performance of the modified protocol can be easily considered as in [37] and [41].

### 5.2.2 Optical CDMA Protocol

In the  $R^3T$  protocol many assumptions were imposed [7]. Briefly, time is slotted with a slot size  $T_s$ . Each node has a single buffer to store only the message being served, connection requests and acknowledgements are exchanged between stations, and finally the ARQ used is a go-back  $n$  protocol that depends on the two-way propagation time which is assumed to be equal to  $t$  time slots. The drawback of



$R^3T$  is that any message that arrives will be dropped unless the buffer is empty. This gives rise to a high blocking probability. In this chapter we introduce a queuing subsystem that is able to store one more message (message waiting to be served) if the main buffer is busy. We impose the following assumptions in our model for optical CDMA protocol:

- A maximum of one message can arrive at each time slot to a station with probability  $A$  (also called user activity) and is stored in the queue if the server is busy.
- Any arrival to a non empty queue is blocked.
- The queue is freed once the stored message is moved to the server for being transmitted.
- A station scans for connection requests only after a successful transmission or reception or when it is idle.
- A priority is given for the reception mode than for the transmission mode.

### **5.3 Mathematical Model**

The state diagram of the  $R^3T$  protocol with a single buffer in the queue is illustrated in Figs. 5.2-5.7 Each state is labeled by its number of users. States marked with a '0' indicate that the buffer is empty while a '1' indicates that the buffer is full. Transition between states is on a slot basis; that is the duration of each state equals to one time slot. Users move from states marked with '0' to states marked with '1' if there is a message arrival (event happening with a probability  $A$ ). Messages will be blocked if the users have their queues full and there is a message arrival except for these three cases:

- 1- After successful transmission
- 2- After successful reception.
- 3- After request.

In these cases, users will move to the requesting mode marked with a '1'.

At any time slot, any user in the network will be in one of the following states or modes:

- Initial state,  $\{m\}$ . Users in the initial state scan across all codes in a round-robin manner. If a connection request (event happening with a probability  $\sigma$ ) is found,

they will proceed to the acknowledgement mode. If there is a message arrival and there is no connection request, they will go to the requesting mode. If there is neither a message arrival nor a connection request, the station will remain in the initial state.

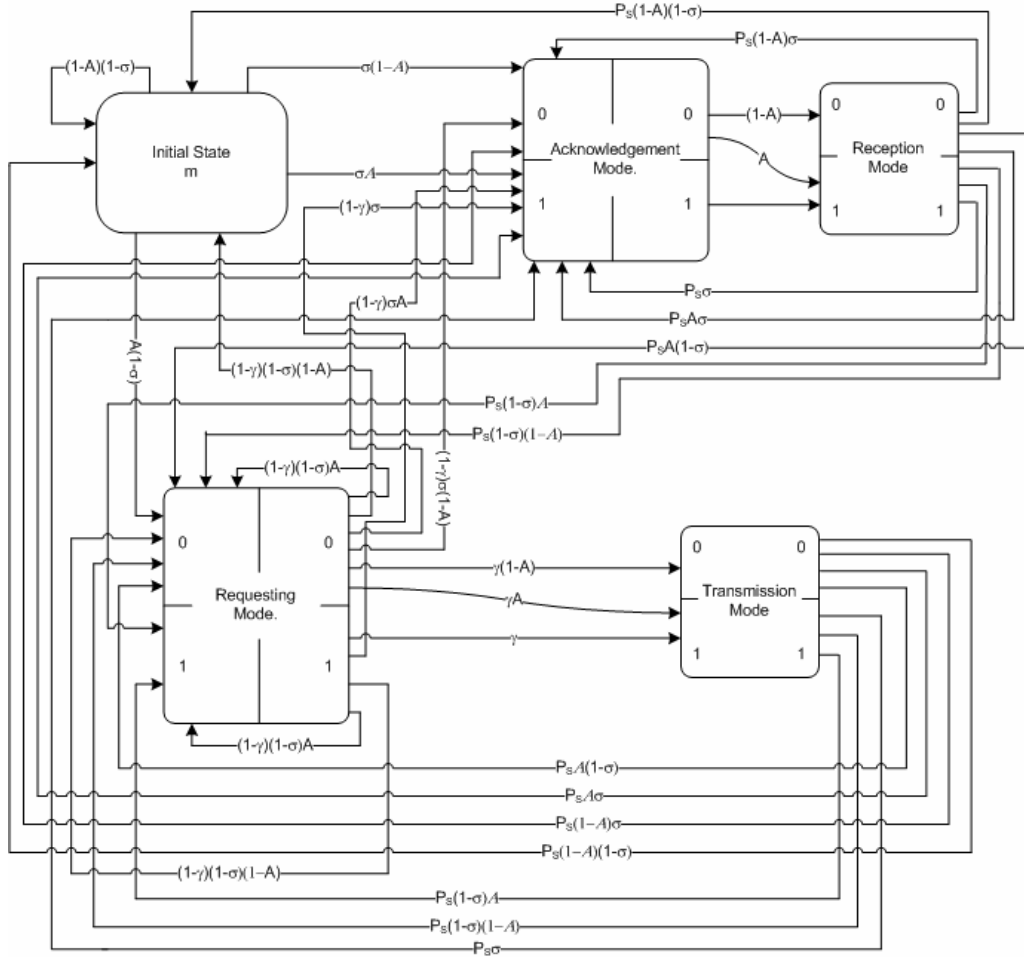


Fig. 5.2. Complete state diagram of the  $R^3T$  optical CDMA protocol with a single buffer in the queue.

- Requesting mode,  $\{q_{1,0}, q_{2,0}, \dots, q_{\tau,0}, q_{1,1}, q_{2,1}, \dots, q_{\tau,1}\}$ . Stations in this mode send repeated requests  $\{q_{1,0}, q_{2,0}, \dots, q_{\tau,0}, q_{1,1}, q_{2,1}, \dots, q_{\tau,1}\}$  for  $\tau$  time slots, where  $1 \leq \tau \leq t$  is the time out duration in time slots. Then the station should wait for a feed back and thus enters a waiting mode  $\{W_{1,0}^q, W_{2,0}^q, \dots, W_{t-1,0}^q, W_{1,1}^q, W_{2,1}^q, \dots, W_{t-1,1}^q\}$ , for  $t-1$  time slots, as depicted in Fig. 5.3. Whenever a waiting station gets a positive acknowledgement (event occurring with a probability  $\gamma$ ) from the destination, it starts sending its message and enters the transmission

mode, otherwise it remains in the waiting mode. In the last waiting state, if an acknowledgement is not received, the station is timed out, it then enters either the initial state or the acknowledgement mode or the requesting mode, depending on the user activity and the connection requests found at that time.

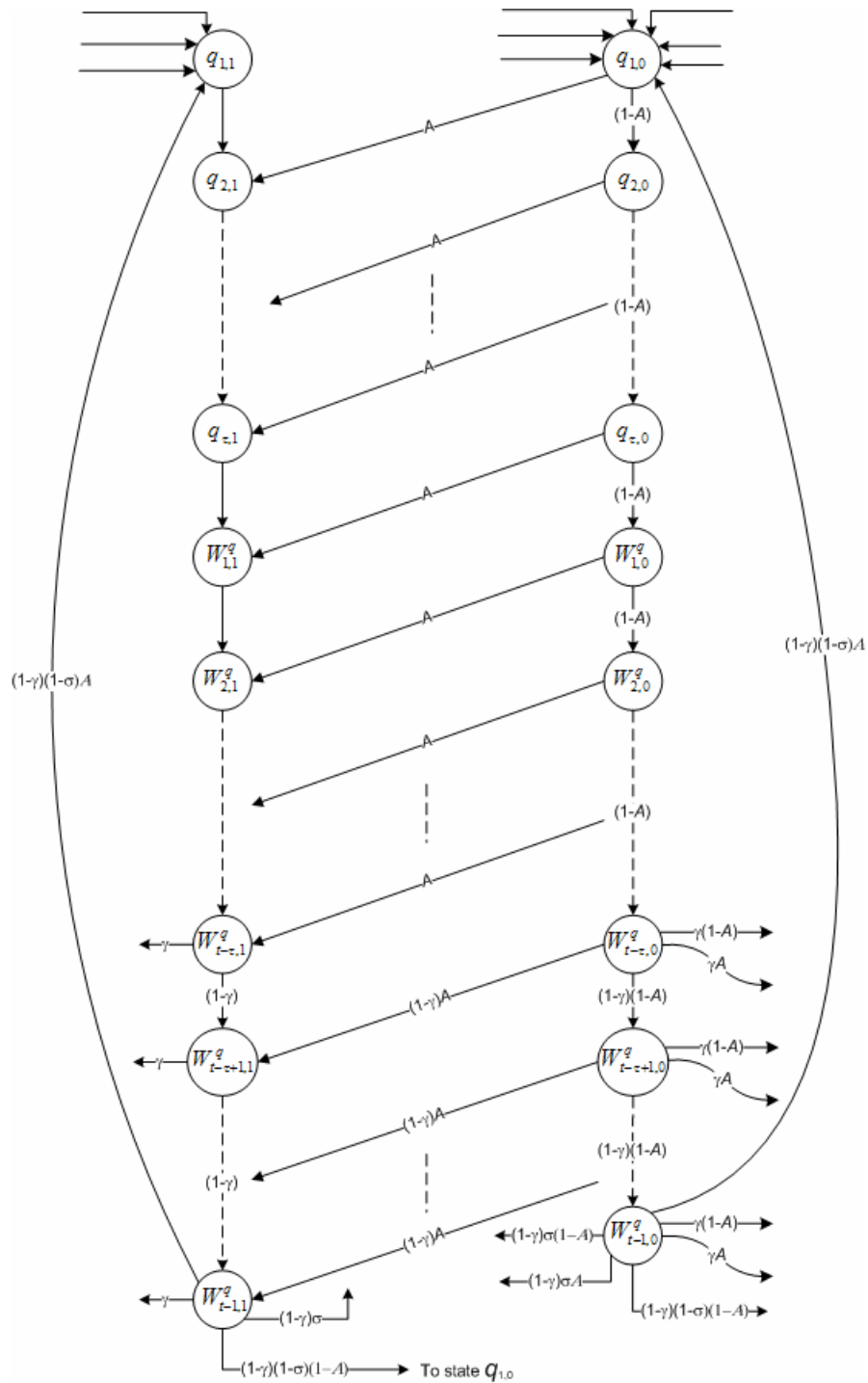


Fig. 5.3. Detailed state diagram of the requesting mode.

- Acknowledgement mode,  $\{a_{1,0}, a_{2,0}, \dots, a_{t,0}, a_{1,1}, a_{2,1}, \dots, a_{t,1}\}$ . Users in this mode send an acknowledgement to the requesting user and wait for  $t$  time slots till the reception of the first packet as inferred from Figs. 5.2 and 5.4.

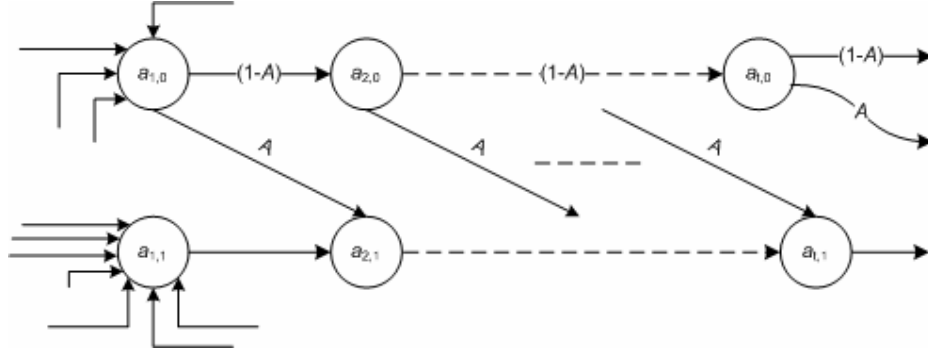


Fig. 5.4. Detailed state diagram of the acknowledgement mode.

- Reception mode,  $\{Rx_1, Rx_2, \dots, Rx_\ell\}$ . A user in the reception mode receives either new packets or retransmitted ones. Figure 5.5 illustrates the structure of the reception mode and the states  $R_{X_i}$ ,  $i \in \{1, 2, \dots, \ell\}$ . In states  $\{s_{i,0}, s_{i,1}\}$ , a user receives packet  $i$ , if it is successfully received, the user will move to states  $\{s_{i+1,0}, s_{i+1,1}\}$ , otherwise he will ask for retransmission and enters a waiting mode  $\{W_{1,0}^{si}, W_{2,0}^{si}, \dots, W_{t-1,0}^{si}, W_{1,1}^{si}, W_{2,1}^{si}, \dots, W_{t-1,1}^{si}\}$ . If the station receives the last packet  $\ell$  successfully it moves to either the initial state or the acknowledgement mode or the requesting mode, depending on the arrivals and the connection requests found at that time.
- Transmission mode,  $\{r_1, r_2, \dots, r_t, Tx_{t+1}, Tx_{t+2}, \dots, Tx_\ell\}$ . Figure 5.6 illustrates the detailed state diagram of the transmission mode. A station is in the state  $r_n$ ,  $n \in \{1, 2, \dots, t\}$  if it is transmitting the first  $t < \ell$  packets, Fig. 5.7a. The station moves to states  $\{r_{t+1,0}, r_{t+1,1}\}$  of  $T_{X,t+1}$  if the first packet was transmitted successfully, otherwise it will retransmit the first  $t$  packets. Users in states  $\{r_{t+i,0}, r_{t+i,1}\}$  of  $T_{X,t+i}$ ,  $i \in \{1, 2, \dots, \ell - t\}$ , shown in Fig. 5.7b are transmitting packet  $t+i$ , and waiting for the status of packet  $i+1$ . If a positive feedback is received, the user will transmit the next packet  $t+i+1$ , otherwise it will retransmit this corrupted packet and all subsequent packets; states

$\{e_{i+1,0}^i, e_{i+2,0}^i, \dots, e_{i+t-1,0}^i, r_{t+i,0}, e_{i+1,1}^i, e_{i+2,1}^i, \dots, e_{i+t-1,1}^i, r_{t+i,1}\}$ . If the last packet is transmitted successfully, the station enters a waiting mode  $\{Wx_1, Wx_2, \dots, Wx_{t-1}\}$  shown in Fig. 5.7c to collect the status of the last  $t-1$  packets. This mode involves two sets of states; retransmitting states and waiting states denoted by  $\{e_{\ell-t+i+1,0}^{\ell-t+i}, e_{\ell-t+i+2,0}^{\ell-t+i}, \dots, e_{\ell,0}^{\ell-t+i}, e_{\ell-t+i+1,1}^{\ell-t+i}, e_{\ell-t+i+2,1}^{\ell-t+i}, \dots, e_{\ell,1}^{\ell-t+i}\}$  and  $\{W_{1,0}^{ei}, W_{2,0}^{ei}, \dots, W_{i-1,0}^{ei}, W_{1,1}^{ei}, W_{2,1}^{ei}, \dots, W_{i-1,1}^{ei}\}$ , respectively. If the station receives a positive status for the last transmitted packet it enters either the initial state or the acknowledgement mode or the requesting mode, according to the message arrival and the connection requests found at that time.

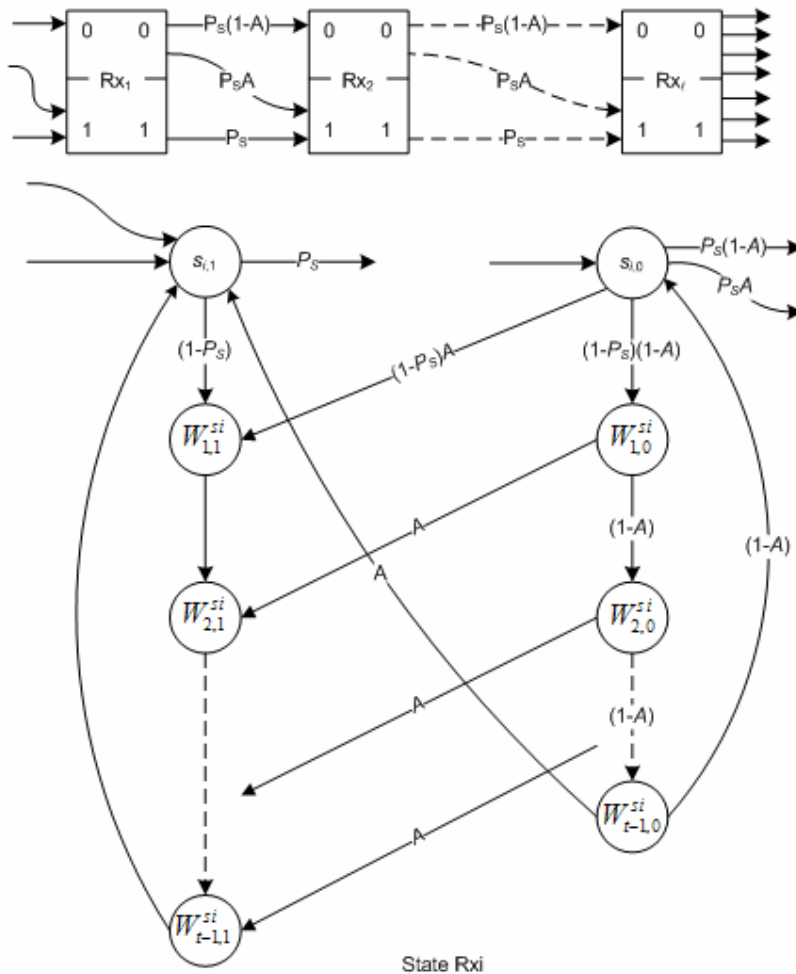


Fig. 5.5. Detailed state diagram of the reception mode.

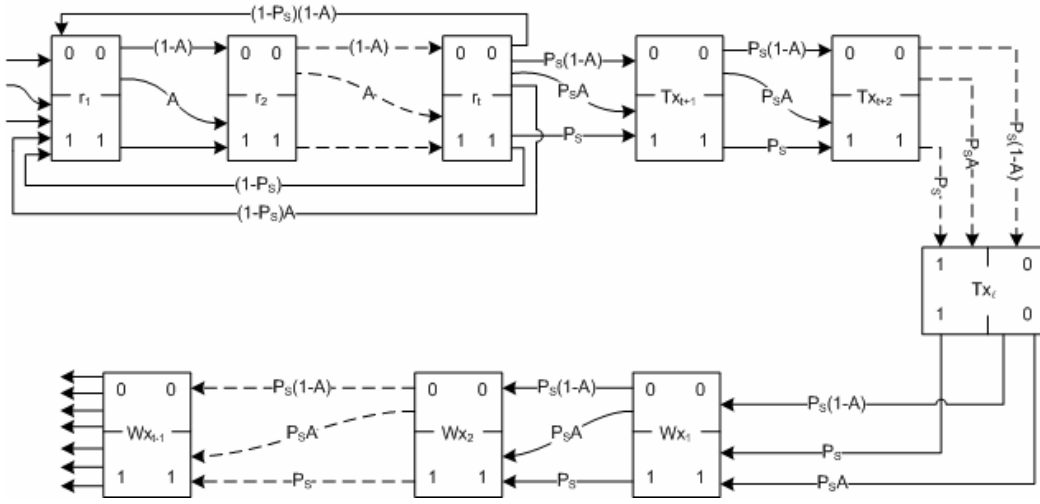


Fig. 5.6. Detailed state diagram of the transmission mode.

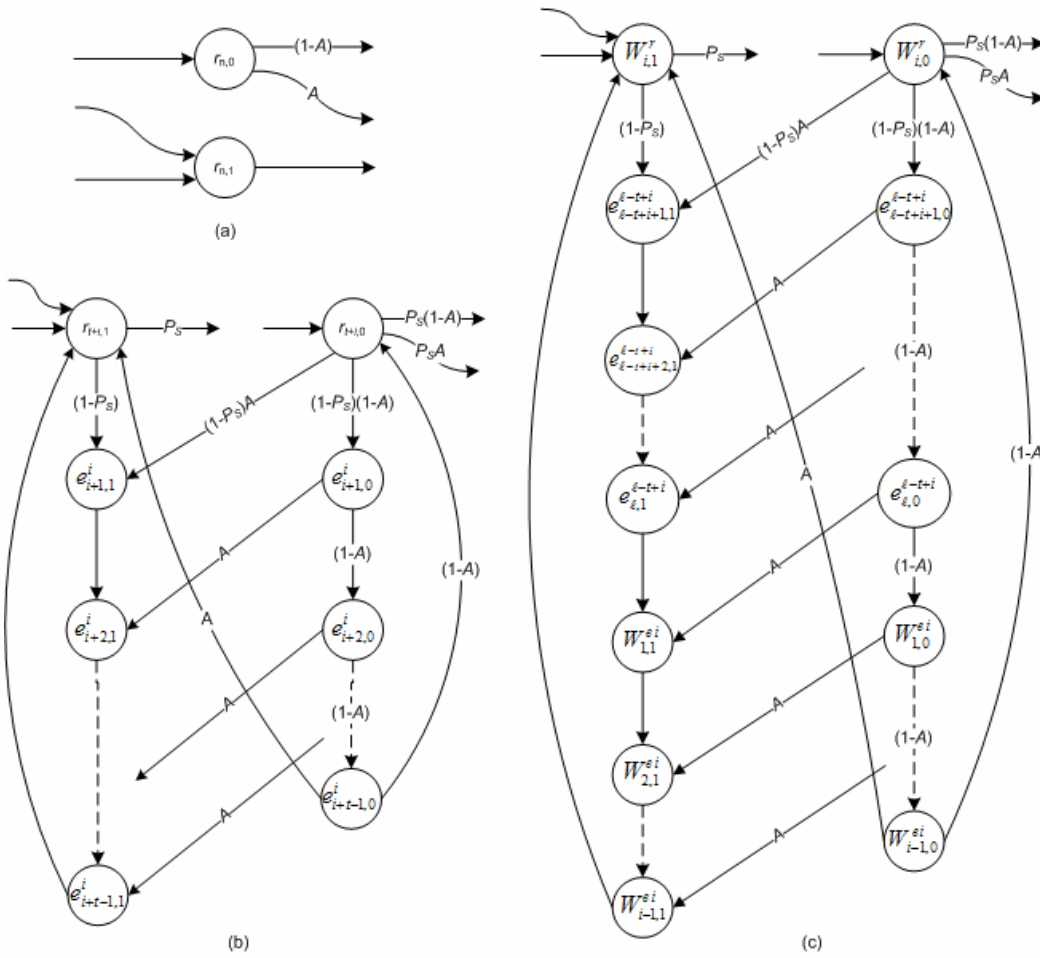


Fig. 5.7. (a) State  $r_n$ , (b) State  $Tx_{t+i}$ , (c) State  $W_{X_i}$ .

## 5.4 Theoretical Analysis

In this section, we evaluate the performance of the  $R^3T$  protocol with a queuing subsystem in terms of the steady state system throughput, the protocol efficiency and the timeout probability.

### 5.4.1 State Diagram Analysis

Because of the complexity of the mathematical model described above, our analysis will be based on the equilibrium point analysis (EPA) to measure the performance of this random access protocol. Each mode will be divided into two sets of states: states marked with '0' indicating that the buffer is empty and states marked with '1' indicating that the buffer is full. By writing down the flow equations for all the states, we can derive the steady state system throughput, protocol efficiency, and the timeout probability.

#### 5.4.1.1. Transmission Mode

This mode involves states  $\{r_1, r_2, \dots, r_t, Tx_{t+1}, Tx_{t+2}, \dots, Tx_\ell\}$ . From Figs. 5.2, 5.6, and 5.7a, we have the following flow equations for  $n \in \{1, 2, \dots, t\}$ :

$$r_{n,0} = (1-A)^{n-1} \cdot r_{1,0} \quad , \quad r_{n,1} = r_{1,1} + [1 - (1-A)^{n-1}] \cdot r_{1,0}. \quad (5.1)$$

From Fig. 5.7b, we can write the flow equations for each state in  $Tx_{t+i}$ ,  $i \in \{1, 2, \dots, \ell - t\}$ :

$$\begin{aligned} r_{t+i,0} &= \chi^i \cdot r_{t,0} \\ r_{t+i,1} &= r_{t,1} + (1 - \chi^i) \cdot r_{t,0} \end{aligned} \quad , \quad \text{where } \chi = \frac{P_S(1-A)}{1 - (1-P_S)(1-A)^t}. \quad (5.2)$$

Whereas for the retransmission states where  $j \in \{1, 2, \dots, t-1\}$ , we have:

$$\begin{aligned} e_{t+j,0}^i &= (1-P_S) \cdot \chi^i (1-A)^j \cdot r_{t,0} \\ e_{t+j,1}^i &= (1-P_S) \cdot r_{t,1} + (1-P_S) \cdot [1 - \chi^i (1-A)^j] \cdot r_{t,0} \end{aligned} .$$

Similarly, for the waiting states  $W_{X_i}$ ,  $i \in \{1, 2, \dots, t-1\}$  shown in Fig. 5.7c we have:

$$W_{i,0}^r = \chi^i \cdot r_{\ell,0} \quad , \quad W_{i,1}^r = r_{\ell,1} + (1 - \chi^i) \cdot r_{\ell,0}, \quad (5.3)$$

$$\begin{aligned}
e_{\ell-t+i+j,0}^{t-i} &= (1-P_S)\chi^i(1-A)^j \cdot r_{\ell,0} \\
e_{\ell-t+i+j,1}^{t-i} &= (1-P_S) \cdot r_{\ell,1} + (1-P_S)\left[1 - \chi^i(1-A)^j\right] \cdot r_{\ell,0}, & j \in \{1,2,\dots,t-i\} \\
W_{k,0}^{ei} &= \chi^i(1-P_S)(1-A)^{t-i+k} \cdot r_{\ell,0} \\
W_{k,1}^{ei} &= (1-P_S) \cdot r_{\ell,1} + (1-P_S)\left[1 - \chi^i(1-A)^{t-i+k}\right] \cdot r_{\ell,0}. & k \in \{1,2,\dots,i-1\}
\end{aligned}$$

Let the set of variables  $[Y_0, Y_1, Y]$  denotes the number of users in state  $Y$  with either empty buffer, or full buffer or regardless of the state of the buffer respectively. We define the following variables:

$$\begin{aligned}
&\left[ r_0 = \sum_{i=1}^{\ell} r_{i,0}, \quad r_1 = \sum_{i=1}^{\ell} r_{i,1}, \quad r = r_0 + r_1 \right] \\
&\left[ W_0^r = \sum_{i=1}^{t-1} W_{i,0}^r, \quad W_1^r = \sum_{i=1}^{t-1} W_{i,1}^r, \quad W^r = W_0^r + W_1^r \right] \\
&\left[ e_0 = \sum_{i=1}^{\ell-t} \sum_{j=1}^{t-1} e_{i+j,0}^i + \sum_{i=1}^{t-1} \sum_{j=1}^{t-i} e_{\ell-t+i+j,0}^{\ell-t+i}, \quad e_1 = \sum_{i=1}^{\ell-t} \sum_{j=1}^{t-1} e_{i+j,1}^i + \sum_{i=1}^{t-1} \sum_{j=1}^{t-i} e_{\ell-t+i+j,1}^{\ell-t+i}, \quad e = e_0 + e_1 \right] \\
&\left[ W_0^e = \sum_{i=1}^{t-1} \sum_{j=1}^{i-1} W_{j,0}^{ei}, \quad W_1^e = \sum_{i=1}^{t-1} \sum_{j=1}^{i-1} W_{j,1}^{ei}, \quad W^e = W_0^e + W_1^e \right]
\end{aligned}$$

Performing the above summations (only for  $Y_0$  and  $Y$ ), which involve mathematical series, we obtain:

$$\begin{aligned}
r_0 &= \left[ \frac{1-(1-A)^t}{A} \right] \cdot r_{1,0} + \left( \frac{\chi}{1-\chi} \right) (1-\chi^{\ell-t}) \cdot r_{\ell,0}, & r = \ell(r_{1,0} + r_{1,1}), \\
W_0^r &= \left( \frac{\chi}{1-\chi} \right) (1-\chi^{\ell-t}) \cdot r_{\ell,0}, & W^r = (t-1)(r_{1,0} + r_{1,1}), \\
e_0 &= (1-P_S) \left( \frac{1-A}{A} \right) \left( \frac{\chi}{1-\chi} \right) \left[ 1 - (1-A)^{t-1} \right] (1-\chi^{\ell-t}) \cdot r_{\ell,0} \\
&+ (1-P_S) \left( \frac{1-A}{A} \right) \left[ \left( \frac{\chi}{1-\chi} \right) (1-\chi^{t-1}) + (1-A)^t \left( \frac{\chi}{\chi - (1-A)} \right) \left( 1 - \left( \frac{\chi}{1-A} \right)^{t-1} \right) \right] \cdot r_{\ell,0}, \quad (5.4) \\
e &= (1-P_S)(t-1)(\ell-t/2)(r_{1,0} + r_{1,1}), \\
W_0^e &= (1-P_S) \left[ \frac{(1-A)^{Y+1}}{A} \right] \left[ \left( \frac{\chi}{\chi - (1-A)} \right) \left( \left( \frac{\chi}{1-A} \right)^{t-1} - 1 \right) - \frac{\chi \cdot (1-\chi^{t-1})}{(1-\chi)(1-A)} \right] \cdot r_{\ell,0} \\
W^e &= (1-P_S)(t-1) \left( \frac{t}{2} - 1 \right) (r_{1,0} + r_{1,1}).
\end{aligned}$$



### 5.4.1.2. Reception Mode

From Figs. 5.2 and 5.5, we can write the flow equations for states  $\{s_{i,0}, s_{i,1}\}$ , for  $i \in \{1, 2, \dots, \ell\}$  as follows:

$$s_{i,0} = \frac{\chi^i}{P_S} \cdot a_{t,0} \quad , \quad s_{i,1} = \frac{1}{P_S} \cdot a_{t,1} + \frac{1}{P_S} (1 - \chi^i) \cdot a_{t,0}. \quad (5.5)$$

From the above equations, it is obvious that

$$s_{i,0} + s_{i,1} = \frac{1}{P_S} (a_{t,0} + a_{t,1}).$$

Relating the reception mode to the transmission mode, we assume that the number of users transmitting the first packet must be equal to the number of users receiving the same packet, yielding

$$r_{1,0} + r_{1,1} = s_{1,0} + s_{1,1} \quad \Rightarrow \quad r_{1,0} + r_{1,1} = \frac{1}{P_S} (a_{t,0} + a_{t,1}). \quad (5.6)$$

Next we write the flow equations for the waiting states for  $j \in \{1, 2, \dots, t-1\}$  as follows:

$$W_{j,0}^{S_i} = \left( \frac{1 - P_S}{P_S} \right) \cdot \chi^i (1 - A)^j \cdot a_{t,0},$$

$$W_{j,1}^{S_i} = \left( \frac{1 - P_S}{P_S} \right) \cdot a_{t,1} + \left( \frac{1 - P_S}{P_S} \right) (1 - \chi^i (1 - A)^j) \cdot a_{t,0}.$$

We define the following variables:

$$\left[ s_0 = \sum_{i=1}^{\ell} s_{i,0} \quad , \quad s_1 = \sum_{i=1}^{\ell} s_{i,1} \quad , \quad s = s_0 + s_1 \right]$$

$$\left[ W_0^s = \sum_{i=1}^{\ell} \sum_{j=1}^{t-1} W_{j,0}^{S_i} \quad , \quad W_1^s = \sum_{i=1}^{\ell} \sum_{j=1}^{t-1} W_{j,1}^{S_i} \quad , \quad W^s = W_0^s + W_1^s \right]$$

Performing the above summations, and using equation (5.6) we obtain:

$$s_0 = \frac{1}{P_S} \left( \frac{\chi(\chi^{\ell} - 1)}{\chi - 1} \right) \cdot a_{t,0} \quad , \quad s = \ell (r_{1,0} + r_{1,1}),$$

$$W_0^s = \left( \frac{1 - P_S}{P_S} \right) \left[ \frac{\chi(\chi^{\ell} - 1)}{\chi - 1} \cdot \frac{(1 - A)(1 - (1 - A)^{t-1})}{A} \right] \cdot a_{t,0}, \quad (5.7)$$

$$W^s = \ell(t-1)(1 - P_S)(r_{1,0} + r_{1,1}).$$

### 5.4.1.3. Acknowledgement Mode

Again by writing the flow equations for the states in this mode, described in Fig. 5.4, and for  $i \in \{1, 2, \dots, t\}$ , we get:

$$a_{i,0} = (1-A)^{i-1} \cdot a_{1,0} \quad , \quad a_{i,1} = a_{1,1} + \left(1 - (1-A)^{i-1}\right) \cdot a_{1,0}. \quad (5.8)$$

Noting that  $a_{i,0} + a_{i,1} = a_{1,0} + a_{1,1}$ , we can rewrite equation (5.6) as follows:

$$r_{1,0} + r_{1,1} = s_{1,0} + s_{1,1} = \frac{1}{P_S} (a_{1,0} + a_{1,1}). \quad (5.9)$$

Similarly, we define the set of variables  $[a_0, a_1, a]$ .

From equation (5.9) and solving for  $a_0$  and  $a$ , one gets:

$$a_0 = \left( \frac{1 - (1-A)^t}{A} \right) \cdot a_{1,0} \quad , \quad a = tP_S \cdot (r_{1,0} + r_{1,1}). \quad (5.10)$$

### 5.4.1.4. Requesting Mode

Figure 5.3 illustrates the requesting states and waiting states in the requesting mode. We write down the flow equations for these states as follows:

$$\begin{aligned} q_{j,0} &= (1-A)^{j-1} \cdot q_{1,0} \\ q_{j,1} &= q_{1,1} + \left(1 - (1-A)^{j-1}\right) \cdot q_{1,0} \end{aligned} \quad , \quad j \in \{1, 2, \dots, \tau\}. \quad (5.11)$$

Considering the waiting states for which  $k \in \{1, 2, \dots, t - \tau\}$  and  $i \in \{1, 2, \dots, \tau - 1\}$  we have:

$$\begin{aligned} W_{k,0}^q &= (1-A)^{\tau+k-1} \cdot q_{1,0} \quad , \quad W_{k,1}^q = q_{1,1} + \left(1 - (1-A)^{\tau+k-1}\right) \cdot q_{1,0} \\ W_{t-\tau+i,0}^q &= (1-A)^{t-1} \left( (1-A)(1-\gamma) \right)^i \cdot q_{1,0} \quad . \\ W_{t-\tau+i,1}^q &= (1-\gamma)^i \cdot q_{1,1} + (1-\gamma)^i \left(1 - (1-A)^{t-1+i}\right) \cdot q_{1,0} \end{aligned} \quad (5.12)$$

To relate the requesting mode to the transmission mode, we will write the flow equations into state  $r_1$  as follows:

$$\begin{aligned} r_{1,0} &= \gamma \cdot (1-A) \cdot \left[ W_{t-\tau,0}^q + W_{t-\tau+1,0}^q + \dots + W_{t-1,0}^q \right] + (1-P_S)(1-A) \cdot r_{t,0} \\ r_{1,1} &= \gamma \cdot A \cdot \left[ W_{t-\tau,0}^q + W_{t-\tau+1,0}^q + \dots + W_{t-1,0}^q \right] + (1-P_S) \cdot A \cdot r_{t,0} \quad . \\ &\quad + \left[ W_{t-\tau,1}^q + W_{t-\tau+1,1}^q + \dots + W_{t-1,1}^q \right] \cdot \gamma + (1-P_S) \cdot r_{t,1} \end{aligned} \quad (5.13)$$

Substituting from equations (5.1) and (5.12) in (5.13) we can get:

$$q_{1,0} = \frac{P_S}{\gamma \cdot \chi \cdot (1-A)^{t-1}} \cdot \left[ \frac{1-(1-A)(1-\gamma)}{1-[(1-A)(1-\gamma)]^\tau} \right] \cdot r_{1,0}$$

$$(r_{1,0} + r_{1,1}) = \frac{1}{P_S} [1-(1-\gamma)^\tau] \cdot (q_{1,0} + q_{1,1})$$
(5.14)

Thus, we can define the following variables:

$$q_0 = \sum_{j=1}^{\tau} q_{j,0} = \left( \frac{1-(1-A)^\tau}{A} \right) \cdot \frac{P_S}{\gamma \cdot \chi \cdot (1-A)^{t-1}} \cdot \left[ \frac{1-(1-A)(1-\gamma)}{1-[(1-A)(1-\gamma)]^\tau} \right] \cdot r_{1,0}$$

$$q_1 = \sum_{j=1}^{\tau} q_{j,1} \quad , \quad q = q_0 + q_1 = \tau \cdot \left[ \frac{P_S}{1-(1-\gamma)^\tau} \right] \cdot (r_{1,0} + r_{1,1})$$

$$W_0^q = \sum_{k=1}^{t-\tau} W_{k,0}^q + \sum_{i=1}^{\tau-1} W_{t-\tau+i,0}^q$$

$$= \left[ \frac{(1-A)^\tau}{A} (1-(1-A)^{t-\tau}) + \frac{(1-A)^\tau (1-\gamma)}{1-(1-A)(1-\gamma)} (1-[(1-A)(1-\gamma)]^{\tau-1}) \right]$$

$$\cdot \left[ \frac{P_S}{\gamma \cdot \chi \cdot (1-A)^{t-1}} \right] \cdot \left[ \frac{1-(1-A)(1-\gamma)}{1-[(1-A)(1-\gamma)]^\tau} \right] \cdot r_{1,0}$$
(5.15)

$$W_1^q = \sum_{k=1}^{t-\tau} W_{k,1}^q + \sum_{i=1}^{\tau-1} W_{t-\tau+i,1}^q$$

$$W^q = W_0^q + W_1^q = \left[ t - \tau - 1 + \frac{1}{\gamma} (1-(1-\gamma)^\tau) \right] \cdot \left[ \frac{P_S}{1-(1-\gamma)^\tau} \right] \cdot (r_{1,0} + r_{1,1}).$$

From Figs. 5.2, and 5.4, we can also write the flow equations into states  $\{a_{1,0}, a_{1,1}\}$ , as follows:

$$a_{1,0} = \sigma(1-A) \cdot m + P_S \sigma(1-A) \cdot (s_{\ell,0} + W_{t-1,0}^r) + (1-\gamma) \sigma(1-A) \cdot W_{t-1,0}^q$$

$$a_{1,1} = \sigma A \cdot m + P_S \sigma A \cdot (s_{\ell,0} + W_{t-1,0}^r) + P_S \sigma \cdot (s_{\ell,1} + W_{t-1,1}^r)$$

$$+ (1-\gamma) \sigma A \cdot W_{t-1,0}^q + (1-\gamma) \sigma \cdot W_{t-1,1}^q$$
(5.16)

Solving the above two equations simultaneously, the initial state can be written as:

$$m = \frac{P_S}{\sigma} \left[ 1 - 2\sigma - \sigma \left( \frac{(1-\gamma)^\tau}{1-(1-\gamma)^\tau} \right) \right] \cdot (r_{1,0} + r_{1,1}) = \left[ \frac{1-\sigma}{\sigma} \right] \cdot a_{1,0}$$
(5.17)

The probability that a request is found by a scanning user,  $\sigma$ , is equal to the probability that another user is in the requesting mode, yielding:

$$\sigma = \frac{1}{N} \sum_{i=1}^{\tau} q_{i,0} + q_{i,1} = \frac{\tau \cdot P_S}{N [1-(1-\gamma)^\tau]} \cdot (r_{1,0} + r_{1,1}).$$
(5.18)

To evaluate  $\sigma$  and  $\gamma$  we need another equation relating  $\sigma$  and  $\gamma$  to be solved with equation (5.18). This relation is obtained by solving the following two equations:

$$\begin{aligned}
q_{1,0} &= A(1-\sigma) \cdot m + P_S A(1-\sigma) \cdot (s_{\ell,0} + W_{t-1,0}^r) + P_S(1-A)(1-\sigma) \cdot (s_{\ell,1} + W_{t-1,1}^r) \\
&\quad + A(1-\sigma)(1-\gamma) \cdot W_{t-1,0}^q + (1-A)(1-\sigma)(1-\gamma) \cdot W_{t-1,1}^q \\
q_{1,1} &= P_S A(1-\sigma) \cdot (s_{\ell,1} + W_{t-1,1}^r) + A(1-\sigma)(1-\gamma) \cdot W_{t-1,1}^q
\end{aligned}$$

## 5.4.2 Performance Measures

In order to evaluate the performance of the proposed model and compare it with the ideal  $R^3T$  protocol, we will derive expressions for the system throughput, the protocol efficiency, and the timeout probability.

### 5.4.2.1 Steady State Throughput

The steady state system throughput  $\beta(N, A, t, \tau, \ell)$  is defined as the average number of successful received packets per slot. It can be calculated as follows:

$$\beta(N, A, t, \tau, \ell) = \sum_{i=1}^{\ell} (s_{i,0} + s_{i,1}) \cdot P_S = P_S(r') \cdot \ell \cdot (r_{1,0} + r_{1,1}). \quad (5.19)$$

Here,  $r'$  denotes the number of users either in transmission states or retransmission states and is given by:

$$r' = r + e = [\ell + (1 - P_S)(t - 1)(\ell - t/2)] \cdot (r_{1,0} + r_{1,1}). \quad (5.20)$$

Substituting back in (5.19), the throughput can be expressed as follows:

$$\beta(N, A, t, \tau, \ell) = \frac{P_S(r') \cdot \ell \cdot r'}{[\ell + (1 - P_S)(t - 1)(\ell - t/2)]} \text{ packets/slot}. \quad (5.21)$$

It is evident that the number of users in the network must be equal to the total number of users in all the states, that is:

$$N = m + r + e + W^r + W^e + s + W^s + a + q + W^q.$$

Substituting with equations (5.4), (5.7), (5.10), (5.15) and (5.17), then using (5.20) one can get:

$$\begin{aligned}
&N[\ell + (1 - P_S)(t - 1)(\ell - t/2)] \\
&= r' \left[ 2\ell + (t - 1) + tP_S + (1 - P_S)(t - 1)(2\ell - 1) + \frac{P_S}{\sigma} - 2P_S \right. \\
&\quad \left. + \left\{ t - 1 - (1 - \gamma)^\tau + \frac{1}{\gamma} (1 - (1 - \gamma)^\tau) \right\} \cdot \frac{P_S}{1 - (1 - \gamma)^\tau} \right]. \quad (5.22)
\end{aligned}$$

That is,  $r'$  is the solution of the above equation.

### 5.4.2.2 Protocol Efficiency

As in the previous chapters, the protocol efficiency  $\eta$  is defined as the ratio between the number of successfully received packets and the number of packets available for transmission:

$$\eta = \frac{\beta(N, A, t, \tau, \ell)}{r'}. \quad (5.23)$$

### 5.4.2.3 Timeout Probability

The timeout probability denoted by  $P_{to}$ , is defined as the probability that a station will time out after entering the requesting mode. For convenience and sake of comparison, we derive the timeout probability for both  $R^3T$  optical random access protocols; with and without transmission queue.

- *$R^3T$  Optical Random Access Protocol without a Queue [7]:*

In this case, the timeout probability is equal to the probability that the station is in the last waiting state  $W_{t-1}^q$  in the requesting mode (Fig. 3.5) and that no acknowledgement is received. Thus, one can write:

$$P_{to} = \frac{W_{t-1}^q}{N} (1 - \gamma).$$

By writing down the flow equation into state  $W_{t-1}^q$  and using equation (3.8), the timeout probability can be expressed as follows:

$$P_{to} = \frac{\beta}{N\ell} \left( \frac{1 - \sigma}{\sigma} \right) A \cdot (1 - \gamma)^\tau. \quad (5.24)$$

- *$R^3T$  Optical Random Access Protocol with a Queue:*

In this case, the timeout probability is given by:

$$P_{to} = \frac{W_{t-1,0}^q + W_{t-1,1}^q}{N} (1 - \gamma).$$

From equation (5.12), we have:

$$W_{t-1,0}^q + W_{t-1,1}^q = (1 - \gamma)^{\tau-1} (q_{1,0} + q_{1,1}).$$

Substituting with equation (5.14) in the above equation and using equation (5.19), the

timeout probability is rewritten as:

$$P_{to} = \frac{\beta}{N\ell} \left[ \frac{(1-\gamma)^\tau}{1-(1-\gamma)^\tau} \right]. \quad (5.25)$$

## 5.5 Simulation Results

In our simulations, we have used a set of OOCs denoted by  $\phi(31,3,1,1)$  as the user signature codes. To guarantee minimal interference between users, we have restricted the auto- and cross-correlation constraints to one. A chip rate of 4 Mchips/s for each user is held constant in our simulations and a packet size of  $K = 127$  bits is considered. It is assumed that a packet should fit in a time slot. We have used the EPA in order to compute the steady state system throughput, the protocol efficiency, and the timeout probability for both  $R^3T$  protocols; with and without a transmission queue. The near-far effect has been neglected since all nodes are uniformly located from the star coupler. Only, the effect of MAI has been taken into account, as it represents the major limitation in CDMA systems. The effect of shot and thermal noise may be added in cases in which physical noise sources are expected to be of interest [37]. Our results are plotted in Figs. 5.8-5.12. A message length of  $\ell = 15$  is imposed in all figures and a timeout duration of  $\tau = 1$  is imposed in all figures but Fig. 5.11. A propagation delay time of  $t \in \{2, 4, 6\}$  is considered in our simulation. This selection of parameters ensures an interstation distance of  $z \in \{200, 400, 600\}$  m.

In Fig. 5.8, we have plotted the throughput versus the number of users  $N$  for both  $R^3T$  protocols with and without a queuing system for different propagation delays (different interstation distances). General trends of the curves can be noticed. As the number of users in the network increases, more packets are available for transmission and thus the throughput increases till it reaches its peak. For the  $R^3T$  protocol without a queuing system, the throughput falls down rapidly as the number of users is further increased, because the effect of MAI becomes more severe. Whereas for the  $R^3T$  protocol with queuing system (buffer), some users may have additional packets stored in their buffer (to be transmitted later on without interference), yielding a slower decay in the throughput. It can be inferred that the throughput is lower for longer propagation delays, which is obvious.

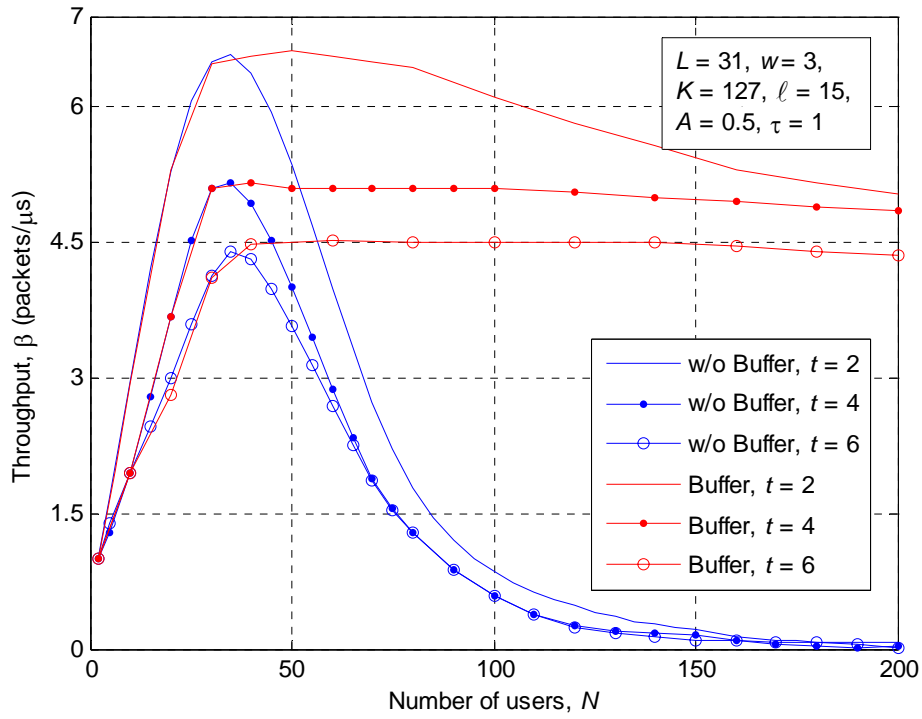


Fig. 5.8. Throughput versus number of users for different propagation delays.

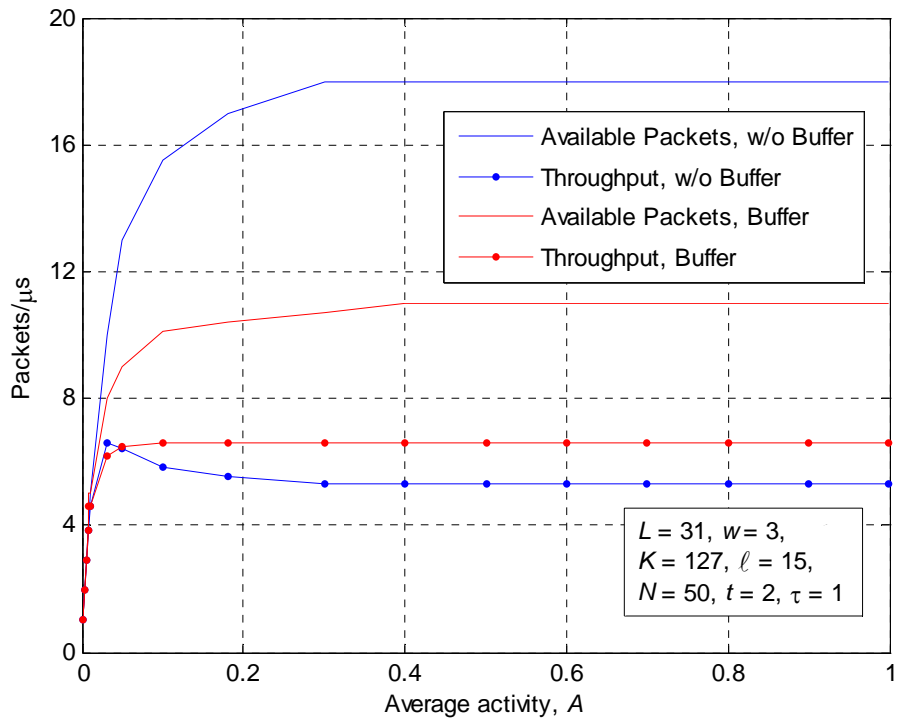


Fig. 5.9. Available packets and throughput versus average activity.

In Fig. 5.9, we have plotted the steady state system throughput and the number of available packets for transmission against the user activity. We have selected  $N = 50$ , as we have argued in Fig. 5.8 that for a certain set of OOCs and for  $N \geq 40$  the throughput of the  $R^3T$  protocol with a queuing system outperforms that of the system without a queue. In fact, the initial increase of throughput is because as  $A$  increases above zero, more packets become available with low interference. It can be noticed that for the system without buffer, the number of available packets for transmission is quite large yielding a significant MAI and thus giving rise to an increased number of retransmitted packets.

Figure 5.10 depicts the relation between the protocol efficiency and the number of users  $N$  in the network. It has been plotted for different values of activities,  $A \in \{0.1, 0.9\}$ . The following results can be extracted: both protocols exhibit high efficiency for a smaller number of users and for relatively small activities. Both  $R^3T$  protocols with and without buffer behave similarly for low population networks, while for larger population networks the system with buffer significantly outperforms the ideal  $R^3T$  protocol.

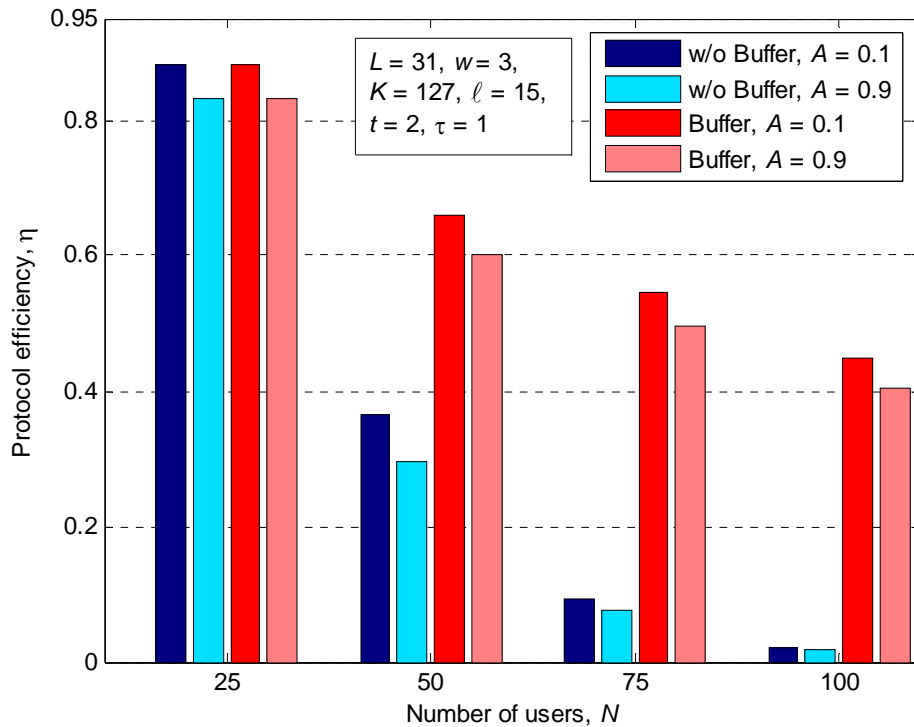


Fig. 5.10. Protocol efficiency versus message length for different number of users.



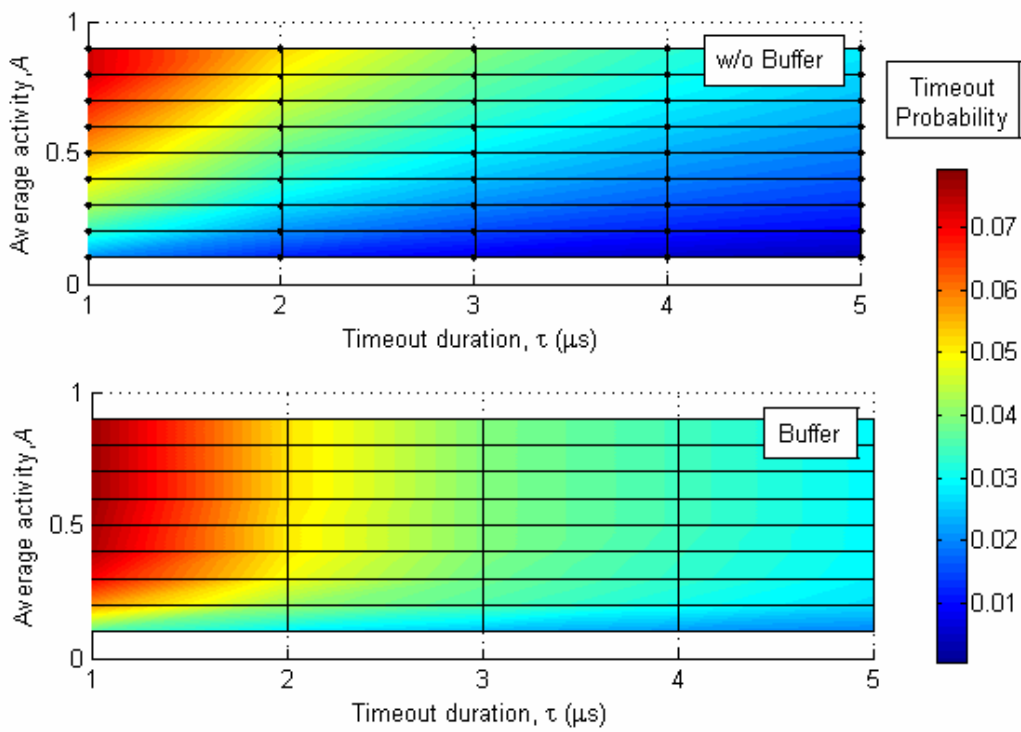
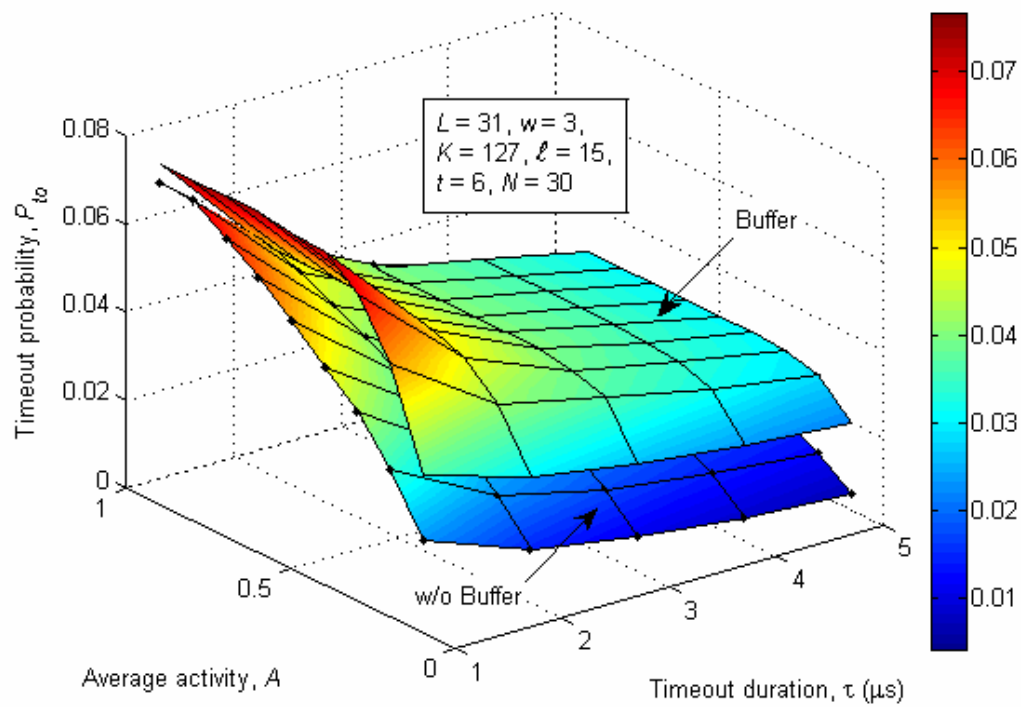


Fig. 5.11. Timeout probability versus average activity and timeout duration.

In Fig. 5.11, the timeout probability has been plotted against the timeout duration and the average activity for both  $R^3T$  protocols. An x-y view has also been plotted for illustration purpose. General trends of the curves can be noticed. As the timeout duration  $\tau$  is increased, users have a greater chance to be acknowledged and thus the timeout probability is decreased. Whereas for larger values of activity, users become busy transmitting their messages and cannot acknowledge further connection requests which makes the timeout probability increases. It is evident that the ideal  $R^3T$  protocol provides a lower timeout probability. This is because when a buffer is added to the system, users will have additional messages (stored in their buffer) to send and thus, they will not have time to acknowledge further requests yielding a higher timeout probability.

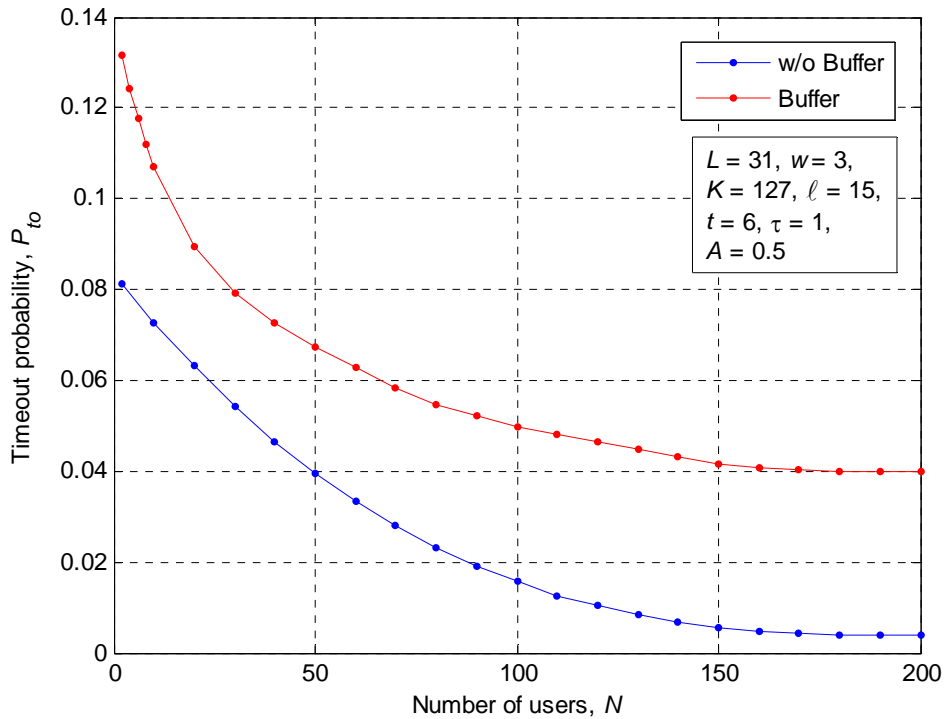


Fig. 5.12. Timeout probability versus number of users.

Finally, the relation between the number of users in the network and the timeout probability is investigated in Fig. 5.12. As argued in Fig. 5.11 and for the same reasons, the  $R^3T$  protocol with a queuing system provides a higher timeout probability. It can be seen that at a given activity level and for larger population

networks, a larger number of users will be able to transmit their messages, yielding a lower timeout probability.

## **5.6 Conclusions**

In this chapter, we have proposed a queuing model to improve the performance of the previously proposed  $R^3T$  protocol. A single buffer was added to each node. Only the effect of MAI was considered. Expressions for throughput, protocol efficiency, and timeout probability have been derived, simulated and compared with that of the  $R^3T$  protocol without queuing. The following concluding remarks can be extracted from our results:

- 1- The proposed modifications to the  $R^3T$  model exhibits better performance for high population networks and under high traffic loads.
- 2- The enhanced  $R^3T$  protocol provides a better efficiency over a wider dynamic range, an asymptotic efficiency of 90 % can be reached, Fig. 5.10.
- 3- The proposed protocol exhibits an acceptable timeout probability.
- 4- Of course the price to be paid for the improvement is the increased system complexity when adding a queuing subsystem.

Other performance metrics such as the blocking probability and the average packet delay can be found in [42]. Therefore, the following conclusions can also be added:

- 5- The blocking probability is significantly reduced by a factor of 50%.
- 6- The queuing delay is added to the total latency of the network, but it is still acceptable.

# CHAPTER 6

## PROPOSED OPTICAL RANDOM ACCESS CDMA PROTOCOL WITH STOP & WAIT ARQ

### Outline:

- Introduction
- System and Hardware Architecture
- Mathematical Model
- Performance Analysis
- Numerical Results
- Conclusions

## CHAPTER 6

# PROPOSED OPTICAL RANDOM ACCESS CDMA PROTOCOL WITH STOP & WAIT ARQ

### 6.1 Introduction

The success of modern communication systems has shifted the focus towards optical fiber networks. Especially, optical code division multiple access (CDMA) systems have been shown to be competitive candidates to support a large number of simultaneous users [4]-[11]. Most of researches in optical CDMA networks were concentrated in the physical layer. There are, however, a few authors that have examined the network or link layer of optical CDMA communication systems, [4]-[8]. In [4] and [5], Hsu and Li have studied the slotted and unslotted optical CDMA networks. In [6], Shalaby has proposed two media access control (MAC) protocols for optical CDMA networks. However the effect of multi-packet messages, connection establishment and corrupted packets haven't been taken into account. Recently, Shalaby [7] has developed a new protocol called round robin receiver/transmitter ( $R^3T$ ) protocol that has solved some of the above problems. The  $R^3T$  protocol is based on a go-back  $n$  automatic repeat request (ARQ), that is when a packet gets corrupted, the transmitter retransmits it and all sub-sequent packets. This scenario gives good performance for low population networks, while the performance is still low for larger population networks. Considering only the retransmission of corrupted packets, a selective reject ARQ has been applied in [8], which yields better results in case of higher population networks.

Our goal in this chapter is to develop a new optical random access CDMA protocol which is based on a stop & wait ARQ in order to reduce the complexity of the previously proposed protocols. At the same time we aim at improving the system performance compared to the  $R^3T$  protocol. Moreover, the proposed protocol is examined for the case of both chip-level and correlation receivers. In most cases of practical interest, thermal noise dominates the receiver performance. Accordingly, in our analysis we will study the effect of thermal noise and its impact on the performance of the proposed protocol.

This chapter is organized as follows. In Section 6.2, we discuss the system and hardware architecture for our optical CDMA network. Section 6.3 is devoted for a description of the proposed protocol. The optical link layer is investigated and a complete state diagram of this protocol is presented. Section 6.4 is maintained for the mathematical model, where derivations of the steady state system throughput, the average packet delay, the protocol efficiency, and the blocking probability are calculated. In Section 6.5, we discuss some of the numerical results obtained. A comparison between the proposed protocol and the  $R^3T$  protocol is also considered. Finally, we give our conclusions in Section 6.6.

## 6.2 System and Hardware Architecture

Considering the network topology at the physical layer, we have a passive optical star network composed of a star coupler connecting  $N$  users as shown in Fig. 6.1. Optical orthogonal codes (OOCs) are used because they have both a peak cross-correlation and a shifted autocorrelation equal to one. The choice of code weight  $w$  and code length  $L$  for OOCs is arbitrary but these quantities determine the cardinality according to [9]:

$$|C| = \left\lfloor \frac{L-1}{w(w-1)} \right\rfloor, \quad (6.1)$$

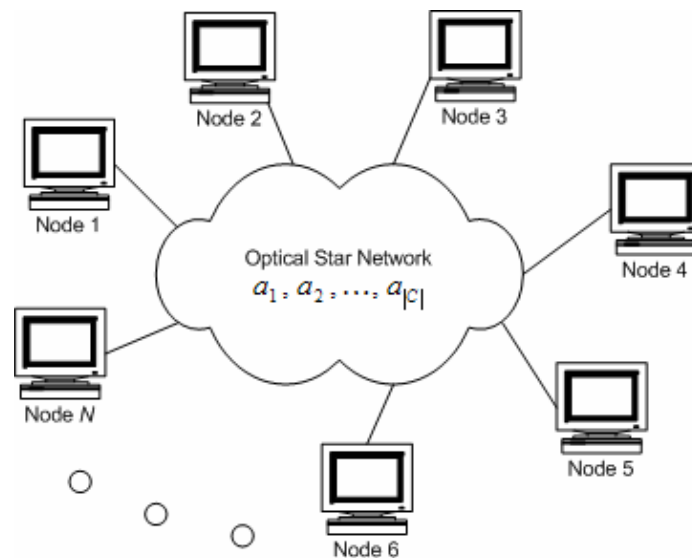


Fig. 6.1. Optical CDMA network topology.

where  $\lfloor x \rfloor$  denotes the integer portion of the real value  $x$ . Due to the bursty nature of the traffic, we allow the number of users to exceed the number of available codes  $|C|$ . In our model, we assume that all codes are always available in a pool, Fig. 6.1. In order to avoid receiver tunability, codes are assigned to users apriori. That is, when a user subscribes to the network, it is given a code (possibly used) randomly. Further, a code is randomly cyclic shifted around itself once assigned. In this way, there is no need for pretransmission coordination. It has been shown that for fixed data rate and chip duration, there is no advantage in using pulse position modulation (PPM) in place of on-off keying (OOK). That's why each user is able to generate an optical OOK-CDMA signal according to its signature code that represents its data.

Chip-level receivers are implemented at the physical layer of our optical CDMA network. In [26], Shalaby demonstrated that the complexity of this receiver is independent of the number of users, and therefore, much more practical than traditional correlation receivers. The packet success probability  $P_s(r')$  given  $r'$  active users for both correlation receivers and chip-level receivers has been derived in subsections 2.5.1 and 2.5.2, respectively, where we have considered only the effect of MAI. The effect of thermal noise on the performance degradation of the proposed protocol can be easily considered by using equation (4.10).

## **6.3 Mathematical Model**

### **6.3.1 Protocol Assumptions**

Because of its simplicity over other ARQs, stop & wait is implemented at the data link layer of our optical CDMA network. After a packet is sent, a user enters a waiting mode to get a feedback of that packet. If a positive acknowledgement is received the user will send the next packet, otherwise he will retransmit another version of the corrupted packet. We impose the following assumptions in our model for optical CDMA protocol:

- Time is slotted with slot size  $T_s$ , a two way propagation delay time is assumed to be equal to  $t$  time slots, and a timeout duration of  $\tau$  time slots is selected such that  $1 \leq \tau \leq t$ .

- A message is composed of  $\ell > t$  packets each having  $K > 0$  bits. One packet should fit in a time slot  $T_s = K \ell T_c$ , where  $T_c$  is the chip duration.
- A maximum of 1 message can arrive at each time slot to a station with probability  $A$  (also called user activity). This message is stored in a buffer till its successful transmission.
- Any arrival to a non empty buffer will be blocked.
- Connection requests and acknowledgements are exchanged between stations.
- Transmission times for requests and acknowledgements are neglected.
- A priority is given for the reception mode than for the transmission mode.
- Receivers use a cyclic redundancy check (CRC) to determine whether a received packet is correctly detected or not.

### 6.3.2 State Diagram Description

The complete state diagram of the proposed optical CDMA random access protocol with stop & wait ARQ is illustrated in Fig. 6.2. Each state is labeled by its number of users. Transition between states is on a slot basis; that is the duration of each state equals to one time slot. At any time slot, any user in the network will be in one of the following states or modes:

- Initial state,  $\{m\}$ . Users in the initial state scan across all codes in a round-robin manner. If a connection request (event happening with a probability  $\sigma$ ) is found, a station will proceed to the acknowledgement mode. If there is a message arrival and there is no connection request, it will go to the requesting mode. If there is neither message arrival nor connection request, the station will remain in the initial state.
- Requesting mode,  $\{q_1, q_2, \dots, q_\tau\}$ . Stations in this mode send repeated requests  $\{q_1, q_2, \dots, q_\tau\}$  for  $\tau$  time slots. Then, the station should wait for a feed back and thus enters a waiting mode  $\{W_1^q, W_2^q, \dots, W_{t-1}^q\}$ , for  $t-1$  time slots, as depicted in Fig. 6.2. Whenever a waiting station gets a positive acknowledgement (event occurring with a probability  $\gamma$ ) from the destination, it starts sending its message and enters the transmission mode, otherwise it remains in the waiting mode. In the



last waiting state, if an acknowledgement is not received, the station is timed out and returns to the initial state.

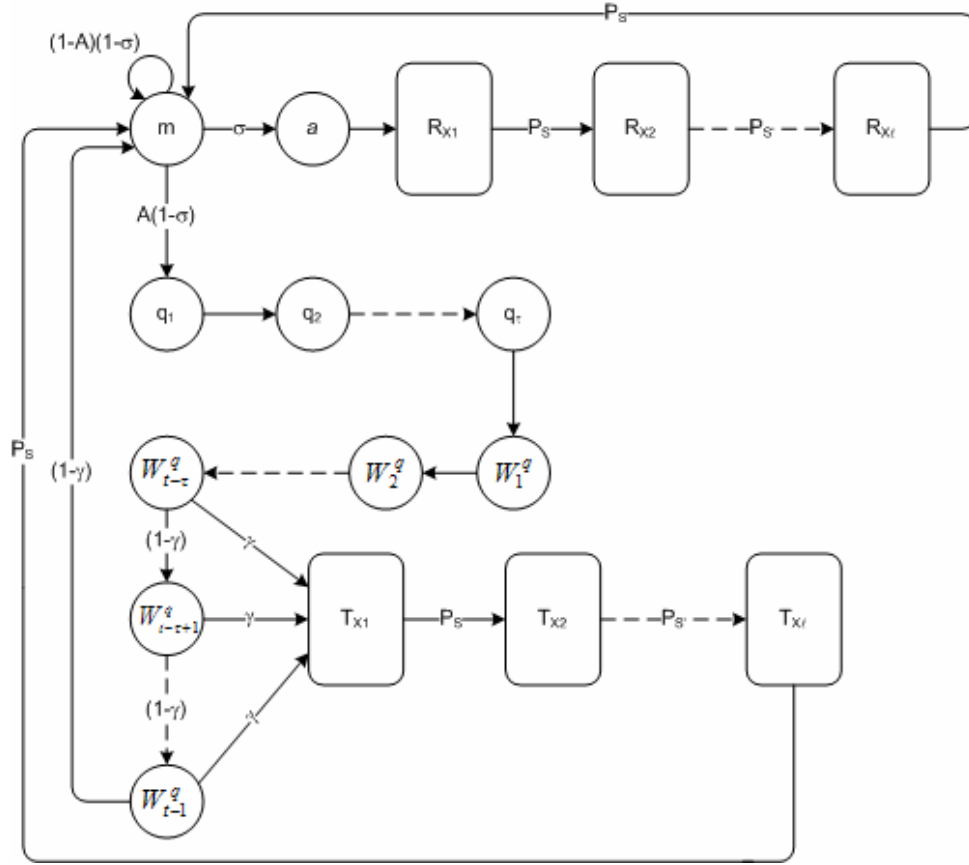


Fig. 6.2. State diagram of the proposed optical CDMA protocol with stop & wait ARQ.

- Acknowledgement state,  $\{a\}$ . In this state, the station sends an acknowledgement to a requesting station and then enters a waiting mode  $\{W_1^{s1}, W_2^{s1}, \dots, W_{t-1}^{s1}\}$  for  $t$  time slots till the reception of the first packet.
- Reception mode,  $\{Rx_1, Rx_2, \dots, Rx_\ell\}$ . A user in the reception mode receives either new packets or retransmitted ones. Figure 2 illustrates the structure of the states  $R_{x_i}$ ,  $i \in \{1, 2, \dots, \ell\}$ . In states  $s_i$ , a user receives packet  $i$ , if it is successfully received, the user will move to states  $\{W_1^{si+1}, W_2^{si+1}, \dots, W_{t-1}^{si+1}\}$  waiting for the next packet, otherwise he will ask for retransmission and enters a waiting mode  $\{W_1^{si}, W_2^{si}, \dots, W_{t-1}^{si}\}$ . If the station receives the last packet successfully it goes back to the initial state.

- Transmission mode,  $\{Tx_1, Tx_2, \dots, Tx_\ell\}$ . This mode involves transmission states  $r_i$ ,  $i \in \{1, 2, \dots, \ell\}$  and waiting states  $W_j^{ri}$ ,  $j \in \{1, 2, \dots, t-1\}$ , Fig. 6.3. A user in state  $r_i$  is transmitting packet  $i$ , then he enters a waiting mode  $\{W_1^{ri}, W_2^{ri}, \dots, W_{t-1}^{ri}\}$  to get the acknowledgement of that packet. If a positive feedback is received the user will proceed to state  $r_{i+1}$  otherwise he will return to state  $r_i$  for retransmission. After successful transmission of the last packet the user will return to the initial state.

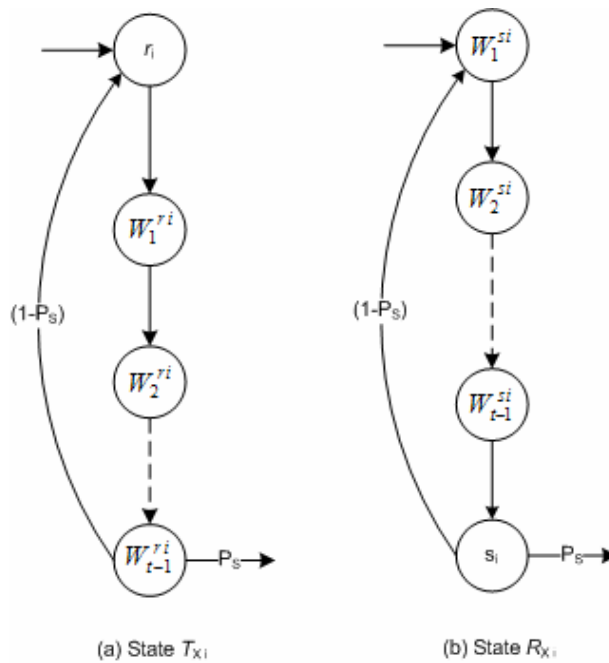


Fig. 6.3. Transmission states,  $T_{xi}$  and reception states,  $R_{xi}$ .

## 6.4 Performance Analysis

### 6.4.1 State Diagram

Because of the complexity of the above model and the prohibitively large number of states, the problem will be analytically intractable if we try to calculate the transition probabilities between states and the stationary probabilities using Markov chains [44]. Fortunately, the equilibrium point analysis (EPA) technique significantly simplifies the problem. In this technique, the system is always assumed to be

operating at an equilibrium point [43]; that is the number of users entering a state is equal to the number of users departing from the same state. By writing down the flow equations for each state, the performance of the proposed optical CDMA protocol can be evaluated.

#### 6.4.1.1 Transmission Mode

This mode involves states  $r_i$  and states  $W_j^{r_i}$ , where  $i \in \{1, 2, \dots, \ell\}$  and  $j \in \{1, 2, \dots, t-1\}$ . From Figs. 6.2 and 6.3, we have the following flow equations.

$$r_1 = r_2 = \dots = r_\ell \quad \text{and} \quad W_j^{r_i} = r_1.$$

Let  $r_o$  denotes the number of transmitting users in a given slot such that

$$r_o = \sum_{i=1}^{\ell} r_i = \ell r_1. \quad (6.2)$$

We define  $W^r$  as the number of users waiting after transmission

$$W^r = \sum_{i=1}^{\ell} \sum_{j=1}^{t-1} W_j^{r_i} = \ell(t-1) \cdot r_1. \quad (6.3)$$

#### 6.4.1.2 Reception Mode

Assuming that the number of users transmitting packet  $i$  is equal to that receiving the same packet, for  $i=1$  we can directly write  $r_1 = s_1$ . From Figs. 6.2 and 6.3, we can write the flow equations for states  $s_i$  and  $W_j^{s_i}$ , for  $i \in \{1, 2, \dots, \ell\}$  and  $j \in \{1, 2, \dots, t-1\}$  as follows:

$$\begin{aligned} W_1^{s_1} &= a + (1 - P_s) \cdot s_1, \\ s_1 = s_2 = \dots = s_\ell &= r_1 \quad \text{and} \quad W_j^{s_i} = r_1. \end{aligned} \quad (6.4)$$

We define the following variables

$$\begin{aligned} s &= \sum_{i=1}^{\ell} s_i = \ell r_1 \\ W^s &= \sum_{i=1}^{\ell} \sum_{j=1}^{t-1} W_j^{s_i} = \ell(t-1) \cdot r_1. \end{aligned} \quad (6.5)$$

### 6.4.1.3 Acknowledgement Mode

Again by writing the flow equations for the states in this mode, described in Fig. 6.2 and using equation (6.4) we get:

$$a = \sigma m = P_s r_1.$$

Therefore

$$m = \frac{P_s}{\sigma} r_1. \quad (6.6)$$

### 6.4.1.4 Requesting Mode

Figure 6.2 illustrates the requesting states and waiting states in the requesting mode. By writing down the flow equations as in [7], we define:

$$q + W^q = \sum_{i=1}^{\tau} q_i + \sum_{i=1}^{t-1} W_i^q = \left[ t - 1 + \frac{1}{\gamma} (1 - (1 - \gamma)^\tau) \right] A \frac{1 - \sigma}{\sigma} P_s r_1. \quad (6.7)$$

The probability that a request is found by a scanning user  $\sigma$  and the probability that a station gets an acknowledgement  $\gamma$  can be computed as follows [7]:

$$\sigma = \frac{1}{2} \left[ \sqrt{\left( AP_s \tau \frac{r_1}{N} \right)^2 + 4 \left( AP_s \tau \frac{r_1}{N} \right)} - AP_s \tau \frac{r_1}{N} \right]$$

$$\gamma = 1 - \left[ 1 - \frac{\sigma}{A(1 - \sigma)} \right]^{1/\tau}.$$

## 6.4.2 Performance Metrics

### 6.4.2.1 Steady State System Throughput

The steady state system throughput  $\beta(N, A, t, \tau, \ell)$  is defined as the average number of successful received packets per slot. It can be calculated as follows:

$$\beta(N, A, t, \tau, \ell) = \sum_{i=1}^{\ell} s_i \cdot P_s = P_s(r') \ell r_1.$$

Substituting with equation (6.2) one gets:

$$\beta(N, A, t, \tau, \ell) = r' P_s(r'). \quad (6.8)$$

To compute  $r'$ , we assume that the total number of users in all states is equal to  $N$ , yielding

$$N = m + r + W^r + s + W^s + a + q + W^q$$

$$= \frac{r'}{\ell} \left[ \frac{P_s}{\sigma} + 2\ell + 2\ell(t-1) + P_s + \left\{ t - 1 + \frac{1}{\gamma} (1 - (1-\gamma)^t) \right\} A \frac{1-\sigma}{\sigma} P_s \right], \quad (6.9)$$

where we have used equations (6.2) – (6.7).

#### 6.4.2.2 Blocking Probability

The blocking probability is defined as the probability of an arrival being blocked. In this case, the blocking probability is equal to the probability that the station is not in the initial state  $m$  and there is a message arrival  $A$  or the station is in the initial state  $m$  but there is a request for connection and at the same time there is a message arrival  $A$ .

Thus, one can write:

$$P_B = \frac{m}{N} \cdot \sigma \cdot A + \left( 1 - \frac{m}{N} \right) \cdot A.$$

Substituting with equations (6.2) and (6.6) we get:

$$P_B = A \left[ 1 - \frac{P_s}{\ell N} \left( \frac{1-\sigma}{\sigma} \right) r' \right]. \quad (6.10)$$

#### 6.4.2.3 Protocol Efficiency and Average Delay

The protocol efficiency  $\eta$  is defined as the ratio between the number of successfully received packets and the number of packets available for transmission:

$$\eta = \frac{\beta(N, A, t, \tau, \ell)}{r'}. \quad (6.11)$$

The average packet delay  $D$  can be calculated from Little's theorem:

$$D = \frac{NA \cdot (1 - P_B)}{\beta(N, A, t, \tau, \ell)} \quad \text{slots}, \quad (6.12)$$

where  $NA \cdot (1 - P_B)$  denotes the total traffic in the network.

Note that equations (6.10) - (6.12) are valid for both optical random access CDMA protocols; with Stop & Wait ARQ and with go-back  $n$  ARQ [7].

## 6.5 Numerical Results

In this section, we discuss some numerical results for the proposed optical random access CDMA protocol. The steady state system throughput, the blocking probability, the average packet delay, and the protocol efficiency derived above have been evaluated and compared to the results in [7]. The performance of the proposed protocol using both chip-level receivers and correlation receivers is also presented. Correlation receivers are only considered in Fig. 6.4. Finally, the effect of thermal noise is taken into consideration in the last figure.

Table 6.1. Parameters used for numerical calculations.

CDMA Parameters	APD Parameters (thermal noise)	
	APD responsivity at unity gain	$R = 0.84 \text{ A/W}$
$R_b = 127 \text{ Mbps}$	APD dark current	$I_d = 1 \text{ nA}$
$L = 31$	Average APD gain	$G = 100$
$w = 3$	APD effective ionization ratio	$k_{eff} = 0.02$
$K = 127$	Receiver noise temperature	$T^o = 300 \text{ K}$
	Receiver load resistor	$R_L = 50 \Omega$

Our results are plotted in Figs. 6.3-6.8. A two way propagation delay time  $t \in \{2, 4, 6\}$  slots (or interstation distances of  $z = vT_s t/2 \in \{200, 400, 600\} \text{ m}$ , where  $v \approx 2 \times 10^8 \text{ m/s}$  is the speed of light inside a fiber) and a timeout duration  $\tau = 1 \text{ slot}$  are imposed in our simulations. Table 6.1 shows the remaining parameters used for the numerical calculations.

In Fig. 6.4, we have plotted the throughput versus the number of users for both chip-level receivers and correlation receivers. General trends of the curves can be noticed. As the number of users in the network increases more packets become available for transmission with low interference. Thus, the throughput increases till it reaches its peak. As the number of users is further increased the effect of MAI becomes significant and the throughput starts to decay. In the case of stop & wait

ARQ the protocol supports a larger number of users and reaches higher values of throughput. This is because the channel is not busy all the time, as users enter a waiting mode after sending each packet. On the other hand, for a protocol depending on a go-back  $n$  ARQ, users continuously send their packets, which contribute to higher traffic loads, yielding lower packet success probabilities and lower throughput values. It can be inferred that the performance of both protocols is reduced when using correlation receivers and that the performance of the stop & wait with correlation receivers is nearly close to that of the  $R^3T$  protocol with chip-level receivers.

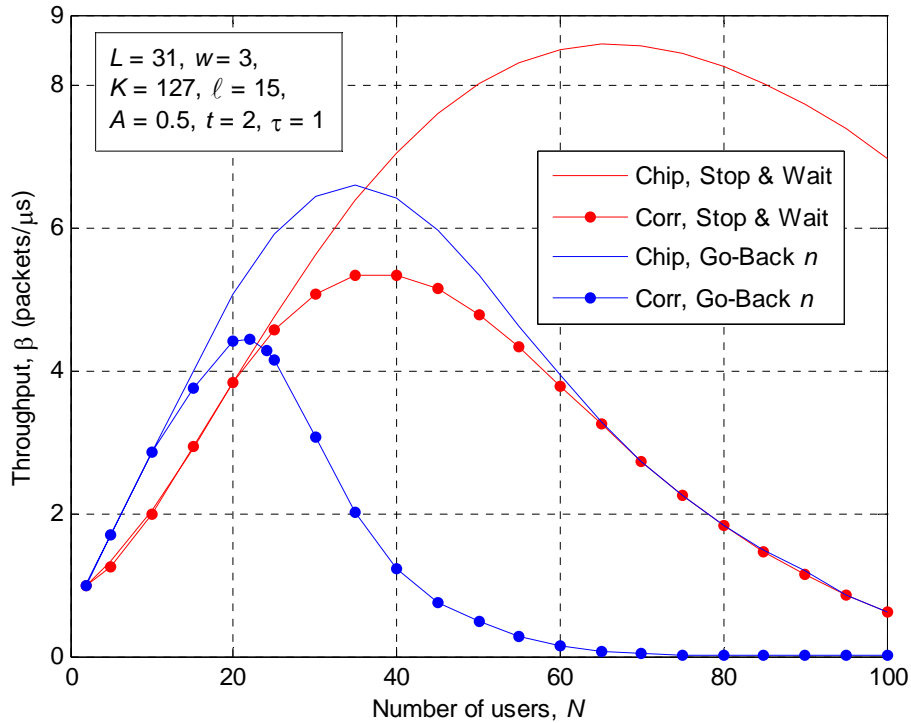


Fig. 6.4. Throughput versus number of users for different receivers.

In Fig. 6.5, the blocking probability has been plotted versus user activity for different activity levels and for different interstation distances. It can be seen that the blocking probability increases significantly for higher activity levels,  $A \in \{0.75, 1\}$ . The proposed protocol (stop & wait) provides lower blocking probabilities because at  $N = 70$ . This protocol can still handle the traffic as depicted in Fig. 6.4. For larger intersation distances, the channel will be busy for longer durations. This gives rise to

a high probability of collision between packets which reduces the throughput, therefore the blocking probability increases.

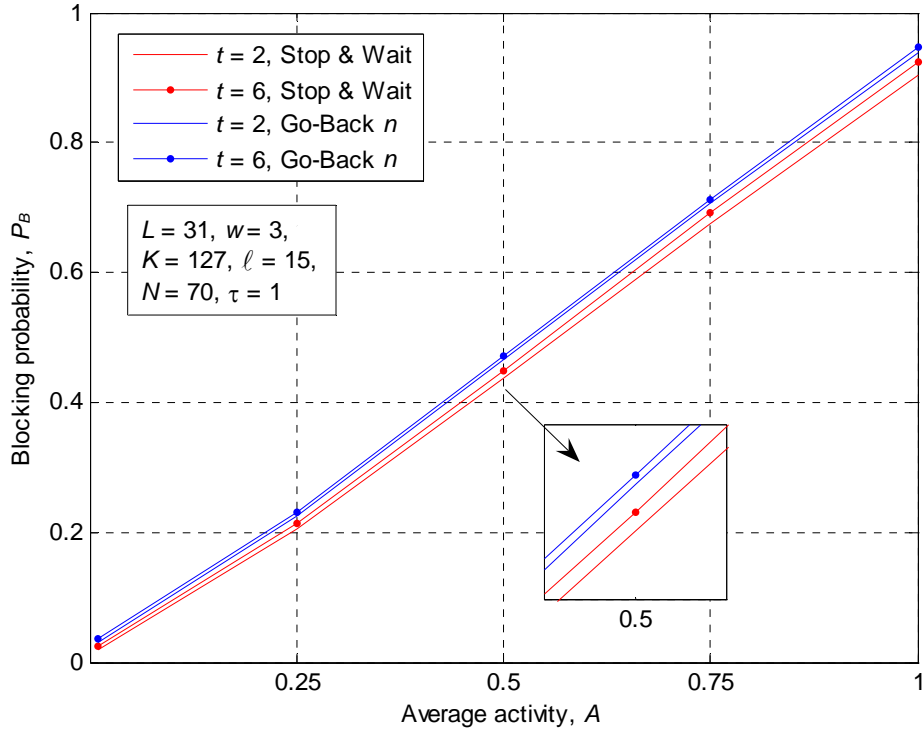


Fig. 6.5. Blocking probability versus user activity for different interstation distances.

In Fig. 6.6, we have plotted the system throughput and the average packet delay versus the average activity for different number of users  $N \in \{30, 70\}$ . It can be noticed that the  $R^3T$  protocol exhibits higher throughput values and lower delays at  $N = 30$ . Whereas the proposed protocol outperforms the  $R^3T$  protocol at  $N = 70$ , as argued in Fig. 6.4. For short interstation distances, as the user activity increases the throughput also increases till it reaches saturation whereas for longer distances the throughput falls after reaching its peak. In fact, the initial increase of throughput is because as  $A$  increases above zero, more packets become available with low interference. The throughput decay in the case of long propagation delays after reaching its peak because the number of active users increases while other users already in the transmission mode are still busy transmitting their messages over long distances. The interference would thus increase rapidly and packet failures become more probable. Finally, it is noticed that for longer interstation distances and with an increase in user activity, the average packet delay increases.



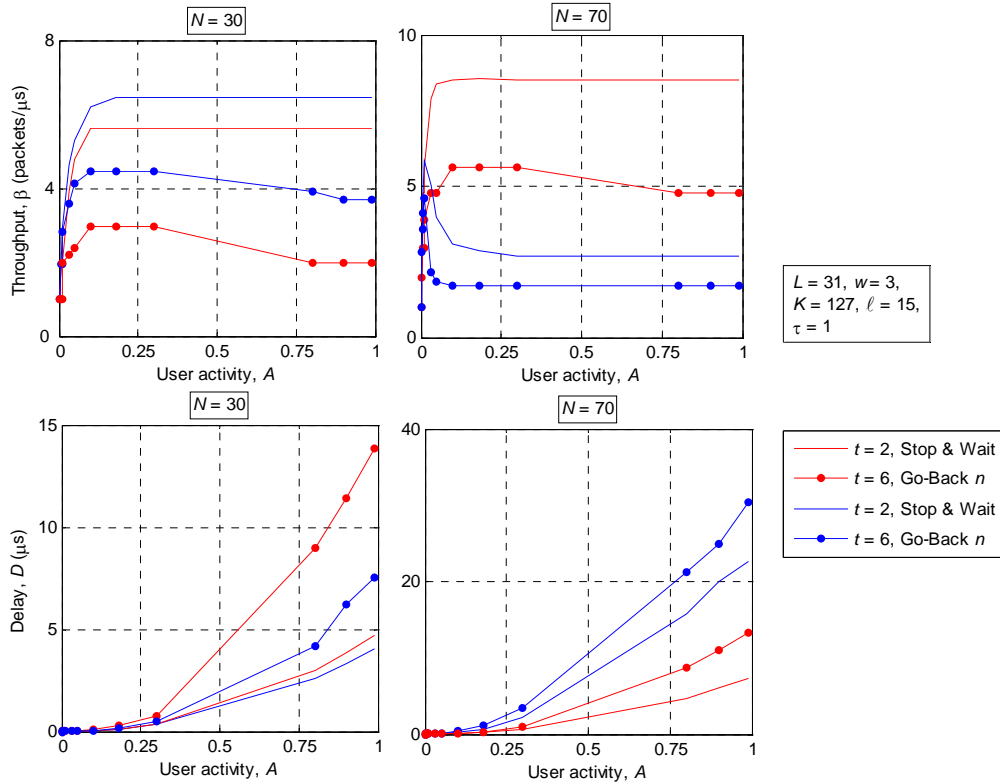


Fig. 6.6. Throughput and delay versus activity for different number of users and different interstation distances.

The relation between the system throughput and the number of users for our proposed protocol is depicted in Fig. 6.7. It can be seen that for longer propagation delays, the proposed protocol accommodates a higher number of users. Also the quality of service (QoS) requirements is achieved in a large dynamic range. This is because as  $t$  increases, users wait longer times after transmitting their packets, giving chance to other users to start transmission.

The protocol efficiency has been plotted against the message length for both protocols in Fig. 6.8. General trends of the curves can be noticed. The efficiency decreases as the message length is increased till it reaches its floor. This can be argued in a similar way as in Fig. 6.6. Both protocols achieve higher efficiency in case of low population networks. It can be noticed that the new protocol provides an improvement in the protocol efficiency for both small and large population networks.

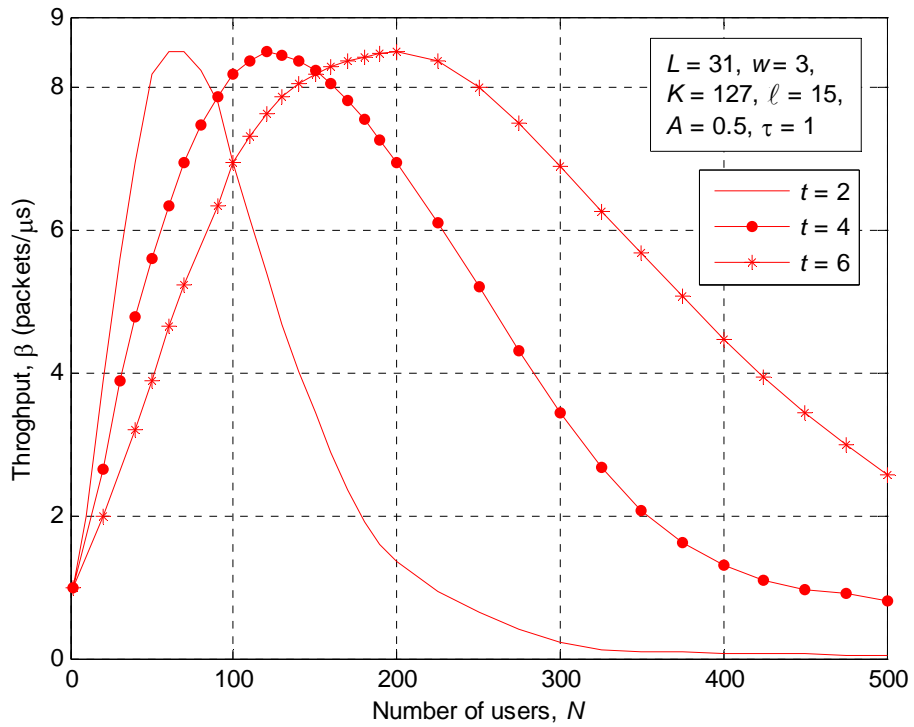


Fig. 6.7. Throughput versus number of users for different interstation distances.

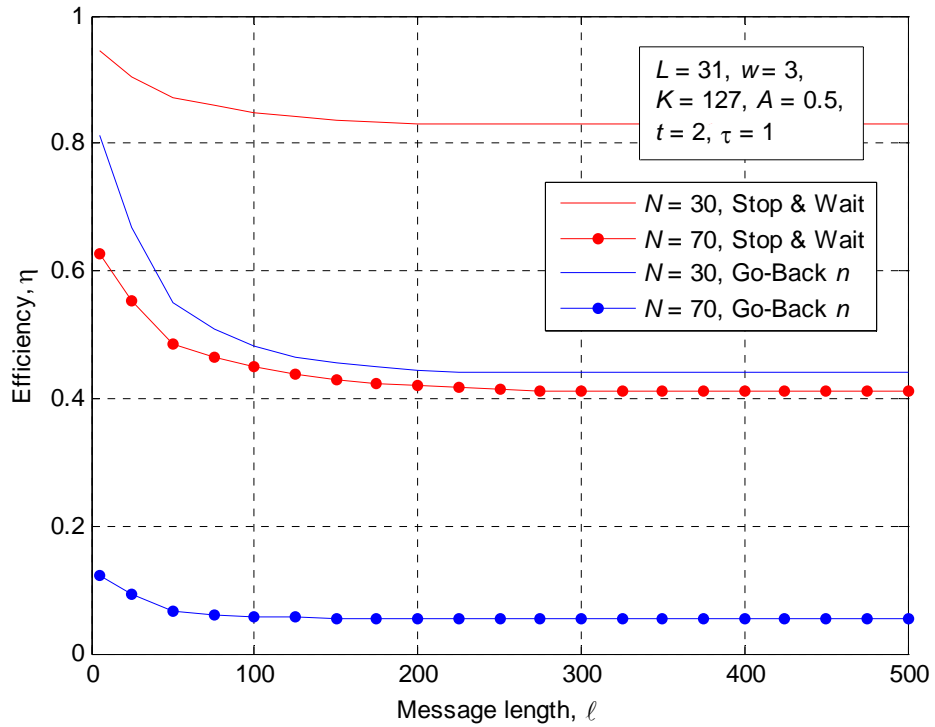


Fig. 6.8. Efficiency versus message length for different number of users.

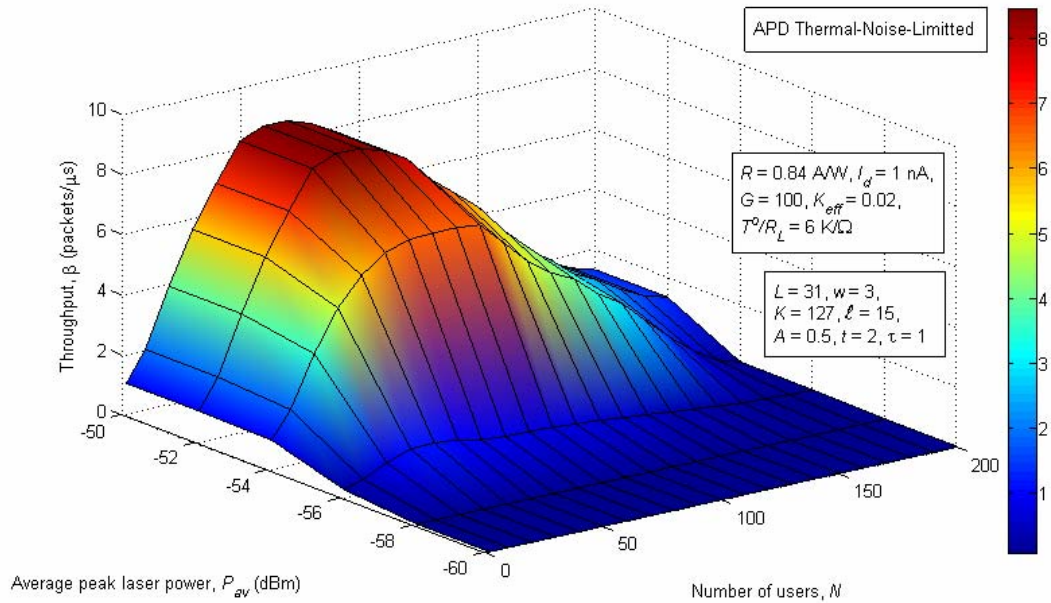


Fig. 6.9. Throughput versus number of users and average peak laser power per chip.

Finally, the impact of thermal noise on our proposed protocol is taken into account in Fig. 6.9 [cf. equation (4.10)]. It can be inferred that by increasing the average peak laser power up to -52 dBm, the receiver can tolerate the effect of the performance degradation and achieves the same throughput as the ideal case (considering only the effect of MAI).

## 6.6 Conclusions

In this chapter, we have proposed an optical random access CDMA protocol based on a stop & wait ARQ. A mathematical description of this protocol has been presented using a detailed state diagram. Several performance measures were considered; namely, the steady state system throughput, the blocking probability, the average packet delay, and the protocol efficiency. In our numerical calculations, we have focused only on the effect of both MAI and receiver thermal noise. Both correlation and chip-level receivers were also examined. Finally, a comparison between our proposed protocol and the  $R^3T$  protocol [7] was discussed. The following concluding remarks can be extracted from our results.

- 1- The performance of the proposed CDMA protocol using correlation receivers is nearly close to that of the  $R^3T$  protocol with chip-level receivers.
- 2- The proposed protocol outperforms the  $R^3T$  protocol (in terms of the system throughput and average packet delay) in high population networks, whereas for smaller size networks the  $R^3T$  protocol slightly outperforms the proposed one.
- 3- Both protocols exhibit satisfactory blocking probability only for small traffic loads. Furthermore, the average packet delay is acceptable under different network parameters.
- 4- For larger interstation distances, the proposed protocol accommodates a higher number of users. Also the quality of service (QoS) requirements can be achieved in a larger dynamic range (wider range of users).
- 5- Our proposed protocol provides an improvement in the protocol efficiency for both small and large population networks. Also it is clear that for an interstation distance  $z = 200$  m, the efficiency of our protocol with  $N = 70$  is as good as the efficiency of the  $R^3T$  protocol with  $N = 30$ .
- 6- We can tolerate the effect of thermal noise by reasonably increasing the average peak power at the transmitter to -52 dBm, [37].
- 7- The complexity of the proposed protocol is significantly reduced compared to the  $R^3T$  protocol. Also the cost is reduced when using correlation receivers.

# CHAPTER 7

## CONCLUSIONS AND FUTURE WORK

### Outline:

- **Conclusions**
- **Future Research Avenues**

## CHAPTER 7

### CONCLUSIONS AND FUTURE WORK

#### **7.1 Conclusions**

In this thesis, we have first reviewed previous work on optical CDMA communication systems. Both physical layer and data link layer of slotted optical CDMA packet networks have been considered. By studying the performance of different optical CDMA receiver structures, we have found out that for a large number of active users in the network and for the same set of spreading codes, the effect of MAI becomes considerable and thus, the performance of these receivers is significantly reduced. There emerges a high need to design a robust data link layer and MAC protocols for optical CDMA networks that ensure a fair access to the network environment.

In this work, we have focused mainly on random access protocols and solutions for LANs, but many of the principles can also be used for access networks. A physical star topology is used in our optical CDMA network. Compared to ring and bus topologies, star networks offer a better optical power budget and are easy to install, configure, manage, and troubleshoot. Optical orthogonal codes (OOCs) with correlation constraints set to one have been used as the users' signature codes to ensure minimal interference level. Optical direct-detection CDMA and binary on-off keying (OOK) have been implemented at the physical layer.

Most studies of optical CDMA use simple channel models where noise and dispersion are neglected. One of the main objectives of this research was to study a model where both thermal noise and dispersion, are taken into account. In Chapter 4, the Gaussian approximation has been used to study the effect of thermal noise on the performance of the round robin receiver/transmitter ( $R^3T$ ) protocol. Also the impact of the dispersion on limiting the user bit rate has been also considered. We have proved by numerical analysis that the effect of thermal noise dominates the performance only for the case of low population networks, whereas the effect of MAI becomes dominant for larger networks. The power penalty to be paid to overcome the degradation in the performance has also been calculated.

Also in this thesis we have suggested a queuing model for the  $R^3T$  protocol in order to enhance its performance especially at large population networks and at high traffic loads. This is because in the  $R^3T$  protocol it was assumed that each node is equipped with only a single buffer to store only the message being served. Any arrival to a non empty buffer was discarded; this of course gave rise to a high blocking probability. In Chapter 3, we have derived an expression for the blocking probability and demonstrated that the blocking probability can reach as high as 95% under certain network conditions. A detailed state diagram for this modified  $R^3T$  protocol has been presented in Chapter 5 and has been analyzed using the equilibrium point analysis (EPA) technique. Our results revealed that significant improvement in the steady state system throughput and the protocol efficiency can be achieved by only adding a single buffer to the system which does not add significantly to the network's complexity. Furthermore, the  $R^3T$  protocol with a queuing subsystem exhibits an acceptable timeout probability under different network parameters.

Finally, we have proposed an optical random access CDMA protocol based on stop & wait ARQ in Chapter 6. A mathematical description of this protocol has been outlined using a detailed state diagram. Several performance measures have been considered; namely, the steady state system throughput, the blocking probability, the average packet delay, and the protocol efficiency. The performance has been also examined for both correlation and chip-level receivers. We have proved by numerical analysis that the proposed protocol is less complex and significantly outperforms the  $R^3T$  protocol which is based on a go-back  $n$  technique. Our results have also showed that the performance of the proposed protocol with correlation receivers is nearly close to that of the  $R^3T$  protocol with chip-level receivers, which reduces the overall system cost.

## **7.2 Future Research Avenues**

Although the objectives of this research have been achieved, it would be interesting to see some of the aspects discussed in this thesis implemented in an experimental set-up. Any experimental results can then be fed back to the simulation model for further performance optimization and validation. Below, we present several directions for future research in the area of optical CDMA networks.

- The design and evaluation of hybrid MAC protocols where nodes apply different protocols according to the current traffic load.
- Channel load sensing protocols (CLSP) and packet avoidance collision (PAC) protocols can be applied.
- The combination of error correction and traffic control by MAC can be studied for further improvement in the performance of optical CDMA networks.
- Studying optical random access CDMA protocols with larger buffers.
- Two dimensional codes may be implemented to provide larger code sets with lower interference levels.
- Power control depending on the number of active users in the network may be used to compensate for the effect of thermal noise. The effect of shot noise and beat noise can also be included.



## **REFERENCES**

## REFERENCES

- [1] Rajiv Ramaswami, "Optical fiber communication: from transmission to network," *IEEE comm. magazine*, 50<sup>th</sup> anniversary commemorative issue, pp. 138-147, May 2002.
- [2] A. Stok, and E. H. Sargent, "System performance comparison of optical CDMA and WDMA in a broadcast local area network," *IEEE Comm. Lett.*, vol. 6, No. 9, pp. 409-411, September 2002.
- [3] A. Stok, and E. H. Sargent, "Comparison of utilization in optical CDMA and WDMA broadcast local-area networks with physical noise," *IEEE International conference on communications (ICC)*, 2003.
- [4] C.-S. Hsu, and V. O. K. Li, "Performance analysis of slotted fiber-optic code-division multiple-access (CDMA) packet networks," *IEEE Trans. Comm.*, vol. COM-45, pp. 819-828, July 1997.
- [5] C.-S. Hsu, and V. O. K. Li, "Performance analysis of unslotted fiber-optic code-division multiple-access (CDMA) packet networks," *IEEE Trans. Comm.*, vol. COM-45, pp. 978-987, August 1997.
- [6] H. M. H. Shalaby, "Optical CDMA random access protocols with and without pretransmission coordination," *IEEE/OSA J. Lightwave Technol.*, vol. LT-21, pp. 2455-2462, November 2003.
- [7] H. M. H. Shalaby, "Performance analysis of an optical CDMA random access protocol," *IEEE/OSA J. Lightwave Technol.*, vol. LT-22, pp. 1233-1241, May 2004.
- [8] M. A. A. Mohamed, H. M. H. Shalaby, and E. A. El-Badawy, "Optical CDMA protocol with selective retransmission," in *Proc. Ninth IEEE Symp. Computers and Communications (ISCC 2004)*, Alexandria, Egypt, pp. 621-626, June 29 - July 1, 2004.
- [9] F. R. Chung, J. A. Salehi, and V. K. Wei, "Optical orthogonal codes: Design, analysis, and applications," *IEEE Trans. Inform. Theory*, vol. 35, pp. 595-604, May 1989.

- [10] J. A. Salehi, "Code division multiple-access techniques in optical fiber networks - Part I: Fundamental principles," *IEEE Trans. Comm.*, vol. 37, pp. 824-833, August 1989.
- [11] J. A. Salehi, and C. A. Brackett, "Code division multiple access techniques in optical fiber networks - Part II: System performance analysis," *IEEE Trans. Comm.*, vol. 37, No. 8, pp. 834-842, August 1989.
- [12] K. Iversen, and D. Hampicke, "Comparison and classification of all-optical CDMA systems for future telecommunication networks," *SPIE Proc.*, vol. 2614, pp. 110-121, October 1995.
- [13] J. Y. Hui, "Pattern code modulation and optical decoding - A novel code-division multiplexing technique for multifiber networks," *IEEE Journal on Selected Areas in Comm.*, vol. SAC-3, No. 6, pp. 916-927, November 1985.
- [14] P. R. Prucnal, M. A. Santoro, and T. R. Fan, "Spread spectrum fiber-optic local area network using optical processing," *IEEE/OSA J. Lightwave Technol.*, vol. LT-4, No. 5, pp. 547-554, May 1986.
- [15] P. R. Prucnal, M. A. Santoro, and S. K. Sehgal, "Ultrafast all-optical synchronous multiple access fiber optical networks," *IEEE Journal on Selected Areas in Communications*, vol. SAC-4, No. 9, pp. 1484-1493, December 1986.
- [16] M. Kavehrad, and D. Zaccarin, "Optical code-division-multiplexed systems based on spectral encoding of noncoherent sources", *IEEE/OSA J. Lightwave Technol.*, vol. 13, No. 3, pp. 534-545, March 1995.
- [17] H. Fathallah, L. A. Rusch, and S. LaRochelle, "Passive optical fast frequency-hop CDMA communications system," *IEEE/OSA J. Lightwave Technol.*, vol. 17, No. 3, pp. 397-405, March 1999.
- [18] H. M. H. Shalaby, "Complexities, error probabilities, and capacities of optical OOK-CDMA communication systems," *IEEE Trans. Comm.*, vol. 50, No. 12, pp. 2009-2017, December 2002.
- [19] S. Zahedi, and J. A. Salehi, "Analytical comparison of various fiber-optic CDMA receiver structures," *IEEE/OSA J. Lightwave Technol.*, vol. LT-18, pp. 1718-1727, December 2000.

- [20] D. V. Sarwate, and M. B. Pursley, "Crosscorrelation properties of pseudorandom and related sequences," *Proc. IEEE*, vol. 68, pp. 593-619, May 1980.
- [21] A. A. Shaar, and P. A. Davies, "Prime sequences: Quasi-optimal sequences for OR channel code division multiplexing," *IEEE Electronics Letters*, vol. 19, No. 21, pp. 888-889, 13 October 1983.
- [22] L. Nguyen, B. Aazhang, and J.F. Young, "All-optical CDMA with bipolar codes," *IEEE Electronics Letters*, vol. 31, No. 6, pp. 469-470, 16 March 1995.
- [23] R. M. H. Yim, L. R. Chen, and J. Bajcsy, "Design and performance of 2-D codes for wavelength-time optical CDMA," *IEEE Photonics Technology Letters*, vol. 14, No. 5, pp. 714-716, May 2002.
- [24] R. M. H. Yim, J. Bajcsy, and L. R. Chen, "A new family of 2-D wavelength-time codes for optical CDMA with differential detection," *IEEE Photonics Technology Letters*, vol. 15, No. 1, pp. 165-167, January 2003.
- [25] T. Ohtsuki, "Performance analysis of direct-detection optical asynchronous CDMA systems with double optical hard-limiters," *IEEE/OSA J. Lightwave Technol.*, vol. LT-15, pp. 452-457, March 1997.
- [26] H. M. H. Shalaby, "Chip-level detection in optical code-division multiple-access," *IEEE/OSA J. Lightwave Technol.*, vol. LT-16, pp. 1077-1087, June 1998.
- [27] M. Azizoglu, J. A. Salehi, and Y. Li, "Optical CDMA via temporal codes," *IEEE Trans. Comm.*, vol. 40, pp. 1162-1170, July 1992.
- [28] J. Muchenheim, and D. Hampicke, "Protocols for optical CDMA local area networks" *Proc. NOC'97, (Antwerpen)*, vol. 1, pp. 255-262, 1997
- [29] L. Lenzini, J. O. Limb, W. W. Lu, I. Rubin, and M. Zukerman, "Analysis and synthesis of MAC protocols," *IEEE Journal on Selected Areas in Communications*, vol. 18, No. 9, pp. 1557-1561, November 2000.
- [30] P. Kamath, J. Touch, and J. Bannister, "The need for media access control in optical CDMA networks," *Proc. IEEE Infocom*, 2004.
- [31] N. Mehravari, "Performance and protocol improvements for very high speed

- optical fiber local area networks using a passive star topology,” *IEEE/OSA J. Lightwave Technol.*, vol. LT-8, pp. 520-530, April 1990.
- [32] H. Takagi, and L. Kleinrock, “Throughput analysis for persistent CSMA systems,” *IEEE Trans. Comm.*, vol. COM-33, No. 7, pp. 627-638, July 1985.
- [33] William Stallings, *Data and Computer Communications*, New York: 6<sup>th</sup> edition, Prentice Hall, 2000.
- [34] G. P. Agrawal, *Fiber-optic Communication Systems*, New York: 3<sup>rd</sup> edition, John Wiley & Sons, Inc., 2002.
- [35] B. Mukherjee, *Optical Communication Networks*, New York: McGraw-Hill, 1997.
- [36] E. K. H. Ng, G. E. Weichenberg, and E. H. Sargent, “Dispersion in multiwavelength optical code-division multiple-access systems: Impact and remedies,” *IEEE Trans. Comm.*, vol. 50, No. 11, November 2002.
- [37] Z. A. El-Sahn, Y. M. Abdel-Malek, H. M. H. Shalaby, and El-S. A. El-Badawy, "Performance limitations in the  $R^3T$  optical random access CDMA protocol," *Submitted for possible publication to OSA J. Optical Networking*, March 2005.
- [38] V. F. B. Mezger, and M. B. Pearce, “Dispersion limited fiber-optic CDMA systems with overlapped signature sequences,” in *Proc. IEEE Laser and Electro-Optics Soc. 9th Annu. Meeting*, pp. 408-409, 1996.
- [39] T. Pfeiffer, M. Witte, and B. Deppisch, “High-speed transmission of broadband thermal light pulses over dispersive fibers,” *IEEE Photon. Technol. Lett.*, vol. 11, pp. 385-387, March 1999.
- [40] M. J. Karol, “Performance of the PAC optical packet network,” *IEEE/OSA J. Lightwave Technol.*, vol 11. No. 8, pp. 1394-1399, August 1993.
- [41] H. M. H. Shalaby, “Effect of thermal noise and APD noise on the performance of OPPM-CDMA receivers,” *IEEE/OSA J. Lightwave Technol.*, vol. 18, No. 7, pp. 905-914, July 2000.
- [42] Z. A. El-Sahn, Y. M. Abdel-Malek, H. M. H. Shalaby, and El-S. A. El-Badawy, "The  $R^3T$  optical random access CDMA protocol with queuing

subsystem," *Submitted for possible publication to the IEEE/OSA J. Lightwave Technol., also a summary submitted to the 31<sup>st</sup> European Conference on Optical Communication, (ECOC 2005), Glasgow, Scotland, 25-29 September 2005.*

- [43] J. R. Sack, and J. Urrutia, *Handbook of Computational Geometry*, North Holland: Elsevier Science, 2000.
- [44] Xi Zhang, and Kang G. Shin, "Markov-chain modeling for multicast signaling delay analysis", *IEEE/ACM Transactions on Networking*, vol. 12, No. 4, pp. 667-680, August 2004.



جامعة الإسكندرية  
كلية الهندسة

# بروتوكولات التوصلية العشوائية للشبكات الضوئية المستقبلية ذات التوصلية المتعددة بالتقسيم الشفري

رسالة مقدمة استيفاءً جزئياً لمتطلبات الحصول على

**درجة الماجستير**

في

**الهندسة الكهربائية**

من المهندس

**زياد أحمد رشاد الصحن**

تحت اشراف

**أ.د. السيد عبد المعطى البدوي**    **أ.د. حسام محمد حسان شلبي**

مسجلة في: سبتمبر ٢٠٠٢

مقدمة في: ابريل ٢٠٠٥

بسم الله الرحمن الرحيم

## الملخص العربي

اكتسبت الاتصالات بالألياف الضوئية أهمية كبيرة في العقدین الأخيرین و ذلك نظرا للزيادة المطردة في كمية البيانات المطلوب نقلها، حيث تتمتع الألياف الضوئية بنطاق ترددي واسع جدا يمكنها من نقل البيانات بمعدلات فائقة تصل الى عشرات التيراهرتز. و للاستفادة من هذا النطاق الترددي الواسع يجب استخدام احدى تقنيات الوصولية المتعددة Multiple Access Techniques. تعد تقنية الوصولية المتعددة بالتقسيم الشفري Code Division Multiple Access (CDMA) هي الطريقة المثلى لتحقيق هذه الاستفادة، بجانب تمتعها بمميزات أخرى مثل سهولة التنفيذ العملي و امكانية تغيير عدد المشتركين في الشبكة بسهولة.

يتعرض هذا البحث لدراسة الشبكات الضوئية ذات الوصولية المتعددة بالتقسيم الشفري على كل من مستويي الطبقة المادية Physical Layer و طبقة وصلة البيانات Data Link Layer حيث تم التركيز على البروتوكولات المستخدمة في الشبكات الوصولية و المحلية و هما:-

- بروتوكولات الوصولية العشوائية Random Access Protocols.

- بروتوكولات تحكم الوصولية الوسائطية Media Access Control (MAC) Protocols.

تبدأ الرسالة بدراسة لتأثير الضوضاء و التشتت الضوئي على أداء بروتوكول الاستقبال و الارسال بالأسلوب الحلقي Round Robin Receiver/Transmitter Protocol ، و توضح النتائج الرقمية أن تأثير الضوضاء الحرارية يغلب على أداء البروتوكول في شبكات الاتصالات ذات الأعداد الصغيرة من المشتركين، بينما يغلب التداخل الوصولي المتعدد Multiple Access (MAI) على الأداء في الشبكات الأكبر حجما. كما تم حساب قيم القدرة المثالية و الطول الموجي المناسب للتغلب على التأثير السلبي لكل من الضوضاء الحرارية و التشتت الضوئي في الألياف الضوئية.

تم دراسة اضافة نموذج تصنيف Queuing Model الى بروتوكول الاستقبال و الارسال بالأسلوب الحلقي بهدف تحسين الأداء و ذلك عن طريق التغلب على الفقد الحادث في الرسائل، حيث تمت زيادة وحدة اضافية لتخزين الرسائل. تم وضع تصور لمخطط الحالة State Diagram لتنفيذ هذه الدراسة و تحليله تفصيلا باستخدام طريقة التحليل النقطي المتزن Equilibrium Point



Analysis. أوضحت النتائج تحسنا فائقا فى الأداء بصفة عامة، و خاصة فى حالة الشبكات ذات الأعداد الكبيرة من المشتركين و ذات الأحمال المرورية العالية.

من أجل تبسيط بروتوكول الاستقبال و الارسال بالأسلوب الحلقي مع الحفاظ على أدائه أو تحسينه تم اقتراح بروتوكول وصولية عشوائية جديد يعتمد على طريقة قف و انتظر Stop & Wait، و بدراسة آليات الاتصال بين المرسل و المستقبل و كيفية التعامل مع الرسائل التى تحتوى على أكثر من حزمة بيانات Data Packets و كذا كيفية التعامل مع حزم البيانات التى لم يتم استقبالها بنجاح أظهرت النتائج أن البروتوكول المقترح يتمتع بمستوى عال من الأداء و ذلك مقارنة ببروتوكول الاستقبال و الارسال بالأسلوب الحلقي علاوة على مقدرته على استيعاب عدد أكبر من المشتركين.

**تتكون هذه الرسالة من سبعة أبواب كالتالى:-**

الباب الأول: مقدمة تتناول أهمية الاتصالات بالألياف الضوئية و خاصة الشبكات ذات الوصولية المتعددة بالتقسيم الشفري، يلي ذلك عرض لمساهمة الباحث فى هذا المجال و ابراز للنقاط البحثية الرئيسية بأبواب الرسالة المختلفة.

الباب الثانى: عرض للتقنيات ذات الوصولية المتعددة بالتقسيم الشفري فى أنظمة الاتصالات الضوئية، و دراسة للأنواع المختلفة للمستقبلات و المقارنة بينها من حيث الأداء و مستوى التعقيد.

الباب الثالث: ملخص للدراسات السابقة فى بروتوكولات الوصولية العشوائية و بروتوكولات تحكم الوصولية الوسائطية المستخدمة فى الشبكات الضوئية ذات الوصولية المتعددة بالتقسيم الشفري.

الباب الرابع: عرض مختصر للعوامل التى تحد من أداء الشبكات الضوئية وكذا دراسة لتأثير الضوضاء الحرارية والتشتت الضوئي فى الألياف الضوئية على أداء بروتوكول الاستقبال و الارسال بالأسلوب الحلقي ثم عرض النتائج التى تم الحصول عليها.

الباب الخامس: دراسة أداء بروتوكول الاستقبال و الارسال بالأسلوب الحلقي بعد اضافة نموذج تصفيف و ذلك للتغلب على الفقد الحادث فى الرسائل، حيث تمت زيادة

وحدة اضافية لتخزين الرسائل، ثم عرض للنتائج التي تم الحصول عليها  
و مقارنتها بالنتائج السابقة.

الباب السادس: عرض اقتراح ليبروتوكول جديد يعتمد على طريقة قف و انتظر و دراسة أدائه  
باستخدام كل من المستقبل الارتباطي Correlation Receiver و مستقبل  
مستوى الجذاعة Chip-Level Receiver و مقارنته ببروتوكول الاستقبال  
و الارسال بالأسلوب الحلقي و أخيرا عرض لنتائج الدراسة.

الباب السابع: عرض لخلاصة ما تم دراسته والنتائج التي تم التوصل اليها، والمقترح المقدم  
للتطوير في مجال نقل المعلومات بالألياف الضوئية.